UNIVERSITY OF
LIVERPOOL

Study of Diodes and Transistors for Organic Circuits

by

Suzanne Michelle Prior

Thesis submitted in accordance with the requirements of the University of Liverpool for the degree of Doctor in Philosophy

September 2009

Department of Electrical Engineering and Electronics

Acknowledgments

It would not have been possible to write this thesis without the help and support of many people, to whom I am extremely grateful.

Firstly, I would like to thank my supervisor, Professor William Eccleston for his guidance, support and patience throughout my study and for sharing his knowledge of solid state electronics.

I would also like to express my thanks to all past and present members of the Solid State research group.

Thanks are due to Kevin Molloy for his technical assistance which enabled this work to be completed.

Finally, I also wish to thank my friends and family, especially my parents, Carol and Bill Prior, for their support and encouragement which has enabled me to complete this work.

Abstract

In recent times much research has been carried out regarding the use of organic materials to fabricate electronic devices, for example diodes and thin film transistors. This thesis examines the use of polymers and small molecule materials to fabricate these devices with the aim of developing a greater understanding of their operation and to provide the basis for the development of circuits. Various materials are used to fabricate Schottky diodes and the measurements enable them to be compared. Equations are developed to describe the operation of the diodes and to facilitate the modelling of circuits.

Schottky diode characteristics were also studied at various temperatures. This is important since many of the materials do not conduct heat very readily and the effect of internal heating may be important. Temperature measurements also provide useful evidence of the nature of the conduction process and demonstrate the validity of the analytical work. Such models often, unintentionally, have temperature as one of the variables.

Capacitance measurements were obtained for the Schottky diodes to establish how the depletion region width alters with frequency, applied voltage and doping. A series of expressions were also derived to establish the theoretical relationships between the parameters and these were checked against experimental results.

The transient response of the diodes was also modelled and compared to experimental results. This was carried out at both a uniform temperature and at varying temperatures.

The final chapter of the thesis moves onto polycrystalline materials as opposed to polymers. The reason for this was the higher carrier mobility. It is practically important to have a single set of equations for both disordered and polycrystalline material if they are to be modelled in design software. This part of the project was to establish how the different transport mechanisms compare and also how parameters such as T_C vary between different kinds of material.

The polycrystalline experiments were completed using TFTs because diodes fabricated with polycrystalline material were not available at the time.

Having completed this work it is apparent that further work could be undertaken to aid the analytical aspects of the subject. Polycrystalline diodes need to be studied and compared with disordered diodes. Assessment of the potential value of the two types, for circuit applications, is essential, particularly from the point of view of circuit performance and cost. This implies an extension of the work to flexible substrates. It would also be of use to fabricate the devices in more ideal conditions to eliminate the effects of air. A wider range of temperatures should also be used to establish how internal heating of the devices affects the results. The effect of temperature on device capacitance and measurements under pulsed inputs would go someway to describing the mechanisms involved with digital circuits.

Contents

Symbol List

A - Contact area of a Schottky diode, m^2

a - Height of the peak of a Gaussian distribution, units dependant on distribution

b - Zero point of a Gaussian distribution, units dependant on distribution

c - Width of a Gaussian distribution, units dependant on distribution

C_d - Depletion region capacitance in a Schottky diode, F

dE - Small but finite energy, eV

dQ_d/dt - Variation in charge with time, A

E - Energy level(s), eV

E_0 - Centre point of a distribution of energy levels, eV

E_C - Conduction level, eV

E_F - Fermi level, eV

E_{Fm} - Fermi level within a metal, eV

E_i - Intrinsic level, eV

E_T - A carrier transport level, eV

F - Electric field, Vm^{-1}

f(E) - Occupancy of energy states, no units

F_D - Electric field strength on the dielectric side of the interface, Vm^{-1}

F_{max} - Maximum electric field, Vm^{-1}

F_S - Electric field strength on the semiconductor side of the interface, Vm^{-1}

f(x) - Gaussian Distribution, no units

I – Current, A

J - Current density, Am^{-2}

K - A constant

k - Boltzmann's constant, 1.38x10-23 m^2 kg s^{-2} K^{-1}

kT_C - Meyer-Neldel energy, m^2 kg s^{-2}

L - Width of the neutral region of a Schottky diode, m

M - Centre point of a Gaussian distribution, units dependant on distribution

m - $T_C/T - 1$, no units

n - Carrier concentration, m^{-3}

N(0) - A constant

N(E) An exponential approximation of the Gaussian distribution of states, no units

N'(0) - Rate of change of trap density per unit energy, $m^{-3}eV^{-1}$

N'(E) - Distribution of states per unit energy, $m^{-3}eV^{-1}$

n_0 - Density of carriers, m^{-3}

N_C - Effective density of states, m^{-3}

N_D - Doping density, m^{-3}

n_f - Free charge, m^{-3}

n_i - Intrinsic carrier density, m^{-3}

n_t - Trapped charge, m^{-3}

q - Electron charge, C

Q_d - Charge in the depletion region, C

$q\Phi_B$ - Energy difference between the Fermi level and the intrinsic Fermi level, CV

R_N - Resistance of the neutral region of a Schottky diode, Ω

T - Absolute temperature in Kelvin, K

T_0 - Characteristic temperature of the carriers, no units

T_C - Characteristic temperature of the traps, K

V_{app} - Applied voltage, V

V_B - Built in potential due to the barrier between materials, V

V_C - Voltage across the depletion region, V

V_D - Drain voltage, V

$V_{G'}$ - Gate voltage minus the threshold voltage, V

V_R - Voltage across the resistor, V

V_{total} - Total voltage = $V_{app} + V_B + 2kT/q$, V

V_x - Voltage at a point x down the channel, V

W - Width of the channel, m

W_d - Width of the depletion region, m

W_n - Width of the neutral region, m

W_t - Width of the polymer film, m

X - A sequence of numbers, no units

x - Distance from the interface, m

x_0 - Peak of the barrier, m

x_t - Length of the channel, m

ε_0 - Permittivity of free space, 8.854 x 10-12 Fm^{-1}

ε_D - Relative permittivity of the dielectric, no units

ε_g - Relative permittivity of the grain material, no units

ε_P - Relative permittivity of the semiconductor, no units

ε_S - Relative permittivity of the semiconductor, no units

η - Ideality factor, no units

θ - Ratio of free to total charge, no units

μ - Drift carrier mobility, $m^2 V^{-1} s^{-1}$

ρ – Resistivity, Ωm^{-1}

σ - Electrical conductivity of the material, Sm^{-1}

σ - Standard deviation, no units

Φ – Potential, V

Φ_B - Built in potential, V

Chapter 1

Introduction

This chapter provides an introduction to organic semiconductors and devices. Also presented is the organisation of the thesis and the experimental techniques used.

1.1 Organic Semiconductors and Devices

A semiconductor is a material which has an electrical conductivity between that of a typical metal and that of an insulator. An organic semiconductor is an organic material which exhibits semiconductor properties. Organic semiconductors can be in the form of single molecules, short carbon chains (oligomers) and long carbon chains (polymers).

Organic semiconductors fall into two main groups, "linear backbone" polymers derived from polyacetylene and "organic charge transfer complexes". It is possible to dope organic materials, to increase the number of carriers available, just as it is possible with inorganic materials. Organic metals also exist; these are very highly doped organic semiconductors and have electrical conductivity comparable to typical metals.

Much research has been carried out on organic semiconductors over the last 30 years. While it is not generally acknowledged, the first report of modern highly conductive polyacetylenes was by Weiss et al in 1963 [1]. In 1977, Shirakawa et al reported similar results using polyacetylene [2], for which they were awarded a Nobel Prize in Chemistry. Further work into this area has produced many useful organic semiconductors which have been successfully used in the fabrication of devices.

The use of organic semiconductors has many advantages, for example, ease of fabrication, flexibility and low cost. They are currently used in a number of devices for example, organic light emitting diodes (OLED) [3,4], organic solar photovoltaic (PV) cells [5] and organic field effect transistors (OFET) [6].

The ease of processing organic materials has also opened up a wide range of future applications where these polymers could be of great use. For example large area electronics is potentially a very large market which crystalline silicon is unlikely to achieve because of its inability to emit light.

Traditional inorganic materials require much more complicated processing techniques and substrates and are therefore more expensive to produce. The use of polymers would be more efficient and cost effective. Another possibility is to produce flexible displays with these materials which can be rolled up and stored.

A major disadvantage in the use of polymers is their sensitivity to air. Oxygen dopes the polymer p-type. This is a major concern because it is difficult to control. Materials have to be developed which are resilient to air exposure, or they must be encapsulated in an oxygen free environment, whilst maintaining both low cost and flexibility.

The work presented in this thesis is mainly concerned with the characterisation and analysis of devices fabricated with polytriarylamine (PTAA). The analysis is initially applied to simple Schottky diodes and once these are understood, more complicated devices are considered. The analysis of the Schottky diodes involves only one polymer, plus various metals that make up the contacts. It has been important to establish the effect of the various metals on the electrical characteristics of the diodes in order to determine which produce the best characteristics.

1.2 Thesis Organisation

Here a brief overview of the content of the thesis is given.

The introduction gives a brief overview of the thesis including an introduction to organic semiconductors and devices, together with the experimental techniques used to complete the experimental work.

Chapter 2 describes the various junctions which can be formed between metals and polymers and how these can be used to fabricate devices.

Derivations of the transport mechanisms for carriers across a Schottky barrier are included together with the effect of space charge limited currents within the devices. Experimental results are also used for comparison to the theoretical work.

The effect of temperature on the characteristics of Schottky diodes is investigated in the third chapter. This details some of the reasons for this behaviour. Also discussed is the relationship found between the temperature of measurement and the current observed.

The capacitance of the depletion region of a Schottky diode is discussed in chapter 4. Included here are derivations for the capacitance of the depletion region, resistance of the neutral region and the width of the depletion region. The effect of frequency, doping and voltage on the observed capacitance of the device is found experimentally.

Chapter 5 investigates the impulse response of Schottky diodes. This was achieved by theoretical analysis of both a simple case, where the neutral region resistance and the depletion region capacitance remains constant and for a more complex case where the resistance and capacitance vary with the applied voltage. Schottky diodes were then analysed experimentally and the results compared. The effect of temperature on the impulse response of Schottky diodes was then examined to determine the effect of temperature on the output observed. This was achieved by obtaining the impulse response at a wide range of temperatures and observing the results. The results were then analysed.

Chapter 6 provides an analysis of the carrier transport methods in small molecule thin film transistors (TFTs). A derivation of the equation to describe the transport mechanism is also included and experimental results analysed.

Finally, chapter 7 provides a discussion of the main conclusions reached and also possibilities for future work.

1.3 Experimental Techniques

To carry out practical work a variety of materials and experimental techniques were used, these are discussed below.

Firstly, the organic polymer polytriarylamine (PTAA) was obtained from Merck Chemicals Ltd (previously Avecia) and the dopant 2,3-dichloro-5,6-dicyano-1,4-benzoquinone (DDQ) was obtained from Aldrich.

To obtain metal contacts for the devices, the metal was thermally evaporated under a vacuum pressure of 10^{-3} torr.

To characterise the diodes their DC characteristics were obtained from a PC controlled Hewlett Packard 4145b parameter analyser which were then plotted in Origin graphing software.

Finally, temperature measurements were performed under vacuum at 10^{-1} torr and cooled within a liquid nitrogen cryostat. The samples were fabricated on a flexible substrate to allow for quicker cooling of the devices, the material used was polyethylene terephthalate (PET). The DC characteristics were then obtained from a Keithley 615 electrometer and 230 voltmeter.

1.4 Contributions

Prior S, Donaghy D, Eccleston W, Stablober B and Haase A. 'Analytical modelling of TFTs and diodes on small molecule organic semiconductor devices'. International Conference on Organic Electronics, Philips High Tech Campus, Eindhoven, 2007.

1.5 References

[1] R. McNeill, R. Siudak, J. H. Wardlaw, D. E. Weiss. Austrian Journal of Chemistry, Volume 16, Issue 663, 1963, p1056-1075.

[2] H. Shirakawa, E. J. Louis, A. G. MacDiarmid, C. K. Chiang, A. J. Heeger. Journal of the Chemical Society, Chemical Communications, Number 16, 1977, p578-580.

[3] J.H. Burroughes, D.D.C. Bradley, A.R. Brown, R.N. Marks, K Mackay, R.H. Friend, P.L.Burns, A.B. Holmes. Nature, Volume 347, Issue 6293, 1990, p 539-541.

[4] G. Gustafsson, Y. Cao, G. M. Treacy, F. Klavetter, N. Colaneri, A. J. Heeger. Nature, Volume 357, Issue 6378, 1992, p 477-479.

[5] C. J. Brabec. Solar Energy Materials and Solar Cells, Volume 83, Issue 2-3, 2004, p 273-292.

[6] M. Fadlallah, W. Benzarti, G.Billiot, W. Eccleston, D. Barclay. Journal of Applied Physics, Volume 99, Issue 10, 2006, Article Number 104504.

Chapter 2

Metal Semiconductor Junctions

Discussed within this chapter is the derivation for the current through a forward biased metal semiconductor junction in both the exponential and in the saturation region of operation. An investigation into the use of various metals as ohmic contacts to PTAA, and how this affects the performance of Schottky diodes, was carried out. This was investigated by fabricating polymer Schottky diodes with a range of different ohmic contact materials and obtaining their electrical characteristics. The effect of the contact material on the current-voltage characteristics and the calculated parameters of the diode are discussed, together with the causes for the observed effects.

2.1 Introduction

It is necessary that polymers produce good junctions with metals, to enable electronic devices to be fabricated. By combining a polymer with two suitable metal contacts it is possible to produce a Schottky diode [1]. Such devices rely heavily on the properties of the materials at the junctions to obtain the desired characteristics of the device. The quality of this interface is particularly important, as residual oxides and surface roughness are both factors, as well as the presence of traps, but there are opposing effects with this. Traps enhance current when they are closely spaced, but when they are not they are likely to give rise to stationary charge which lowers the overall average mobility of carriers.

In order to obtain a rectifying junction, a potential barrier must form at the interface with the metal. The height of the barrier depends on the difference in work function of the two materials. Work function is a measure of the energy required to remove an electron from a surface and this may depend on the way the surface has been treated. If the work function of an n type semiconductor is less than that of the metal, a barrier is formed to the flow of electrons into the metal. This barrier is distributed across a relatively thick depletion region and this can also absorb a large applied voltage. The applied voltage then lowers the barrier. The barrier to electron flow across the metal is much more abrupt so needs a very high field to reduce it.

Schottky diodes were fabricated with aluminium as the rectifying contact, polytriarylamine (PTAA) doped with 2,3-dichloro-5,6-dicyano-1,4-benzoquinone (DDQ) with a range of experimental ohmic contacts. The main ohmic contacts used were gold, platinum/palladium and copper. Discussed are the differences obtained by using different materials and the effects that the materials have on the current-voltage characteristics and parameters of the diode.

2.2 Metal Polymer Contacts

Schottky barriers have a large range of applications and are therefore of most interest. It has been suggested that the dominant method of carrier transport across a Schottky barrier is diffusion opposing the drift imposed by the presence of the field associated with the depletion region [2,3].

The theory detailing the carrier transport mechanisms across a Schottky barrier in the exponential rise of current is detailed below. Space charge limited currents, in saturation, are also discussed. Included are experimental results for Schottky barriers formed with various ohmic contact materials.

2.2.1 Carrier Concentration within Disordered Semiconductors

Disordered semiconductors have effectively more widely spread energy levels for the transportation of carriers [4] compared with single crystal materials [5]. This is due to single crystal materials behaving as though they have a single conduction band edge for the transportation of carriers, whereas within disordered semiconductors the density of energy levels rises rapidly with energy and cannot be treated as a single band edge. The exponential rise in energy levels results in an increase in the number of carriers which are available to the current. This occurs not only because there are more energy levels for carrier transportation but also, at higher energy levels, they are physically closely spaced, and carriers are more able to hop between the adjacent energy levels. If the energy levels are very localised and widely spaced, they immobilise the carriers making them unable to hop, they are therefore unable to contribute to the current. The states have an energy distribution which is random and a Gaussian distribution [6], f(x), is assumed

$$f(x) = a\exp\frac{-(X-b)^2}{2c^2} \qquad 2.2.1.$$

where X is a sequence of numbers, a determines the height of the peak of the distribution, b is a measure of where the zero value of X is located and c determines the width of the distribution. These can be replaced as shown in *eqn 2.2.2*

$$f(x) = \frac{1}{\sigma(2\pi)^{1/2}}\exp\frac{-(x-M)^2}{2\sigma^2} \qquad 2.2.2.$$

where σ is the standard deviation and M is a measure of the centre point of the distribution. The Gaussian distribution was named after Carl Friedrich Gauss. The distribution is a symmetrical bell shaped curve which quickly drops off with distance away from the centre point and tails off towards +/- infinity. This can be adapted to apply to energy levels

$$N(E) = \frac{N(0)}{\sigma(2\pi)^{1/2}}\exp\frac{-(E-E_0)^2}{2\sigma^2} \qquad 2.2.3.$$

where N(E) is the Gaussian function of energy levels, N(0) is a constant , E is a sequence of energies and E_0 is a measure of the centre point of the distribution. *Fig 2.2.1* details the Gaussian distribution when the width of the Gaussian function is altered, as can be seen this effects the exponential slope of the graphs.

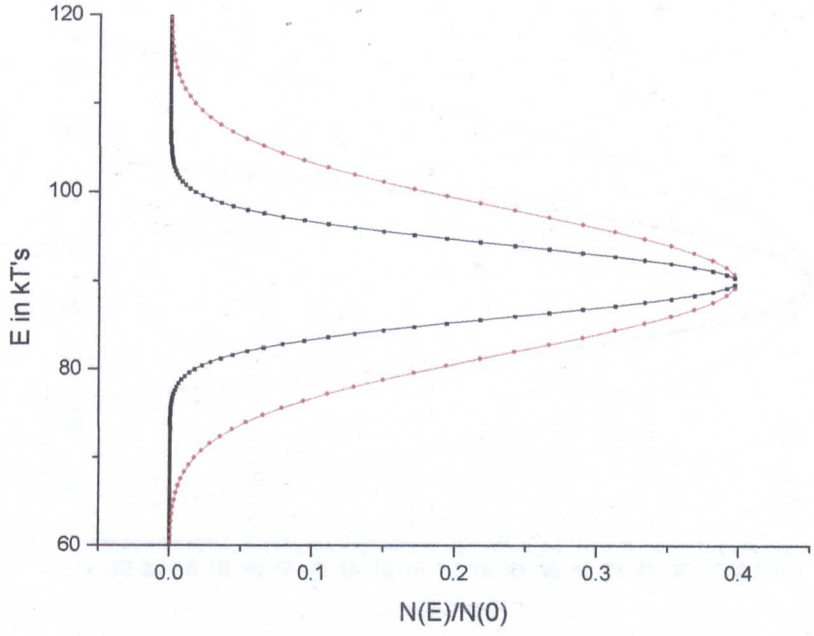

Fig 2.2.1. Details the Gaussian distribution for Eqn 2.2.3 with varying widths on a linear scale.

As can be observed in *fig 2.2.1* the tail end of a Gaussian distribution appears exponential, this can be further observed in *fig 2.2.2* on a semi logarithmic scale.

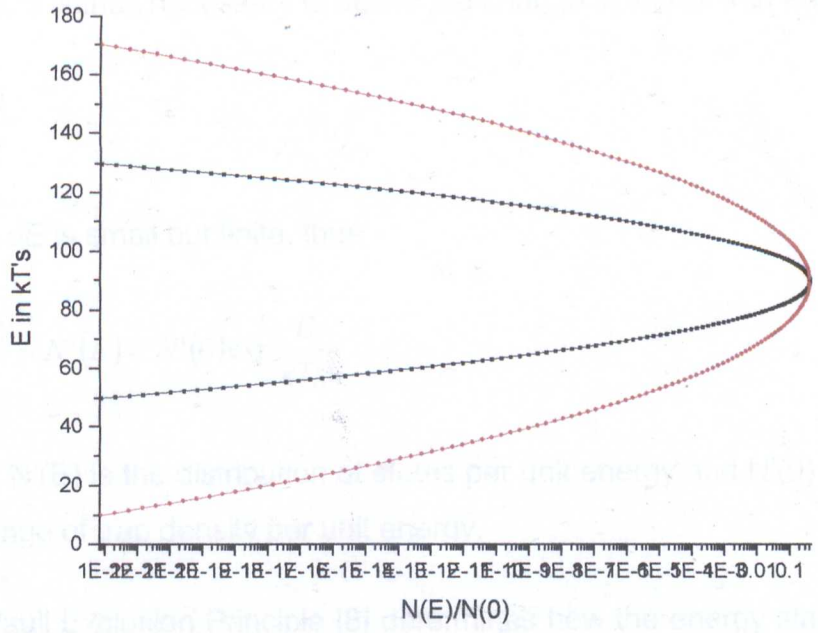

Fig 2.2.2. Details the Gaussian distribution for Eqn 2.2.3 with varying widths on a semi logarithmic scale.

The linear region of the graph indicates that the tail end of the Gaussian distribution is exponential over a certain range, it is then possible to approximate the distribution of energy levels by an exponential of the form

$$N(E) = N(0)\exp\frac{E}{kT_C} \qquad 2.2.4.$$

where N(E) is an exponential approximation of the distribution of states, E is an energy level and kT_C is the Meyer-Neldel energy [7] where k is Boltzmann's constant and T_C is the characteristic temperature of the material, the value of which will vary at different points on the Gaussian curve. This expression however is not of much use as for any value of

energy, the range of E is infinitely small, this means that it can contain zero charge. It is thus necessary to define the change in states with energy

$$\frac{dN(E)}{dE} \qquad 2.2.5.$$

where dE is small but finite, thus

$$\frac{dN(E)}{dE} = N'(E) = N'(0)\exp\frac{E}{kT_C} \qquad 2.2.6.$$

where N'(E) is the distribution of states per unit energy and N'(0) is the rate of change of trap density per unit energy.

The Pauli Exclusion Principle [8] determines how the energy states fill with electrons. It states that for electrons within a collection of atoms in close proximity, that no two electrons can have the same 4 quantum numbers. This means that if n, l and m_l are the same, then m_s must be different, where n is the principle quantum number, l is the azimuthal quantum number, m_l is the magnetic quantum number and m_s is the spin quantum number. This means that 2 electrons can exist in the same state if they have three identical quantum numbers but one is different, for example opposite spin. It is a good approximation to treat the electrons as each having slightly different energies so that the occupancy can be obtained from the Fermi-Dirac statistics [9]

$$f(E) = \frac{1}{1+\exp\left(\frac{E-E_F}{kT}\right)} \qquad 2.2.7.$$

where f(E) is the occupancy of the states, E_F is the Fermi level, and T is the absolute temperature in Kelvin. In a metal, the states below the Fermi level are assumed to be full of carriers and the states above are assumed to be empty. In reality, there are occupied states above the Fermi level and

unoccupied states below, thus the Fermi level is defined as the point where the fraction of states occupied is one half. If the occupancy of states above the Fermi level increases, the position at which the fraction of states occupied equals one half rises and thus so does the Fermi level.

This can be approximated by the Maxwell Boltzmann statistics [10] when

$$E - E_F >> kT \qquad 2.2.8.$$

The approximation is then

$$f(E) = \exp\left(-\left(\frac{E - E_F}{kT}\right)\right) \qquad 2.2.9.$$

This can be used as an approximation to the Fermi Dirac statistics as the lower states are due to dopant and have a low mobility, it is therefore possible to ignore the effect of these states. The density of carriers with energy, which are assumed to be electrons has the form

$$\int f(E)N'(E)dE = \int_{E_F}^{\infty} \exp-\left(\frac{E - E_F}{kT}\right) N'(0) \exp\frac{E}{kT_C} dE \qquad 2.2.10.$$

The limits of the integration are between E_F and infinity, however, close to the Fermi level the condition is not met. In practice, where current is of the most interest, the effective mobility of the carriers increases with increased energy, therefore, the states near to the Fermi level carry much less current and can be ignored. Once the expression is integrated the following expression is obtained

$$n_0 = kT_0 N'(0) \exp\left(\frac{E_F}{kT_C}\right) \qquad 2.2.11.$$

where n_0 is the density of carriers with energy and T_0 is defined as detailed in *eqn 2.2.12.*

$$\frac{1}{T_0} = \frac{1}{T} - \frac{1}{T_C} \qquad 2.2.12$$

where T is the absolute temperature in Kelvin and T_C is the characteristic temperature.

It is possible to obtain an expression for the intrinsic carrier concentration by replacing n_0 by n_i and E_F by E_i in *eqn 2.2.11*

$$n_i = kT_0 N'(0) \exp\left(\frac{E_i}{kT_C}\right) \qquad 2.2.13.$$

Where n_i is the intrinsic carrier density with energy and E_i is the intrinsic level. *Eqn 2.2.11* and *2.2.13* can then be combined

$$n_0 = n_i \exp\left(\frac{E_F - E_i}{kT_C}\right) \qquad 2.2.14.$$

The quantity E_F-E_I can then be replaced as illustrated in *fig 2.2.3.*

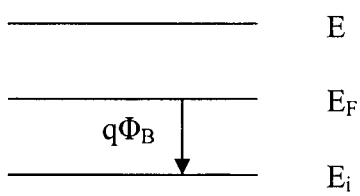

Fig 2.2.3. Schematic representation of the structure of energy levels within a semiconductor to indicate how $q\Phi_B$ is defined.

$$n_0 = n_i \exp\left(\frac{q\phi_B}{kT_C}\right) \qquad 2.2.15.$$

where $q\Phi_B$ is the energy difference between the Fermi level and the intrinsic Fermi level, where q is equal to the electron charge and Φ_B is the built in potential. The result is an expression for the equilibrium carrier concentration, n_0, within a disordered semiconductor.

This expression is quite similar for a material with a transport level such as a conduction band edge. In deriving this we start from the Fermi Dirac equation and assume that the Fermi level is much less than a carrier transport level, E_T. This leads to the Maxwell Boltzmann approximation to Fermi Dirac Statistics. The resulting equation for the equilibrium carrier concentration is

$$n_0 = N_C \exp\left(-\frac{E_T - E_F}{kT}\right) \qquad 2.2.16.$$

where N_C is an effective density of states. A similar expression can be obtained for the intrinsic carrier density

$$n_i = N_C \exp\left(-\frac{E_T - E_i}{kT}\right) \qquad 2.2.17.$$

Eqns 2.2.16 and *2.2.17* can be combined [11]

$$n_0 = n_i \exp\left(\frac{E_F - E_i}{kT}\right) \qquad 2.2.18.$$

Again, the term E_F-E_i can be replaced by the electronic charge and the effective potential difference between the two levels

$$n_0 = n_i \exp\left(\frac{q\phi_B}{kT}\right) \qquad 2.2.19.$$

The resulting expressions for the two cases differ in the fact that one has T and the other is the effective temperature T_c of the trap distribution. It is

expected that this would be T_0, however, only the carriers above the Fermi level have been assumed to be free. This is a much better approximation for a disordered semiconductor than it would be for a crystalline material because of the exponential rise in the density of states, which in turn comes from the Gaussian approximation.

2.2.2 Schottky Barrier Transport Mechanisms

As discussed earlier, if two materials are brought together to form a junction, one metal and one semiconductor, a variety of junctions can be formed depending on the work functions of each material. The work function is the energy required to take an electron from the Fermi level to the vacuum level. In this example a metal and an n type semiconductor are used. If the metal has a larger work function than the semiconductor, the energy level diagram for the two materials would have a structure as shown in *fig 2.2.4.*

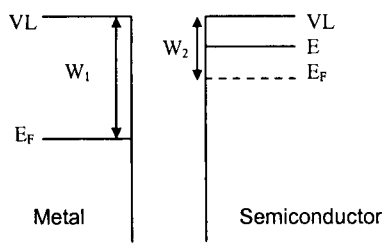

Fig 2.2.4. Details the energy levels within a metal and an n type semiconductor. Here the metal has a larger work function than the semiconductor. The quantity E is one value in the exponential rise on the density of states with energy.

The same two materials are first connected by an external wire. The Fermi levels are aligned as the two sets of electrons come into equilibrium. There is then a potential difference between the two materials, and a field in the gap, but also the vacuum levels are now at different levels. When the two materials are placed in contact, the difference in potential falls across the semiconductor surface region, which becomes accumulated. The metal might be thought to deplete, but this is prevented by the very large concentration of charged atoms in such materials. The energy level diagram for this is detailed within *Fig 2.2.5.*

The charge concentration in the accumulation region depends on the difference in the two work functions. The distance over which the carriers in the accumulation are spread is measured by the Debye Length.

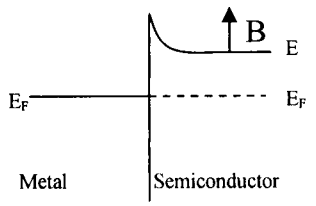

Fig 2.2.5. Details a Schottky barrier formed between a metal and an n type semiconductor.

Fig 2.2.6 shows a schematic representation of a Schottky diode. As can be seen there is a Schottky contact on the left hand side and an ohmic contact on the right hand side with the semiconductor between the contacts. The semiconductor contains both a depletion region and a neutral region. The depletion region was discussed previously and opposes the flow of carriers due to fixed centres of opposite charge to the majority carriers and the neutral region has no net charge.

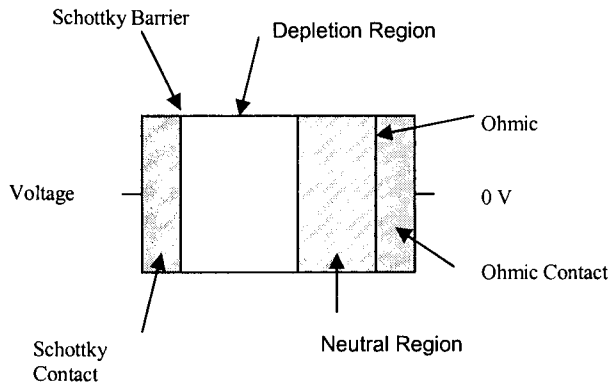

Fig 2.2.6. Schematic representation of a Schottky diode.

In forward bias the whole distribution of energy levels in the neutral region rises, with respect to those in the metal, by the application of the applied voltage. This Fermi level in the neutral region rises by the same amount. In the depletion region it is assumed that the Fermi level also rises, so that it is flat from the ohmic contact to the peak in the potential barrier next to the metal. In the depletion region this is termed the quasi Fermi level. Implicit in making this assumption is that Maxwell Boltzmann approximation still applies. This would not be the case were the carriers to be come hot however, this is unlikely in a depletion region where the built-in field opposes current flow. The entire distribution is lifted in energy with little deviation from Maxwell-Boltzmann, except where they are accelerated into the metal. The rise in energy levels with applied potential is illustrated in *fig* 2.2.7.

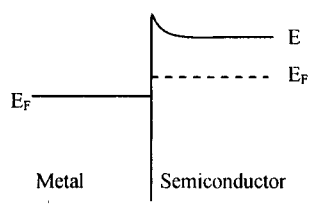

Fig 2.2.7. Details a Schottky barrier under forward bias.

During forward bias, the current passing into the metal increases exponentially with increased applied voltage, this is due to the exponential increase in carrier density as described by Maxwell Boltzmann statistics. Closer to the Fermi level this approximation to the Fermi Dirac statistics fails. However in these low energy regions the density of states and hence conduction is very low. The existence of an exponential rise in the current is evidence of the validity of Maxwell Boltzmann statistics.

The equation for the state density per unit energy N'(E) needs to be altered to account for the rise in the energy level to incorporate the voltage applied to the Schottky barrier. The equation then becomes

$$N'(E) = N'(0)\exp\frac{E - qV_{app}}{kT_C} \qquad 2.2.20.$$

where V_{app} is the negative applied voltage to the ohmic contact to obtain the forward bias with an n type semiconductor. As the current density is proportional to the carrier concentration at the top of the barrier next to the metal, it is clear that the current density is

$$J \propto \exp\frac{qV_{app}}{\eta kT} \qquad 2.2.21.$$

where J is the current density and η is the ideality factor. This assumes that the quasi Fermi level is flat. The value expected for the ideality factor in the disordered materials used is expected to be greater than 1 as similar materials have produced these results [12], however silicon does not have the carriers distributed according to the trapping levels and therefore a different ideality factor is obtained, here η =1 which is only slightly increased by trapping.

When a voltage is applied to the diode so that it is forward biased, a current flows across the diode, this is the forward current. At higher applied

voltages the resistive neutral region cannot deliver the current and some of the additional applied voltage falls across it. There is a resistance associated with the neutral region and this means that a very large applied voltage would be required to continue supplying the current.

When the diode is in reverse bias, the energy levels in the semiconductor lower with respect to the energy levels in the metal. This causes the Fermi level to alter its position and a quasi Fermi level is produced lower than the original position of the Fermi level. As with forward bias, the applied potential causes the entire distribution of carriers to alter their position. With reverse bias, the distribution of carriers lowers as the Fermi level does. *Fig 2.2.8* illustrates the structure of the junction during reverse bias.

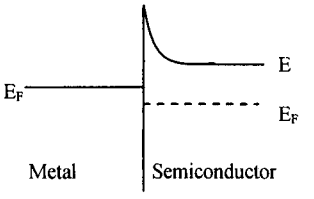

Fig 2.2.8. Details a Schottky barrier under reverse bias.

It is first necessary to consider the field present within a Schottky diode due to the depletion region created when a metal and semiconductor are joined. The field due to the depletion region is shown in *fig 2.2.9.*

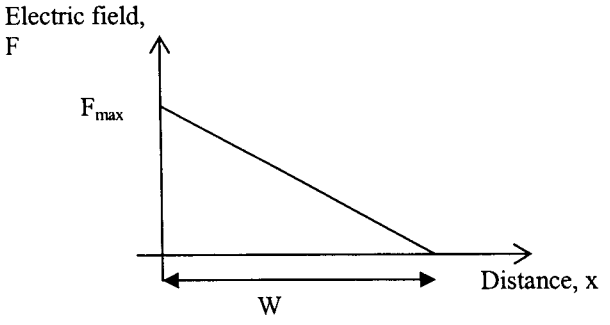

Fig 2.2.9. Details the field present within the depletion region of a Schottky diode, where W is the width of the depletion region and F_{max} is the maximum field at the metal-polymer interface.

It is possible to derive an equation for this maximum field from Poisson's equation. The expression obtained for the maximum field F_{max} is

$$F_{max} = -\left(\frac{2\,q\,N_D \left(V_{app} + V_B + \frac{2\,k\,T}{q} \right)}{\varepsilon_o\,\varepsilon_p} \right)^{1/2} \qquad 2.2.22.$$

where N_D is the doping density of the material, V_B is the built in potential of the junction, ε_0 is the permittivity of free space and ε_P is the relative permittivity of the semiconductor. The maximum potential and minimum field, actually seen by a carrier at a Schottky barrier is at the point where the field due to the depletion region is equal and opposite to the field due to the image charge of the carriers. This is illustrated in *fig 2.2.10.*

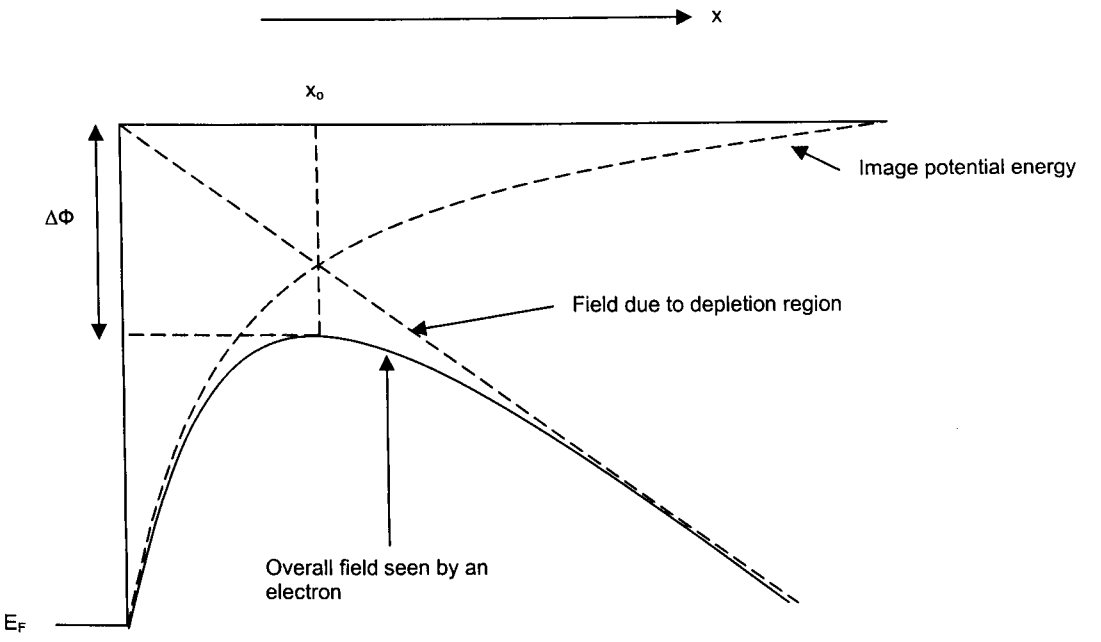

Fig 2.2.10. Schematic representation of the peak of a Schottky barrier detailing the fields present.

There is a force associated with each carrier in the semiconductor; this gives rise to the image charge, which is equal but opposite in sign to the carrier, and is seen on the opposite side of the junction to the carrier itself. If the carrier is at a distance x from the metal, the opposite charge is induced on the metal surface, at a distance –x. This therefore means that there is a force of attraction, between the real and apparent charges.

At the junction, the field lines between the charges, are perpendicular to the boundary of the junction. This is due to the fact that any horizontal component of field, causes a lateral redistribution of charge along the interface, until it is cancelled. The force between the two opposite charges, is given by *eqn 2.2.22* (using x, as the distance between the carrier and the junction). This is the general equation, called Coulomb's Law, for the force between two particles, when the carrier is at a distance x from the junction.

The distance used should be the distance between the centres of the real and apparent charged particles, so for this general equation, the distance is 2x. To obtain the equation for the potential at the peak of the barrier, x_0 will be used instead of x. q^2 is used in this equation as it is the charge of each of the particles multiplied together, here the charges are equal and opposite therefore it is acceptable to use q^2.

Shown in *fig 2.2.11* is a schematic representation of the image charge. It is important to note that the image charge field line distribution within the metal reflects the charge within the semiconductor. This means that the distribution is equal but opposite on both sides of the junction if it is assumed that both materials have the same dielectric constant.

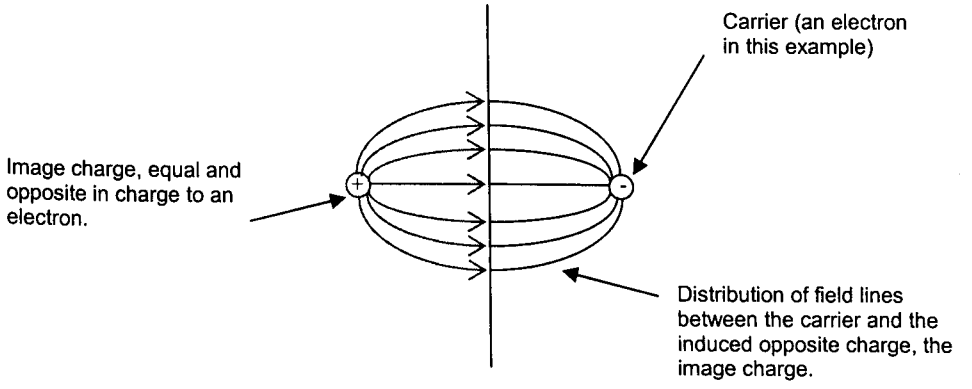

Fig 2.2.11. Details the image charge at the interface between metal and semiconductor.

From Coulombs law,

$$\text{Force} = -\frac{q^2}{4\pi\varepsilon_0\,\varepsilon_p\,(2x)^2} \qquad 2.2.23.$$

The field is,

$$\text{Field} = -\frac{q}{4\pi\varepsilon_0\,\varepsilon_p\,(2x)^2} \qquad 2.2.24.$$

The two equations for the field, *eqn 2.2.22* and *eqn 2.2.24* can then be set equal to one another as at the peak of the barrier the fields are equal and opposite, thus the field at the top of the barrier is equal to zero.

By rearranging these equations the distance x_0 where the peak of the barrier is can be obtained,

$$x_0 = \left(\frac{q}{512\pi^2\,\varepsilon_0\,\varepsilon_p\,N_D V_{total}}\right)^{1/4} \qquad 2.2.25.$$

where $V_{total} = V_{app} + V_B + 2kT/q$, and Vapp is the applied voltage, V_B is the built in potential due to the barrier, k is Boltzmann's constant, T is the temperature in Kelvin and q is the electronic charge. It is then possible to obtain the potential by which the barrier is lowered due to the effect of the depletion region and the image charge. This can be obtained from,

$$\Delta\varphi = F_{max}\,x_0 \qquad 2.2.26.$$

F_{max} and x_0 can be substituted into *eqn 2.2.26* and rearranged to obtain

$$\Delta\varphi = \left(\frac{q^3\,N_D V_{total}}{128\pi^2\left(\varepsilon_0\,\varepsilon_p\right)^3}\right)^{1/4} \qquad 2.2.27.$$

From *eqn 2.2.21* the current density in the reverse direction can be obtained from

$$J \propto \exp\left(\frac{q\,\Delta\varphi}{k\,T}\right) \qquad 2.2.28.$$

Thus, an equation for the current density can be obtained when the image force of the carriers is taken into account and the barrier lowering due to this is considered. This is given by [13],

$$J_R = J_0 \exp\left[\frac{q}{kT}\left(\frac{q^3 N_D V_{total}}{128\pi^2 \varepsilon_0 \varepsilon_s}\right)^{1/4}\right] \qquad 2.2.29.$$

This has previously been derived by Sze for silicon which has an abrupt band edge[14].

This expression for the reverse current density can be used to obtain the doping density of the material by plotting log(J) versus $V^{1/4}$.

2.2.3 Universal Mobility Law

The universal mobility law states how the carrier mobility and carrier concentration are related. It shows that the mobility is dependent on the number of carriers and is thus an important relationship to consider. It will be derived in this section, starting from relationships for carrier density for both ordered and disordered material.

From *eqn 2.2.11*, the carrier density within a disordered semiconductor is defined as

$$n = N'(0)kT_0 \exp\left(\frac{E_F}{kT_C}\right) \qquad 2.2.30$$

Similarly for an ordered semiconductor

$$n = N_C \exp\left(\frac{E_F}{kT}\right)\exp\left(\frac{-E_T}{kT}\right) \qquad 2.2.31$$

Each of these equations can be rearranged for $\exp(E_F/kT)$. They can then be equated and rearranged for n. This is detailed below

$$n = N_C \exp\left(\frac{-E_T}{kT}\right)\left(N'(0)kT_0\right)^{\frac{T}{T_C}} n^{\frac{T_C}{T}} \qquad 2.2.32$$

It is then possible to define an equation for J using *eqn 2.2.32* as J=nqμF

$$J = qK_1 F N_C \exp\left(\frac{-E_T}{kT}\right)\left(N'(0)kT_0\right)^{\frac{T}{T_C}} n^{\frac{T_C}{T}} \qquad 2.2.33$$

The mobility can then be found from *eqn 2.2.33* by dividing the equation for the current density by n q and F.

$$\mu = K_1 N_C \exp\left(\frac{-E_T}{kT}\right)\left(N'(0)kT_0\right)^{\frac{T}{T_C}} n^{\frac{T_C}{T}-1} \qquad 2.2.34$$

This is the universal mobility law [15] with all parameters included. It is possible to more simply represent the universal mobility law as [16]

$$\mu = Kn^m \qquad 2.2.35$$

where:

$$K = K_1 N_C \exp\left(\frac{-E_T}{kT}\right)\left(N'(0)kT_0\right)^{\frac{T}{T_C}}$$

$$m = \frac{T}{T_C} - 1$$

The latter is the same equation as that described by Vissenberg and Matters which in their case involved percolation theory [17].

2.2.4 Space Charge Limited Current for a Perfect Insulator

Space charge limited current occurs when there are many slow moving carriers. This means that to supply a particular current, more carriers are required compared with supplying the same current with high mobility carriers. There is a variation in both carrier density and electric field throughout the device, the product of which remains constant. The theory of Space charge limited current is initially derived for a perfect insulator. This assumes that the insulator is free from traps and has a negligible number of free carriers at equilibrium. This means that the charge within the insulator does not become trapped and contributes to the space charge limited current.

The theory of space charge limited current was first developed by Rose [18] and Lampert and Mark [19, 20].

The presence of diffusion currents are also ignored although they must be present if there is a variation of charge density with distance. If the current is limited by drift we have

$$J = nq\mu F \qquad 2.2.36.$$

where n is the carrier concentration, μ is the drift carrier mobility and F is the field. It is possible to obtain the concentration of free carriers from Poisson's equation as the space charge is driven by the injected carriers. This is ,

$$\frac{d^2\phi}{dx^2} = \frac{-qn}{\varepsilon_0 \varepsilon_s} \qquad 2.2.37.$$

where Φ is the potential and x is the distance from the interface. It is then possible to represent Poisson's equation as,

$$\frac{dF}{dx} = \frac{qn}{\varepsilon_0 \varepsilon_s} \qquad 2.2.38.$$

This equation can then be rearranged to obtain an expression for qn and this substituted into *eqn 2.2.33*. This results in,

$$J = \varepsilon_0 \varepsilon_s \mu F \frac{dF}{dx} \qquad 2.2.39.$$

It can then be integrated with respect to the distance, x, between 0, at the interface and x at the edge of the depletion region. The electric field, F, is integrated between 0 at the point x at the edge of the depletion region and F at the interface. This is then rearranged to obtain an equation for the field,

$$F = \left(\frac{2Jx}{\varepsilon_0 \varepsilon_s \mu} \right)^{1/2} \qquad 2.2.40.$$

The electric field can then be replaced by –dV/dx and then the expression integrated with respect to V and x. Here, V is integrated between 0 and the applied voltage V_{app} and, x is taken between 0 and x. The resulting equation is,

$$J = \frac{9}{8} \varepsilon_0 \varepsilon_s \mu \frac{V_{app}^{\ 2}}{x^3} \qquad 2.2.41.$$

This is known as the Mott-Gurney square law [21].

It is possible to plot the variation of carrier concentration and field throughout the device, this is shown in *fig 2.2.12*.

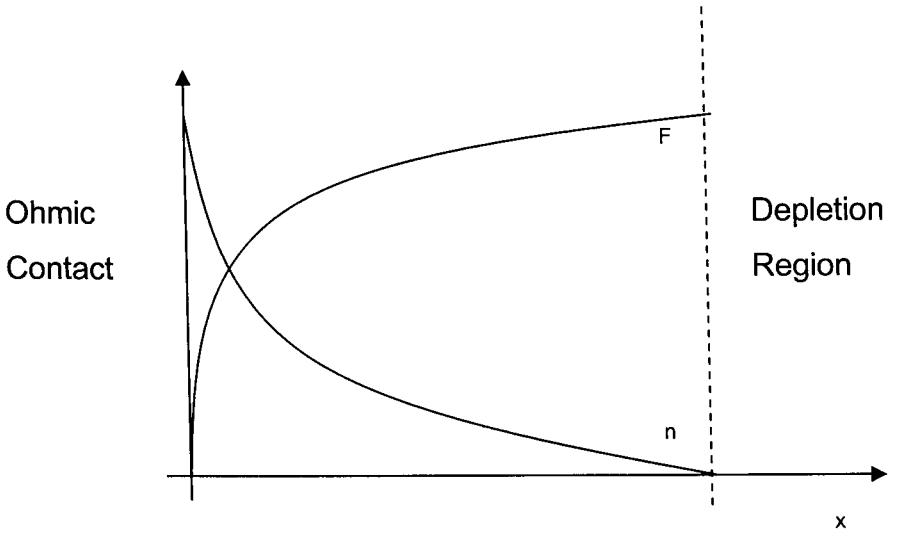

Fig 2.2.12. Representation of the variation in both carrier density and electric field with distance.

As can be seen from the figure, the carrier concentration drops as the electric field rises. The product of the two values is constant as the current is constant across the device.

2.2.5 Space Charge Limited Current for an Insulator with Traps

The previous derivations for the space charge limited currents have assumed that the semiconductor is ideal and that it does not contain traps. If however the semiconductor is non-ideal and includes traps then both the free and trapped charge contributes to the space charge limited current. To derive an expression for the space charge limited current with traps it is necessary to define θ which is the ratio of free carrier density to total carrier density as,

$$\theta = \frac{n_f}{n_f + n_t} \qquad 2.2.42.$$

where n_f is the free carrier concentration and n_t is the trapped carrier concentration. This is assuming that all carriers below the Fermi level are trapped and all above the Fermi level are free and is thus a very rough approximation. It is then possible to rearrange the equation to obtain an expression for the charge contributing to the space charge limited current, this is,

$$n_f + n_t = \frac{n_f}{\theta} \qquad 2.2.43.$$

This can then be substituted into Poisson's equation,

$$\frac{d^2\phi}{dx^2} = \frac{-qn_f}{\varepsilon_0 \varepsilon_s \theta} \qquad 2.2.44.$$

It is then possible to represent Poisson's equation as,

$$\frac{dF}{dx} = \frac{qn_f}{\varepsilon_0 \varepsilon_s \theta} \qquad 2.2.45.$$

This can then be substituted into the current density equation and results in,

$$J = \varepsilon_0 \varepsilon_s \theta \mu F \frac{dF}{dx} \qquad 2.2.46.$$

This expression can then be integrated with respect to x and F as in the previous derivation for a perfect insulator and re-arranged to obtain an equation for F,

$$F = \left(\frac{2Jx}{\varepsilon_0 \varepsilon_s \theta \mu} \right)^{1/2} \qquad 2.2.47.$$

F can then be replaced by –dV/dx and then the expression integrated with respect to V and x. The resulting equation is,

$$J = \frac{9}{8} \varepsilon_0 \varepsilon_s \theta \mu \frac{V_{app}^{\ 2}}{x^3} \qquad 2.2.48.$$

This is the space charge limited current equation for a non-ideal semiconductor. In comparison to the first derivation for an ideal semiconductor not taking the universal mobility law into account, the two equations are very similar; the only difference is that the current is reduced due to the incorporation of theta into the expression.

2.2.6 Space Charge Limited Current in a Perfect Insulator Incorporating the Universal Mobility Law

The mobility of the carriers is dependent on the carrier concentration which has not been considered in the previous derivation of the space charge limited current. The mobility of the carriers and carrier concentration are related by the universal mobility law

$$\mu = Kn^m \qquad 2.2.49.$$

where μ is the mobility of the carriers, K is a constant, n is the carrier density and m is $T_C/T - 1$. This can be substituted into the equation for the drift current density, $J = nq\mu F$, to give,

$$J = qFKn^{m+1} \qquad 2.2.50.$$

An expression for $n^{(m+1)}$ can be obtained from Poisson's equation,

$$n^{m+1} = \left(-\frac{d^2\phi}{dx^2} \frac{\varepsilon_0 \varepsilon_s}{q} \right)^{m+1} \qquad 2.2.51.$$

From *eqn 2.2.36*,

$$J = qFK \left(\frac{dF}{dx} \frac{\varepsilon_0 \varepsilon_p}{q} \right)^{m+1} \qquad 2.2.52.$$

This expression can then be integrated with respect to x and F and re-arranged to obtain an equation for the electric field,

$$F = \left(\frac{J}{qK} \right)^{1/m+2} \left(x \frac{q}{\varepsilon_0 \varepsilon_P} \frac{m+2}{m+1} \right)^{m+1/m+2} \qquad 2.2.53.$$

F can then be replaced by –dV/dx. *Eqn 2.2.53* can then be integrated with respect to V_{app} and x,

$$J = qK \left(\frac{\varepsilon_0 \varepsilon_P}{q} \frac{m+1}{m+2} \right)^{m+1} \left(\frac{2m+3}{m+2} \right)^{m+2} \frac{V_{app}^{\ m+2}}{x^{2m+3}} \qquad 2.2.54.$$

If m=0 is substituted into this equation the previously derived equation, *eqn 2.2.41*, is obtained.

2.3 Schottky Diode Experimental Results

2.3.1 Aluminium Schottky Diodes with Gold Ohmic Contacts

This section provides an analysis of experimental results obtained from Schottky diodes fabricated with gold as the ohmic contact, aluminium as the Schottky contact and PTAA as the polymer, doped with DDQ.

A diagram of the structure of PTAA is shown in *fig 2.3.1* [22].

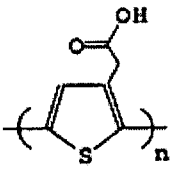

Fig 2.3.1 Diagram of the structure of PTAA

The chemical structure of DDQ [23] is shown in *Fig 2.3.2.*

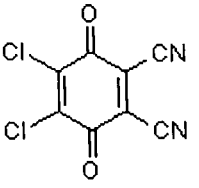

Fig 2.3.2 Diagram of the structure of DDQ

To fabricate these diodes, gold was used as the base contact and treated with pentafluorobenzenethiol. This is a strong electron withdrawing agent which therefore provides the holes which contribute to the current flow. The molecular formula for pentafluorobenzenethiol is C_6HF_5S and its chemical structure is shown in *fig 2.3.3* [24].

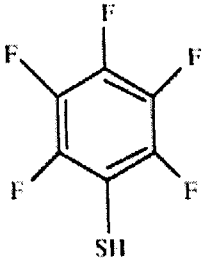

Fig 2.3.3 Structure of Pentafluorobenzenethiol

The doped polymer was then cast over the surface of the base contact and the Schottky contact evaporated onto the surface of the polymer. An

example of the structure of the Schottky diodes is detailed in *Fig 2.3.4.* The Schottky contact was vacuum evaporated onto the polymer through a metal mask in the form of dots of diameter 1mm.

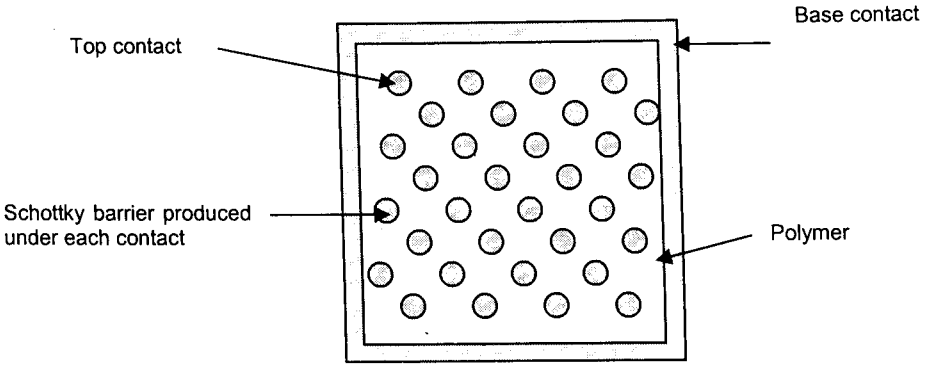

Fig 2.3.4 Schematic representation of the Schottky diodes structure.

To electrically characterise the Schottky diodes, voltage was applied to the gold contact, from -10 to +10 Volts, and the output current recorded. This was achieved by the use of a probe on each contact to supply the voltage across them.

A typical current voltage characteristic for an aluminium-PTAA-gold Schottky diode is detailed within *fig 2.3.5.* As can be observed, the rectification ratio of the diodes is approximately three orders of magnitude.

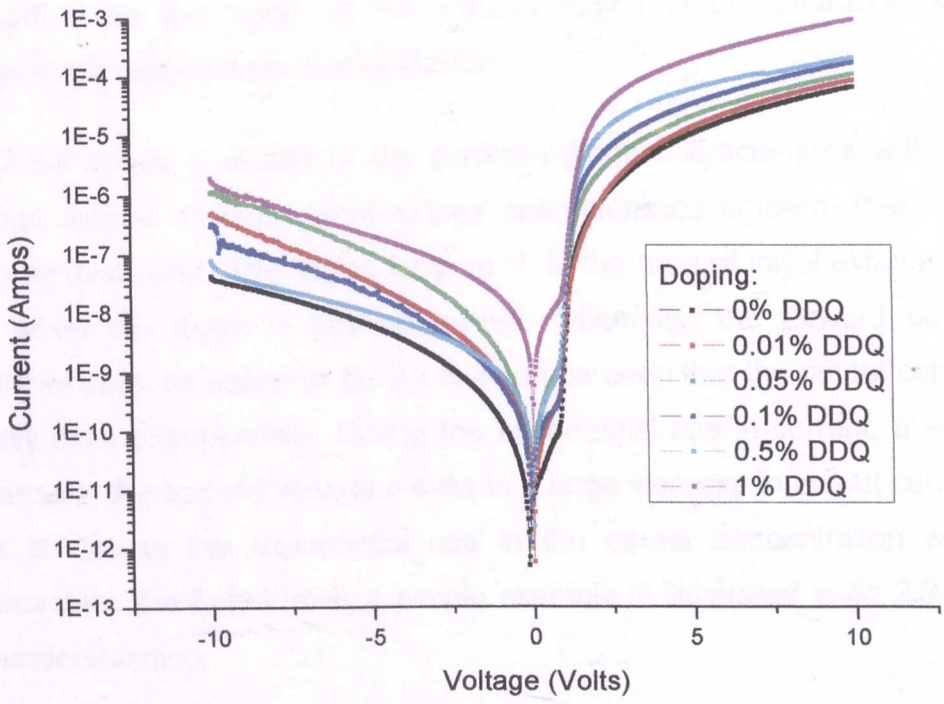

Fig 2.3.5 Typical current-voltage characteristics for gold-PTAA-aluminium Schottky diodes

It is possible to calculate both the carrier mobility and ideality factor from these characteristics. The carrier mobility was calculated using a linear-linear plot of the forward current-voltage characteristics and was found to range from 1.8×10^{-8} cm^{-3} to 1.3×10^{-10} cm^{-3}. The ideality factor was calculated from the exponential region of the forward characteristics and ranges from 1.6 to 4.1. Observing the results obtained for the ideality factor, it is apparent that the diodes have an ideality factor of greater than 1; this indicates that there may be an interfacial layer between the aluminium and the polymer and the results obtained from the diodes are not ideal. The interfacial layer is thought to be an oxide present on the metal and is due to air exposure on the device. It is known that a thin layer of alumina will form on the surface of aluminium after exposure to air, this has been observed

as a 4nm layer of alumina after 100ps air exposure [25]. This is also thought to be the cause of the plateau region in the characteristics, however will require further investigation.

Fig 2.3.6 shows a sketch of the current-voltage characteristics with the various regions of the current-voltage characteristics labelled, these will each be discussed. The region labelled '1' is the area of initial exponential rise when the diode is forward biased. Observing the forward output characteristics, as shown in *fig 2.3.5*, it can be seen that the output current initially rises exponentially. During the exponential rise in current, a small increase in the applied voltage results in a large increase in output current. This is due to the exponential rise in the carrier concentration when approaching the Fermi level, a simple example is illustrated in *fig 2.3.7* to aid understanding.

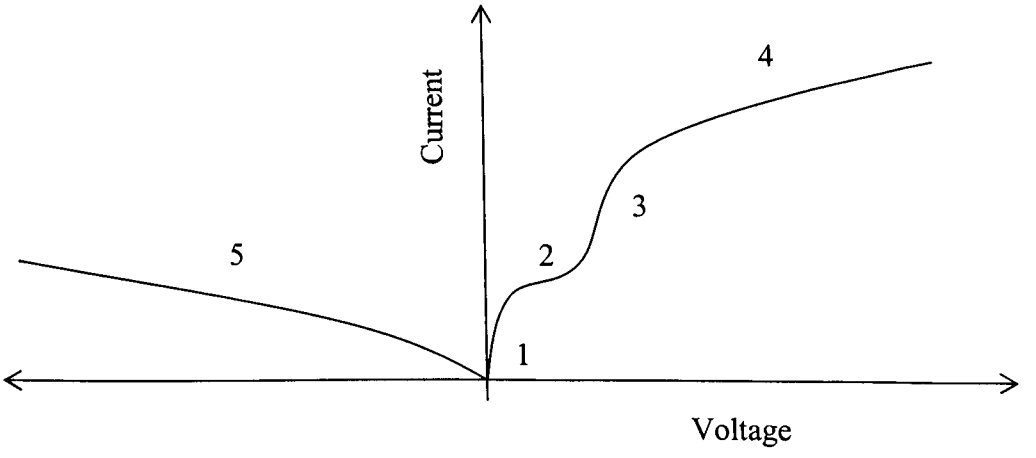

Fig 2.3.6. A sketch of the current-voltage characteristics obtained from a Schottky diode. Various regions of the characteristics have been labelled and are discussed within the text.

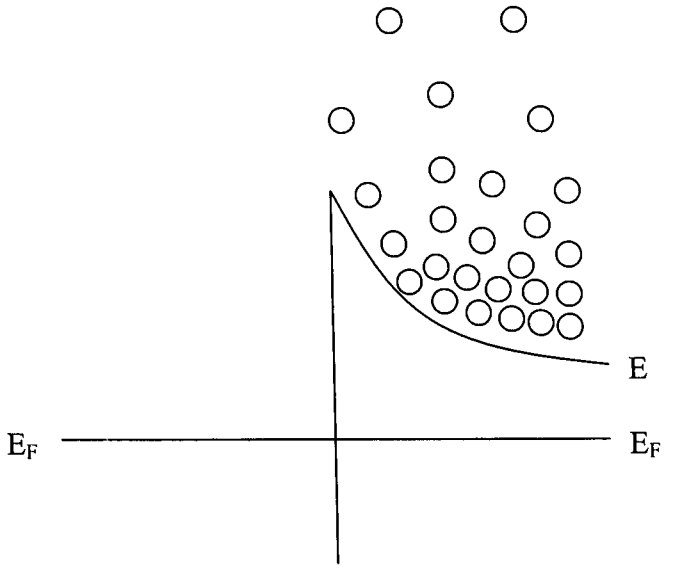

Fig 2.3.7. Schottky barrier indicating the exponential rise in the carrier concentration when approaching the Fermi-level.

When the diode is forward biased, as shown in *fig 2.3.8*, the depletion region contracts, the barrier becomes smaller in height and carriers can more easily pass into the metal from the semiconductor. The energy levels and Fermi level rise allowing more carriers to pass over the Schottky barrier. The increase in carriers allowed to cross the barrier is exponential as the carrier distribution increases exponentially closer to the Fermi level and the whole distribution has risen. This therefore results in an exponential increase in current. In this exponential region, the majority of the applied voltage falls across the depletion region and very little is taken up by the neutral region.

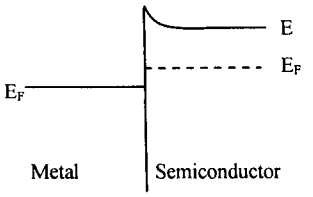

Fig 2.3.8. Forward biased Schottky diode.

The forward characteristics however rapidly reach a plateau region, this is illustrated in *fig 2.3.6* and labelled '2', this occurs when approximately 1 volt is applied to the diodes. This region is thought to be due to the oxidation of the aluminium contact; therefore, carrier traps are present at a particular level of energy. These traps fill with carriers as voltage is applied to the diode and thus prevent all of the carriers contributing to the current. Once the traps are filled, all of the carriers are once again able to contribute to the current flow. It is assumed that the oxide on the aluminium is thin enough for the carriers to tunnel through, if the diodes were exposed to air for too long it is possible that the oxide would become too thick to allow carriers to pass.

Region 3 on *fig 2.3.6* is the second region of exponential rise and behaves in the same way as region 1. The current continues to rise exponentially until the characteristics saturate.

With saturation, the resistance of the neutral region prevents all of the applied potential falling across the depletion region, therefore, voltage falls across the neutral region, thus, the output current does not increase as rapidly for an increase in the applied potential. This is shown in *fig 2.3.6* as region 4.

The reverse characteristics, as shown on region 5 on *fig 2.3.6*, are expected to be proportional to the fourth root of the applied voltage according to *eqn 2.2.28*. This means that on the semi logarithmic scale,

there is a gradual increase in the reverse current with applied reverse voltage.

When the diode is in reverse bias, the energy levels and the Fermi level fall in energy, making it more difficult for carriers to overcome the barrier. This is due to the whole distribution of carriers lowering, therefore, there will be exponentially fewer carriers available due to the exponential distribution of carriers as shown in *fig 2.3.7.* A schematic representation of a reverse biased Schottky diode is given in *fig 2.3.9.* During reverse bias, the depletion region expands and provides further resistance for the carriers to overcome if they are to pass over the Schottky barrier. However, carriers are actually able to tunnel through the barrier if it is sufficiently thin and can then contribute to the current seen on the output.

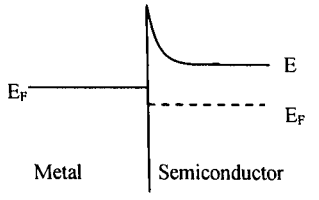

Fig 2.3.9. Reverse biased Schottky diode.

The addition of dopant to the polymer is expected to increase the output current of the forward characteristics as with increased dopant more carriers are available to contribute to the current flow. The reasons for this are that the addition of dopant decreases the resistance of the neutral region and also decreases the barrier at the ohmic contact. The characteristics indicate that they follow the order of doping, i.e. with more dopant a higher current is obtained and vice versa. It is important to note however, that it has been assumed that the dopant remains uniform throughout the devices during the measurements, this may not be the case as the dopant may actually move during the measurements, this could

cause instability in the output characteristics and should be considered in future work.

Also, it has been established that if the voltage is swept from negative to positive and back to negative, it is possible to see hysteresis within the output characteristics, this could be due to the movement of the dopant however would require further consideration.

Shown in *fig 2.3.10* is the output current against the fourth root of the reverse voltage on a semi-logarithmic plot. As can be observed, the characteristics approximate to a straight line which means that the current is approximately proportional to the fourth root of the reverse voltage and this indicates a good agreement with the theory and expected results when image charge lowering is taken into consideration.

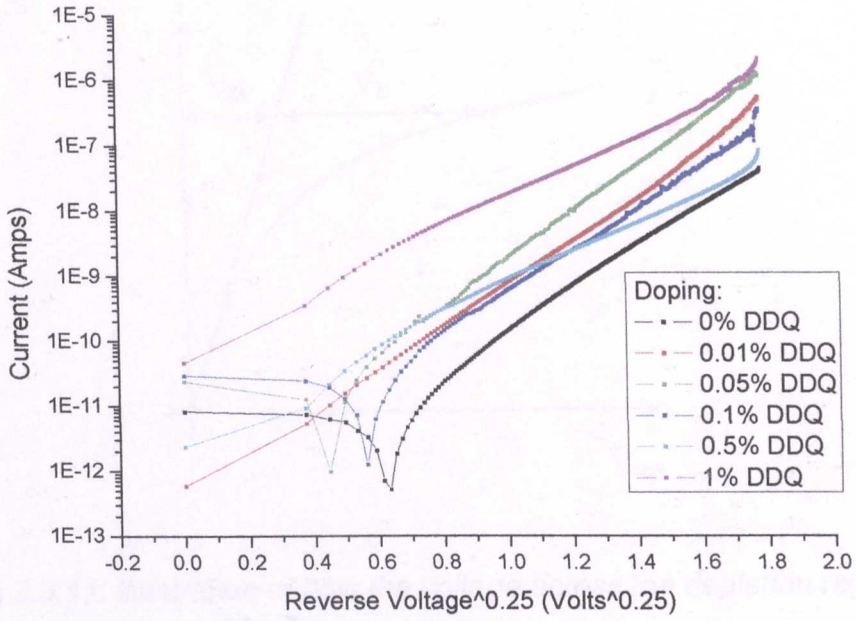

Fig 2.3.10. Semi-logarithmic plot of output current against the fourth root of the reverse voltage for a reversed biased gold-PTAA-aluminium Schottky diode.

From the reverse characteristics it is possible to calculate the doping density of the material, this ranges from $1x10^{18}$ cm^{-3} to $7x10^{18}$ cm^{-3}.

The universal mobility law states how the mobility of the carriers is related to the doping density of the material. This is shown previously in *eqn 2.2.57.*

It is possible to determine the value of the constant, K, from the characteristics of the Schottky diodes. *Fig 2.3.11* shows how the voltage across the depletion region, V_D, and the voltage across the neutral region V_N, can be obtained from the diode characteristics.

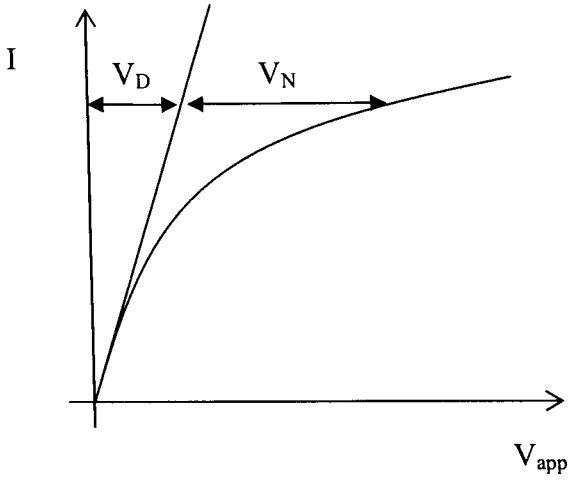

Fig 2.3.11. Illustration of how the voltage across the depletion region, V_D, and the voltage across the neutral region, V_N, can be obtained from the current-voltage characteristics of a Schottky diode on a semi logarithmic plot.

From the obtained value for the voltage across the neutral region, it is possible to calculate the resistance of the neutral region as

$$R_N = \frac{V_N}{I} \qquad 2.3.1$$

From the characteristics obtained, shown in *Fig 2.3.5* using the diode doped at 1% DDQ, the value obtained for R_N was found to be 11075 Ω.

The resistance is related to the resistivity as shown in *eqn 2.3.2*

$$R_N = \frac{\rho L}{A} \qquad 2.3.2$$

Where ρ is the resistivity, L is the width of the neutral region and A is the area of the Schottky diode. The conductivity of the material is the inverse of the resistivity of the material. The conductivity is equal to the product of the

carrier concentration, electronic charge and the effective mobility of the carriers. This is illustrated in *eqn 2.3.3*

$$\rho = \frac{1}{\sigma} = \frac{1}{nq\mu} \qquad 2.3.3$$

It is therefore possible to calculate the effective mobility of the carrier from this equation. The mobility was found to be equal to 6.78×10^{-8} $m^2 s^{-1} V^{-1}$.

It was then necessary to calculate the value of the characteristic temperature obtained from the saturation region of the diode characteristics. It was necessary to use the saturation region as this is the region of the characteristics that corresponds to the neutral region of the diode. This was achieved by collecting data from a number of diodes and plotting a graph to show conductivity against doping density on a log-log scale. A line of best fit was established for the results and the gradient of this line obtained. This was equal to T_C/T. It was then easy to obtain the value of T_C if it were assumed that the value of T was 300K. Following this method, the value of T_C was found to equal 483K. The graph used to determine the value of T_C is given in *fig 2.3.12*

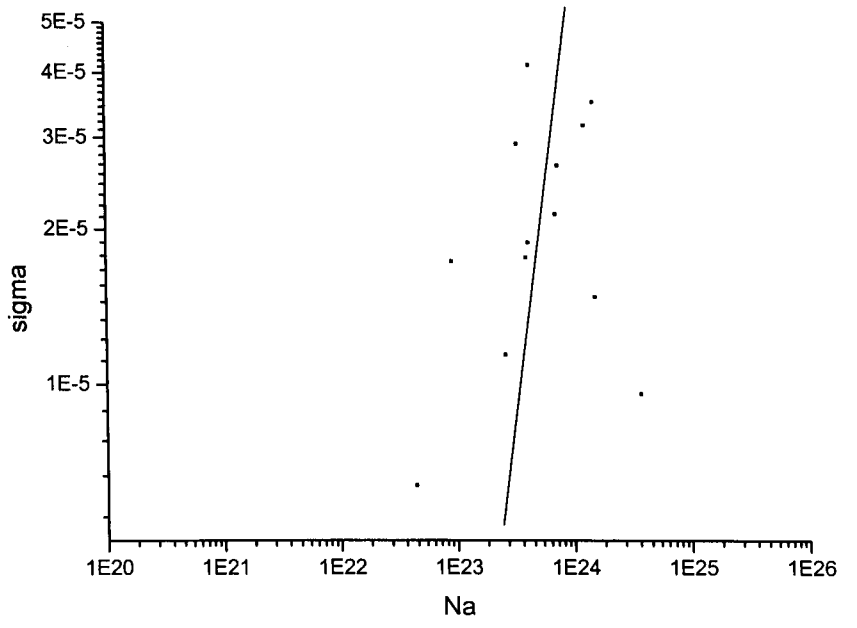

Fig 2.3.12 graph showing the doping density of PTAA plotted against the conductivity.

The value of m can then be obtained from

$$m = \frac{T_C}{T} - 1 \qquad 2.3.4$$

and was found to equal 1.6.

As a comparison to this, the value of T_C was also obtained for the exponential region. To obtain T_0, the following equation was used together with data from the exponential region of the Schottky diode characteristics.

$$\log_{10}\left(\frac{I_1}{I_2}\right) = 0.43\frac{q}{kT_0}(V_1 - V_2) \qquad 2.3.5$$

Once this value of T_0 was calculated, it was possible to calculate the value of T_C from

$$\frac{1}{T_0} = \frac{1}{T} - \frac{1}{T_C} \qquad 2.3.6$$

Having calculated the mobility and the carrier density, the value of m was found using *eqn 2.3.4*. The value calculated for m was 0.35. K was found to be 5.92×10^{-16} $m^5S^{-1}V^{-1}$.

2.3.2 Aluminium Schottky Diodes with Platinum/Palladium Ohmic Contact

Within this section of the thesis is the use of platinum/palladium as an ohmic contact to PTAA is investigated. The diodes were fabricated by casting doped PTAA over the surface of the platinum/palladium contact and then evaporating aluminium onto the polymer as the top contact. Once fabricated, the diodes were characterised by applying a voltage range of -10 volts to +10 volts to the platinum/palladium contact and recording the output current. The obtained results are detailed in *fig 2.3.13*.

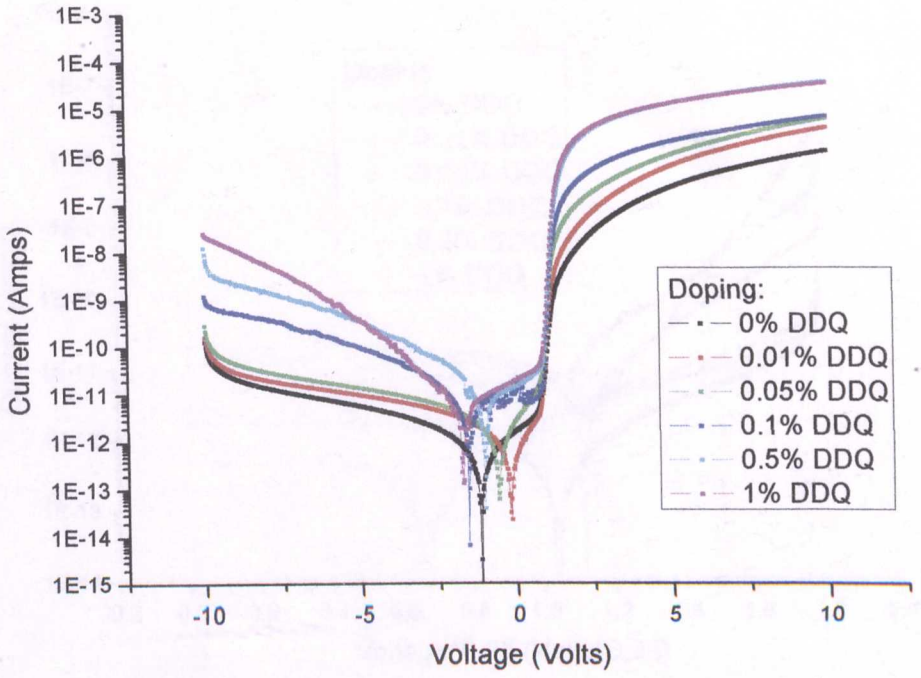

Fig 2.3.13. Current-Voltage characteristics for Platinum/Palladium – PTAA – Aluminium Schottky diodes.

The output characteristics indicate that the rectification of these diodes is approximately three orders of magnitude.

Fig 2.3.14 details the reverse current plotted on a logarithmic scale against the fourth root of the voltage, as can be seen, the characteristics can be approximated by a linear relationship, this shows that there is a close agreement with the theory.

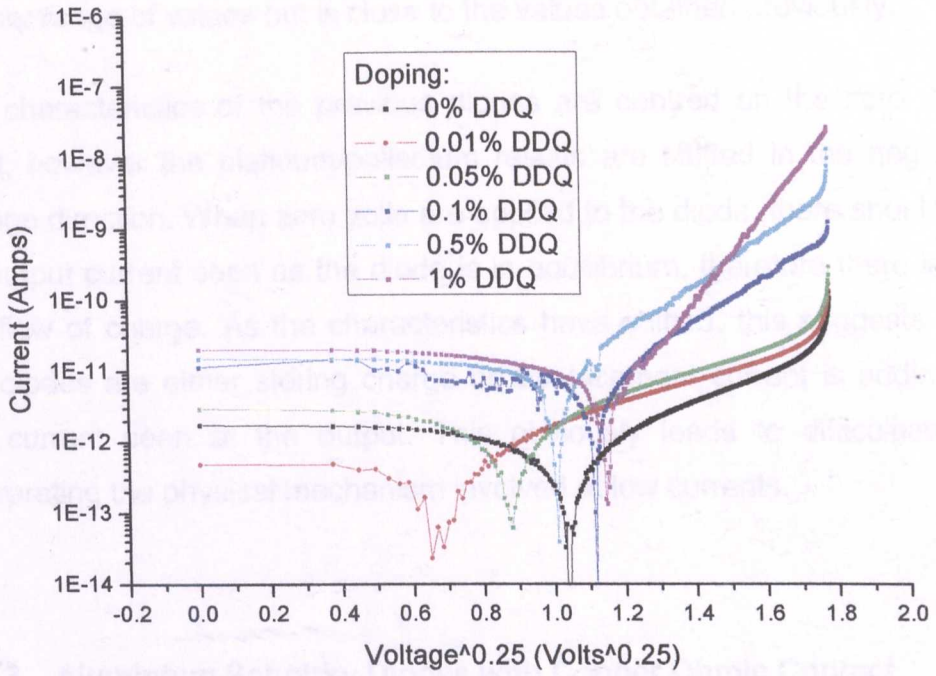

Fig 2.3.14. Semi-logarithmic plot of output current against the fourth root of the voltage for reversed biased platinum/palladium-PTAA-aluminium Schottky diodes.

Parameters were calculated for the diodes discussed within this section of the thesis. Firstly the doping density of the material was found to range from $2x10^{16}$ cm^{-3} to $6.9x10^{18}$ cm^{-3}. The carrier mobility was also calculated and found to be between $5.1x10^{-8}$ cm^2 s^{-1} $V^{-1}$and $3.5x10^{-6}$ cm^2 s^{-1} V^{-1}. These low values are expected for such low values of carrier density compared with the peak value in TFT channels. The final parameter to calculate was the ideality factor and this was found to lie between 1.92 and 3.3, this high value of ideality factor indicates that there is an interfacial layer between the Schottky contact and the polymer. In comparison to the gold diodes, the doping density of the diodes appears to be over a larger

range of values, the carrier mobility is lower and the ideality factor is over a smaller range of values but is close to the values obtained previously.

The characteristics of the previous diodes are centred on the zero volts point, however the platinum/palladium results are shifted in the negative voltage direction. When zero volts are applied to the diode, there should be no output current seen as the diode is in equilibrium, therefore there is no net flow of charge. As the characteristics have shifted, this suggests that the diodes are either storing charge or displacement current is adding to the current seen at the output. This obviously leads to difficulties on interpreting the physical mechanism involved at low currents.

2.3.3 Aluminium Schottky Diodes with Copper Ohmic Contact

Detailed within this section is the use of copper as an ohmic contact to PTAA. Copper is a good choice for the interconnect in organic circuits since flex covered with thick copper is readily available commercially and low in cost. Therefore by also using a copper diode, the technology would be simplified. Integration of diodes is made easier if the copper were to be used for the ohmic contact. To fabricate the diodes, PTAA was cast over the surface of the copper contact and aluminium was then evaporated onto the polymer as the top contact. To characterise the diodes, a voltage range of -10 volts to +10 volts was applied to them and the output current obtained was recorded. The obtained results are detailed in *fig 2.3.15.*

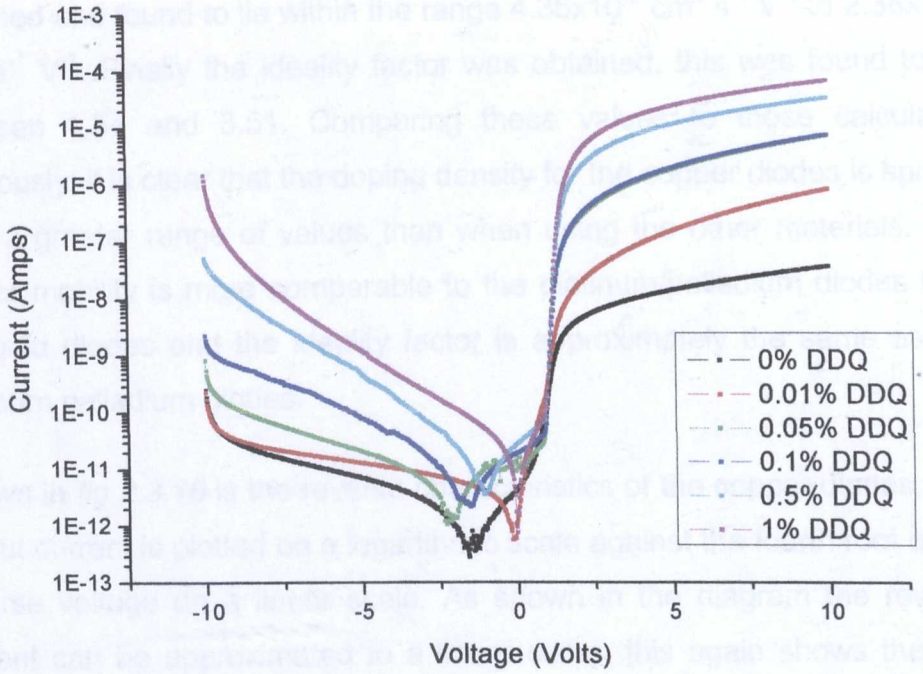

fig 2.3.15 Current-Voltage characteristics for Copper – PTAA – Aluminium Schottky diodes.

As can be seen from the characteristics, the rectification ratio of the diodes is again approximately 10^3. Also with increased doping of the material, a higher forward and reverse current is obtained. The copper diodes show the characteristic plateau region from the use of Aluminium as the Schottky contact.

In comparison to the previously discussed Platinum/Palladium diodes, the output characteristics of the copper diodes are quite similar. For example, the copper diodes also shift from the zero volts point suggesting that at zero voltage applied, some current actually flows, this means that these diodes must again be storing charge within them.

Parameters were obtained from the copper diodes and are detailed below. Firstly the doping density was calculated, this was found to range from

6.31×10^{15} cm^{-3} to 3.71×10^{18} cm^{-3}. The mobility of the carriers was then obtained and found to lie within the range 4.36×10^{-9} cm^2 s^{-1} V^{-1} to 2.38×10^{-6} cm^2 s^{-1} V^{-1}. Finally the ideality factor was obtained, this was found to be between 1.54 and 3.51. Comparing these values to those calculated previously, it is clear that the doping density for the copper diodes is spread over a greater range of values than when using the other materials. The carrier mobility is more comparable to the platinum/palladium diodes than the gold diodes and the ideality factor is approximately the same as the platinum palladium diodes.

Shown in *fig 2.3.16* is the reverse characteristics of the copper diodes. The output current is plotted on a logarithmic scale against the fourth root of the reverse voltage on a linear scale. As shown in the diagram the reverse current can be approximated to a linear curve, this again shows that the results are approximately consistent with theory.

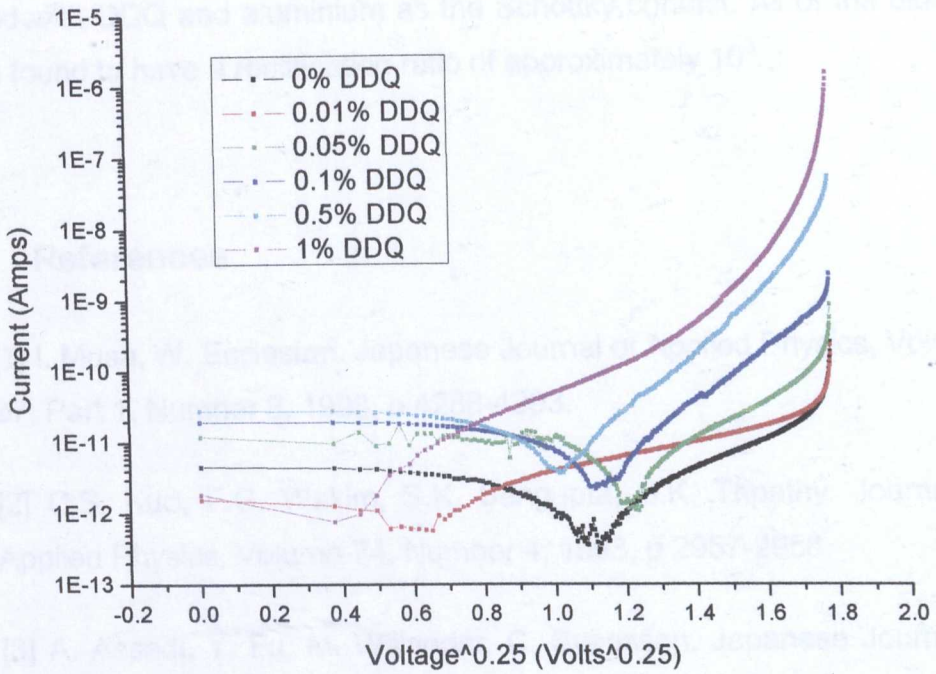

fig 2.3.16 Semi logarithmic plot of output current against the fourth root of the voltage for reversed biased copper-PTAA-aluminium Schottky diodes.

2.4 Summary

Various analyses were discussed within this section of the thesis. Firstly, equations were derived to represent the carrier concentration within disordered semiconductors. The transport mechanisms within Schottky diodes were then discussed and expressions derived for current flow. Space charge limited current was discussed and expressions derived for various conditions. Finally, an expression was derived for the universal mobility law.

Gold, platinum/palladium and copper diodes were fabricated using PTAA doped with DDQ and aluminium as the Schottky contact. All of the diodes were found to have a rectification ratio of approximately 10^3.

2.5 References

[1] I. Musa, W. Eccleston. Japanese Journal of Applied Physics, Volume 37, Part 1, Number 8, 1998, p 4288-4293.

[2] C.S. Kuo, F.G. Wakim, S.K. Sengupta, S.K. Tripathy. Journal of Applied Physics, Volume 74, Number 4, 1993, p 2957-2958.

[3] A. Assadi, Y. Fu, M. Willander, C. Svensson. Japanese Journal of Applied Physics, Volume 32, 1993, p 1696-1699.

[4] M. A. Abkowitz. Philosophical Magazine B- Physics of Condensed Matter Statistical Mechanics Electronic Optical and Magnetic Properties, Volume 65, Issue 4, 1992, p 817-829.

[5] R. Enderlein, N. J. Horing. Fundamentals of Semiconductor Physics and Devices, World Scientific, 1997, p 557.

[6] K. A. Stroud (with additions by D. J. Booth). Advanced Engineering Mathematics, 4th Edition, Palgrave Macmillan, 2003, p 682.

[7] W. Meyer, H. Neldel. Z. Tech. Phys. Volume 18, 1937, p 588.

[8] N. Ashby, S. Miller. Principles of Modern Physics, Holden-Day, Inc. 1970, p 254.

[9] E. A. Irene. Electronic Materials Science, John Wiley and Sons, 2005, p 232.

[10] D. A. Neaman. Semiconductor Physics and Devices: Basic Principles, 3rd Edition, McGraw Hill, 2003, p 95.

[11] D. A. Neaman. Semiconductor Physics and Devices, 3rd Edition, McGraw Hill, 2003, p 124.

[12] C. H. Chen, I. Shih. Journal of Materials Science: Materials in Electronics, Volume 17, Number 12, 2006, p 1047-1053.

[13] D.M. Taylor, H.L. Gomes. Journal of Physics D: Applied Physics, Volume 28, 1995, p 2554.

[14] S.M. Sze, C.R. Crowell, D. Kahng. Journal of Applied Physics, Volume 35, 1964, p2534-2536.

[15] A. R. Brown, D. M. de Leeuw, E. E. Havinga, A. Pomp. Synthetic Metals, Volume 68, 1994, p 65-70.

[16] M. Fadallah, G. Billiot, W. Eccleston, D. Barclay. Solid-State Electronics, Volume 51, Issue 7, 2007, p1047-1051.

[17] M. C. J. M. Vissenberg and M. Matters. Physical Review B, Volume 57, Number 20, 1998, p 12964-12967.

[18] A. Rose. Physical Review, Volume 97, Number 6, 1955, p1538-1544.

[19] M. A. Lampert, P. Mark. Physical Review, Volume 103, Number 6, 1956, p 1648-1655.

[20] M. A. Lampert, P. Mark. Current injection in solids, Academic Press, New York, 1970.

[21] N. F. Mott, R. W. Gurney. Electronic Processes in Ionic Crystals, Clarendon Press, Oxford, 1940.

[22] K. H. Hsieh, K. S. Ho, Y.Z. Wang, S. D. Ko, S. C. Fu. Synthetic Metals, Volume 123, Issue 2, 2001, p217 – 224.

[23] G.G. Mohamed, F.A. Nour El-Dien, E. U. Farag. Spectrochimica Acta Part A: Molecular and Bio molecular Spectroscopy, Volume 65, Issue 1, 2006, p 11-19.

[24] R. Noguchi, A. Haro, A. Sugie, K. Nimoya. Inorganic Chemistry Communications, Volume 9, Issue 1, 2006, p 60-63.

[25] T. Campbell, R. K. Kalia, A. Nakano, P. Vashishta, S. Ogata, S. Rogers. Physical Review Letters, Volume 82, Issue 24, 1998, p 4866-4869.

Chapter 3

The Effect of Temperature on Schottky Diodes

This chapter presents an investigation into the effect of temperature on the performance of Schottky diodes. This was investigated by fabricating polymer Schottky diodes and obtaining their current-voltage characteristics over a range of temperatures. Discussed within this chapter is the effect of temperature on the current-voltage characteristics and the calculated parameters of the diode, together with the causes for the observed effects.

3.1 Introduction

It is necessary to investigate into the effect of temperature on the operation of organic Schottky diodes, since for insulating materials on insulating substrates there is the possibility of internal temperature changes. Also, if the diodes were required to be operated at temperatures well above or below room temperature, changes to the circuit design may be required. To allow circuits to account for such temperature changes, it is required that the effect of temperature is modelled both theoretically and experimentally. Ideally individual equations are developed which operate across a wide range of temperature.

Discussed within this chapter is the theoretical temperature dependence of Schottky diodes together with experimental observation of the effects on the current-voltage characteristics of PTAA Schottky diodes when operated at low temperatures.

3.2 Theoretical Temperature Dependence

3.2.1 Occupancy of Energy Levels with Temperature

To understand the temperature dependence of Schottky diodes it is necessary to consider the application of the Fermi-Dirac statistics to an exponential distribution of states. The Fermi-Dirac statistics show how the occupancy of the energy levels changes with energy and therefore with temperature. This is shown in *fig 3.2.1* [1].

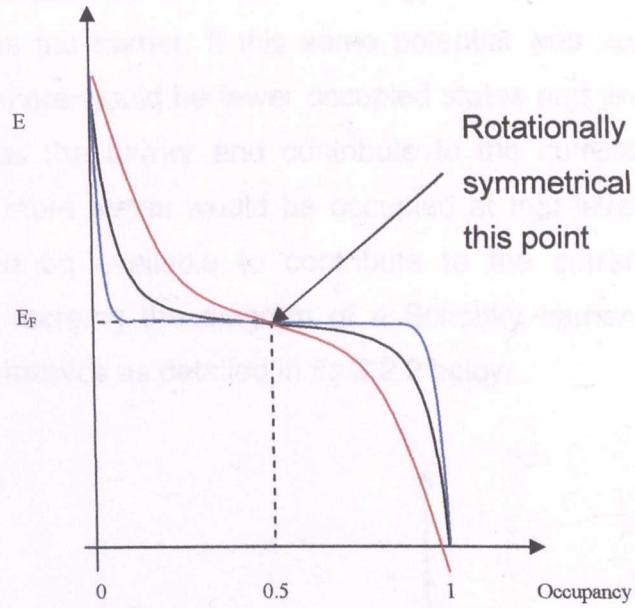

Fig 3.2.1 The Fermi-Dirac statistics under different temperatures. Black represents the Fermi-Dirac distribution at a reference temperature, blue represents below the reference temperature and red represents above the reference temperature.

It is important to note that the Fermi-Dirac distribution is symmetrical around the Fermi level energy, E_F. The curve shown in black is the reference temperature, for example room temperature. The red plot is at a temperature greater than the reference temperature and the blue plot at a lower temperature. It is apparent that at lower temperatures, the distribution becomes more compacted around the Fermi level energy and there is less spread in the distribution of occupied energy levels. In comparison, at higher temperatures it is apparent that there is a much greater spread in the occupancy of energy levels.

This temperature dependence will affect the currents obtained from devices, for example Schottky diodes. For example, in forward bias, the

application of a potential will raise the energy levels for the transportation of carriers across the barrier. If this same potential was applied at a lower temperature, there would be fewer occupied states and fewer carriers able to pass across the barrier and contribute to the current. With a higher temperature, more states would be occupied at that level and thus more carriers would be available to contribute to the current. This can be illustrated by merging the diagram of a Schottky barrier and that of the Fermi-Dirac statistics as detailed in *fig 3.2.2* below.

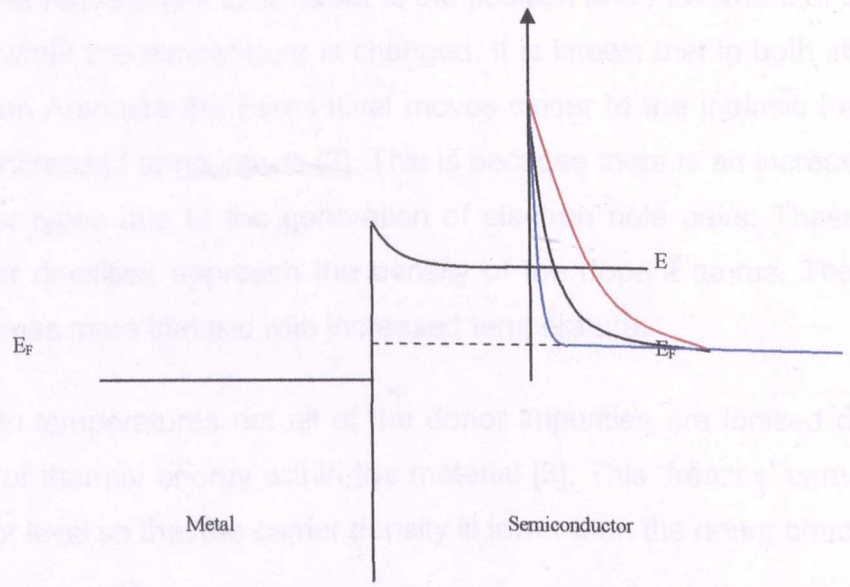

Fig 3.2.2 details the Fermi Dirac distribution within a Schottky barrier.

Fig 3.2.2 shows the Fermi-Dirac distribution from the Fermi level combined with the energy level diagram of a Schottky diode. As can be seen, there is an energy level, E, for the transportation of carriers across the barrier. The occupancy of the states at the energy level E can be observed from the Fermi-Dirac statistics. This theory predicts that the variation in output current with temperature would be exponential due to the exponential

nature of the Maxwell Boltzmann approximation to Fermi Dirac statistics and hence the occupancy of the energy levels.

However, this is based on the Fermi level position remaining constant with temperature, this therefore needs to be considered.

3.2.2 Fermi-Level Position with Temperature

Another requirement to consider is the position and movement of the Fermi level when the temperature is changed. It is known that in both silicon and Gallium Arsenide the Fermi level moves closer to the intrinsic Fermi level with increased temperature [2]. This is because there is an increase in both carrier types due to the generation of electron hole pairs. These intrinsic carrier densities approach the density of the dopant atoms. The material becomes more intrinsic with increased temperature.

At low temperatures not all of the donor impurities are ionised due to the lack of thermal energy within the material [3]. This 'freezes' carriers at the donor level so that the carrier density is lower than the donor concentration.

There is a relatively wide region where the carrier density is equal to that of the dopant atoms and it is known as the extrinsic region. This plateau is shown schematically in *fig 3.2.3.*

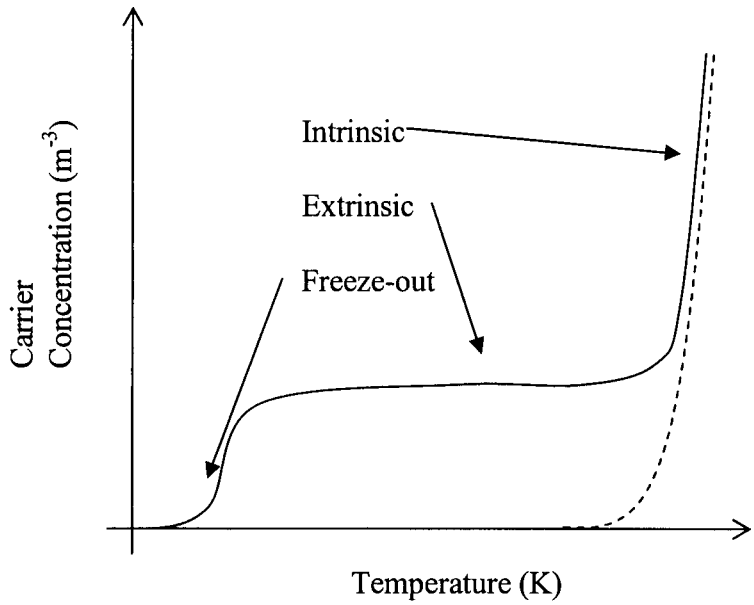

Fig 3.2.3 Details the carrier concentration as a function of temperature.

Within intrinsic ordered semiconductors, there is an energy gap between the electron and hole conducting states. If the material is cooled, the energy gap between electron and hole conducting states increases, the difference between the Fermi level and intrinsic Fermi level also increases and the height of the barrier from the semiconductor to the metal is increased.

The important question is how this behaviour changes when the material is disordered. If it assumed that disordered material behaves in a similar way to that described for ordered material, then a similar effect as above should be seen when disordered material is cooled.

It is also important to note that the position of the Fermi level within the semiconductor can be altered with the addition of dopant to the material [4]. Also, there is residual doping present which occurs due to the fabrication process. This may therefore also require consideration.

In contrast, it is assumed that the Fermi level within the metal is independent of the temperature of measurement. This is due to the high density of states within the metal which pins the Fermi level.

3.2.3 Temperature Dependence of θ in Disordered Material

An equation for space charge limited current which takes into account the effect of free and trapped charge is discussed in Chapter 2: *eqn 2.2.47.* It has a quantity θ which is the ratio of free to total charge and there is a temperature dependence of this quantity. This temperature dependence is due to the temperature dependence of E_F and to the widening of the Fermi Dirac curve already discussed. Both contribute to the value of θ which, in terms of carrier densities is given by [5]

$$\theta = \frac{n_f}{n_f + n_t} \qquad 3.2.1$$

The use of the terms 'free-charge' and 'trapped-charge' are unexpected when there is an exponential distribution of traps as apposed to the classical conduction and valence bands. There are also dopant related states to consider which have a separate Gaussian distribution. Conduction through these states is difficult and carriers have difficulty jumping out of these states. Under equilibrium conditions they are filled with carriers and the Fermi level is likely to sit between them and the intrinsic states due to the disorder in the film where the motion of charge is easier. It is these states that contain the free charge as well as some deeper trapped charge.

It is important to note that this varies between materials. For example the dopant levels dominate the SCLC region with a Schottky Diode made with poly thiophene and so the calculated Meyer Neldel Temperature is 450K: this is the normal value. This is characteristic of intrinsic states rather than those associated with dopant (extrinsic states) and as expected it is found at higher currents where sufficient energy is needed to lift the energy of these deep lying states to an energy where they have a much higher chance of crossing the barrier from semiconductor to metal. This however occurs at lower applied voltage, and energy, in PTAA diodes, and it is the exponential region that shows the characteristic doubling in the Meyer Neldel energy. Poly (3-Hexylthiophene) is another organic polymer, its structure is shown in *Fig 3.2.4* [6]

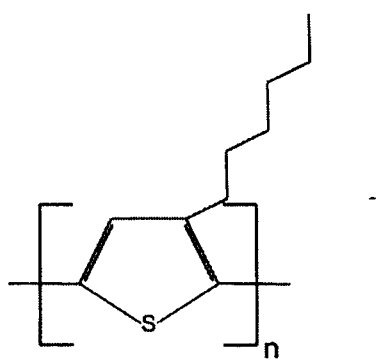

Fig 3.2.4 Chemical structure of P3HT

With P3HT the Fermi level is above the dopant states whereas with PTAA the Fermi level is probably at the cross-over between the two Gaussian distribution curves. At this level carriers have the chance of contributing to the barrier current. Below this level, therefore, the indications are that the extrinsic traps are full and variable range hopping is very difficult

To obtain an expression for the free carriers it is first necessary to consider the occupancy of the energy levels, which must obey Fermi Dirac statistics.

It is assumed that the number of free carriers is equal to the dopant density within the material. It is also assumed that the free carriers are all those which are above the Fermi level and extend to infinity, this is a simplified case and is detailed in *fig 3.2.5.*

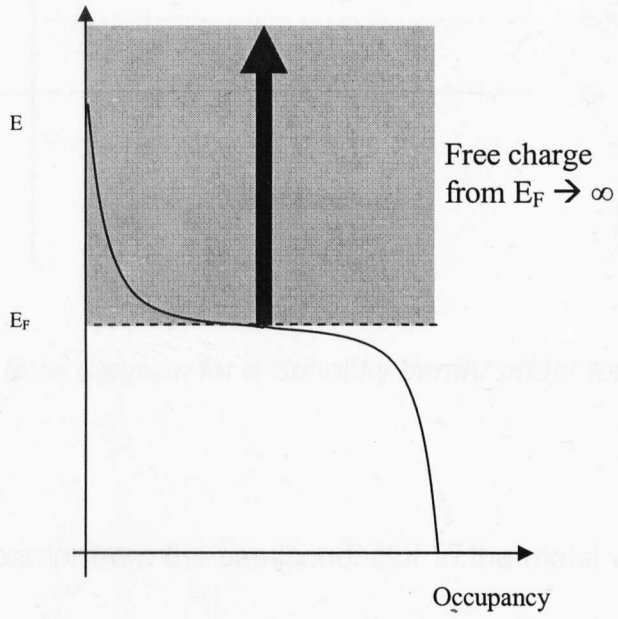

Fig 3.2.5 details the free charge within the Fermi Dirac distribution.

To derive an expression for the density of free carriers, it is necessary to integrate with respect to energy, dE, between the Fermi level and infinity. Below this level the carriers are assumed to be immobile. This is a poor approximation to a Gaussian distribution, as a Gaussian distribution does not extend to infinity. However, it can be justified as the higher states contain very few carriers and are therefore negligible.

With the application of a potential to the Schottky barrier to supply the forward current, the Fermi level and energy levels for carrier transport are raised, this is detailed within *fig 3.2.6.*

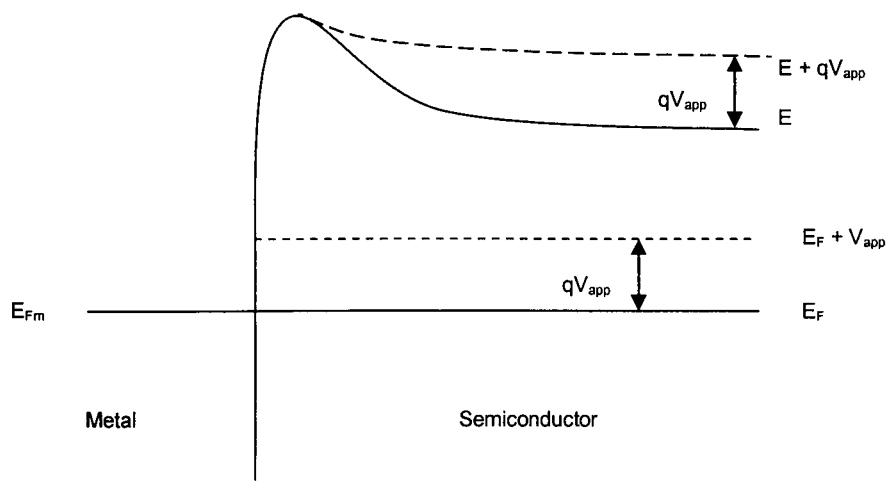

Fig 3.2.6. Energy level diagram for a Schottky barrier under forward bias.

It is clear that the barrier from the semiconductor to the metal will have the form:

$$E_B = E_{Fm} - E_F + qV_{app} \qquad 3.2.2$$

where E_{Fm} is the Fermi level within the metal, E_F is the Fermi level within the semiconductor and V_{app} is the applied potential which is negative for an n type semiconductor. Here, E_{Fm} is independent of temperature, whereas, E_F is temperature dependent.

The free carrier density can then be derived from the integral of the product of the carrier density with energy and occupancy of the states

$$n_f = kT_0 N'(0) \exp\left(\frac{-qV_{app}}{kT_0}\right) \exp\left(\frac{-E_F}{kT_C}\right) \qquad 3.2.3$$

The current density, J, will be proportional to this carrier density.

It is clear from this equation that there is a temperature dependence which will be dependent on the value of T_0 and also E_F.

The trapped charge can again be obtained from the product of the occupancy of the energy levels and the density of carriers with energy below E_F. With the trapped charge it is assumed that all states below the Fermi level are trapped and therefore the occupancy is equal to 1. This then means that the trapped carrier density can be obtained from the integral of the carrier density with energy alone as the occupancy is equal to 1. One effect of the exponential distribution of states is that there are many fewer states below E_F compared with above it. This means that there are very few electrons and still fewer states for the carriers to jump into, compared with the states above E_F. As an approximation, all of the states below the Fermi can be assumed to be full of carriers. This model is shown in *fig 3.2.7.*

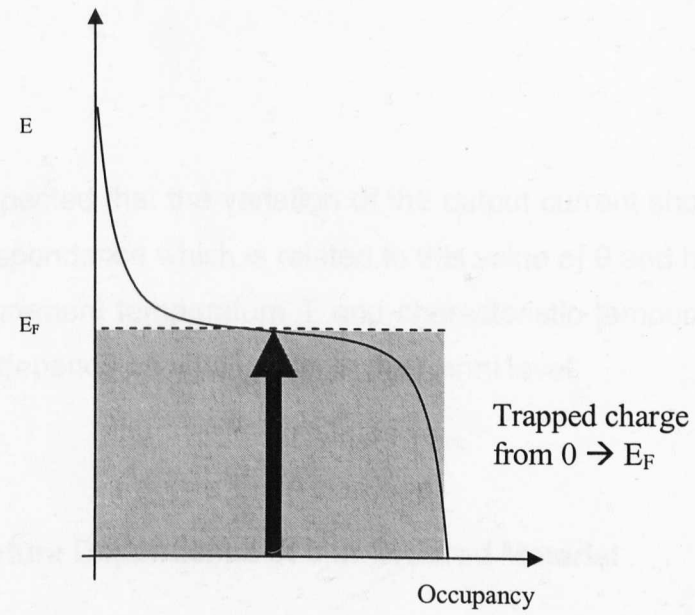

Fig 3.2.7 Details the trapped charge within the Fermi Dirac distribution.

This integral, between E=0 and E_F gives

$$n_t = kT_C N'(0)\exp\left(\frac{qV_{app}}{kT_0}\right)\exp\left(\frac{E_F}{kT_C}\right) \qquad 3.2.4$$

This expression shows that the trapped carrier concentration is dependent on the value of T_C and also the exponential term.

It is now possible to obtain an expression for θ in terms of T_0 and T_C, by substituting into *eqn 3.2.1*. This is detailed below

$$\theta = \frac{T_0}{T_0 + T_C} \qquad 3.2.5$$

It is possible to simplify this expression with the use of the equation

$$\frac{1}{T_0} = \frac{1}{T} - \frac{1}{T_C} \qquad 3.2.6$$

This simplifies to

$$\theta = \frac{T}{T_C} \qquad 3.2.7$$

It is therefore expected that the variation of the output current should have a temperature dependence which is related to this value of θ and hence the values of measurement temperature T and characteristic temperature T_C. However, much depends on small shifts in the Fermi level.

3.2.4 Temperature Dependence of θ in Ordered Material

It is also helpful to compare the result with the temperature dependence of ordered semiconductors which have a transport level, E_T, and conduction band, E_C, as illustrated in *fig 3.2.8*

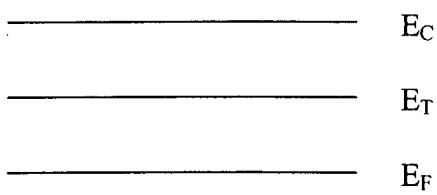

Fig 3.2.8 Schematic representation of a material with transport and conduction bands

For a crystalline semiconductor the equations for free and trapped charge are

$$n_f \propto \exp\left(-\frac{E_C - E_F}{kT}\right) \qquad 3.2.8$$

Where n_f is the free charge within a crystalline semiconductor, E_C is the conduction energy level, E_F is the Fermi level, k is Boltzmann's constant and T is the temperature.

$$n_t \propto \exp\left(-\frac{E_T - E_F}{kT}\right) \qquad 3.2.9$$

Where n_t is the trapped charge within a crystalline semiconductor, and E_T is the transport level.

Thus the ratio of free to trapped charge is

$$\theta = \frac{1}{1 + \exp\left(-\frac{E_T - E_C}{kT}\right)} \qquad 3.2.10$$

If the separation of the conduction band and transport level remains constant then the value of the ratio of free to trapped charge will only be dependent on the variation in temperature. It is possible that the disordered materials studied within this thesis act as ordered material. This could occur when the energy levels are positioned as illustrated in *fig 3.2.9*

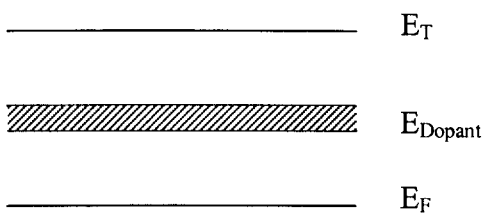

Fig 3.2.9 energy levels present in a disordered material

This situation could occur when the dopant levels enable transport. This would require that each is separated by a significant distance to imitate the energy levels within ordered material. If this is the case then the current dependence with temperature for disordered material will be exponential.

Having studied various possibilities for the effect of temperature on Schottky diodes theoretically, is it necessary to determine the experimental behaviour.

3.3 Experimental Results

3.3.1 Experimental Procedure

To investigate into the effect of temperature on the flow of carriers through organic Schottky diodes, a series of diodes were fabricated on a flexible substrate. A flexible substrate was chosen to allow the diode to fall in temperature more quickly than glass when placed within a liquid nitrogen cryostat. The diode was fabricated with crossover contacts of width 2mm. this therefore means that the area of the diode is a 2mm by 2mm square, ie its area is $4x10^{-6}$ m^2.To fabricate the devices, a set of horizontal bars of gold were evaporated onto the substrate material, these were treated with pentaflourobenzenethiol. The gold was then covered with PTAA doped with DDQ. The second contact was evaporated onto the polymer perpendicular to the first contacts, Aluminium was used for this. The intersection of the two sets of bars corresponded to a number of Schottky diodes. The structure of the Schottky diodes fabricated is shown in *fig 3.3.1*.

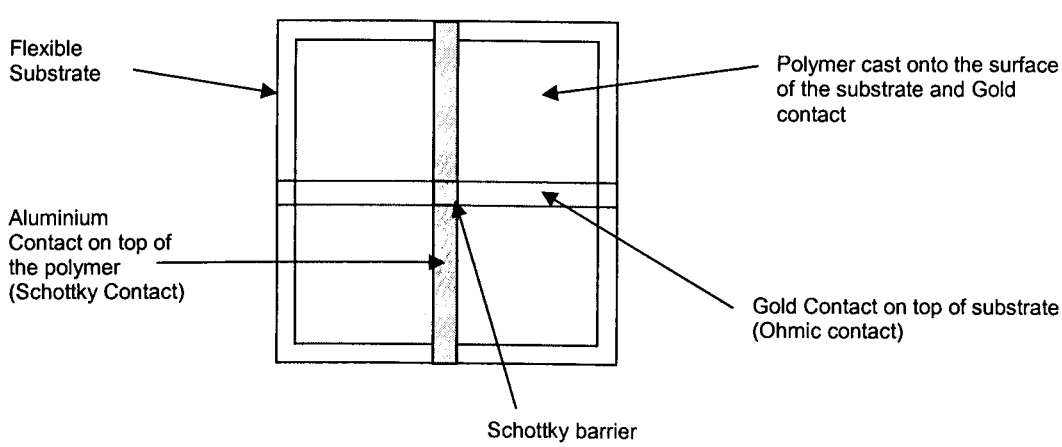

Fig 3.3.1 Schematic representation of the structure of the Schottky diodes fabricated.

Current-Voltage characteristics were obtained from the fabricated Schottky diodes, this was achieved by placing the diode into a cryostat which was then evacuated of air. Liquid nitrogen was then circulated through the cryostat, cooling the chamber holding the diode, until a minimum temperature was obtained. The output characteristics were then obtained by removing the supply of liquid nitrogen, thus allowing the diode to gradually increase temperature and applying +10 volts to -10 volts on the aluminium contact and recording the output characteristics obtained. The temperature of measurement was obtained by recording the value of a calibrated resistor at the beginning and end of each measurement and taking the average of this.

3.3.2 Effect of Temperature on Diode Characteristics

The characteristics obtained from the Schottky diodes are detailed within *fig 3.3.2*. The figure shows the output current plotted against the voltage applied to the diode at various temperatures in Kelvin. The Measurement temperatures are detailed on the right hand side of the graph and range from 107K to 295K.

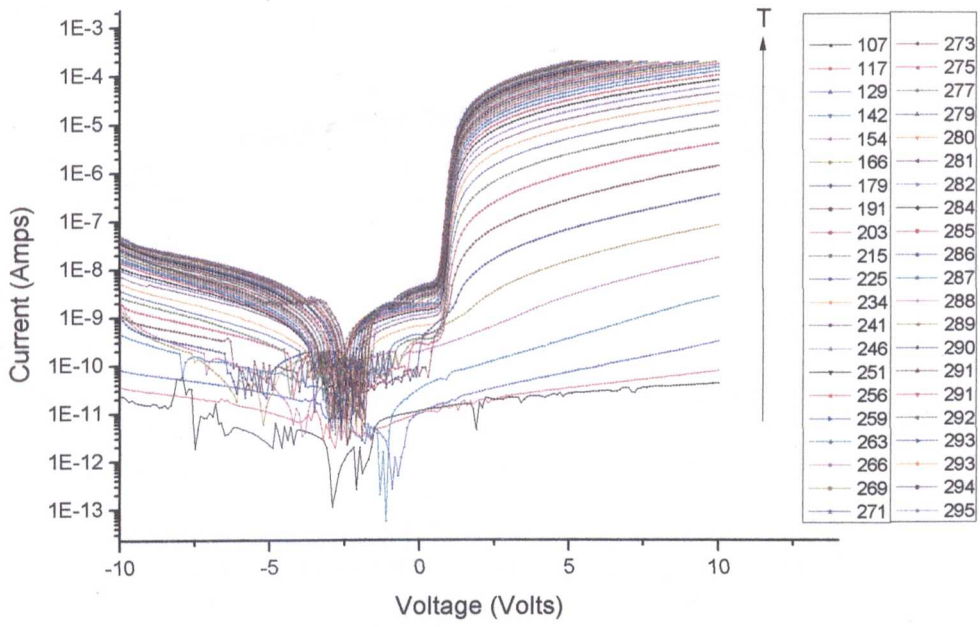

Fig 3.3.2. Output characteristics obtained from a Schottky diode at various temperatures.

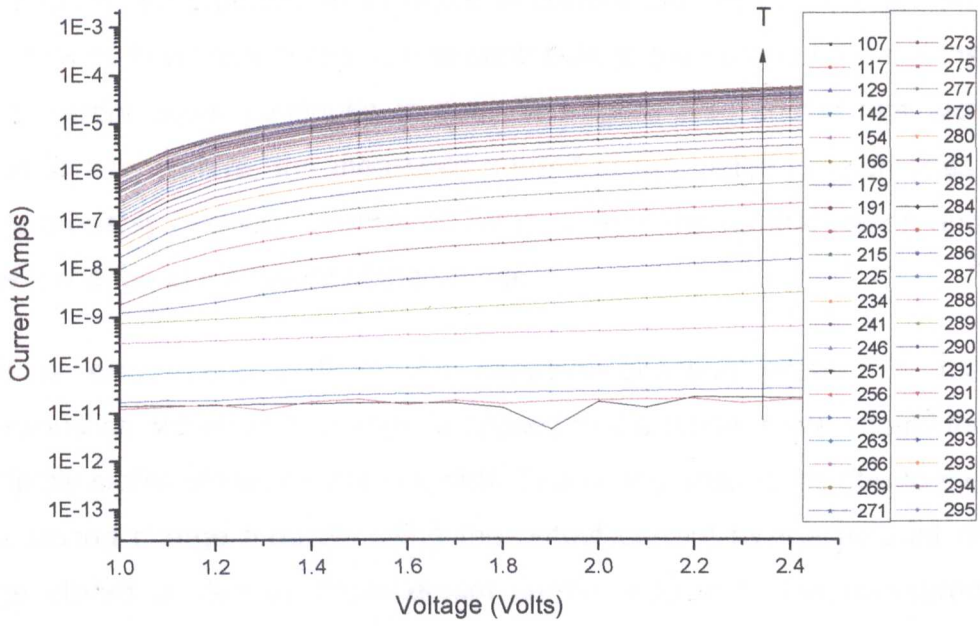

Fig 3.3.3. Output characteristics obtained from a Schottky diode at various temperatures enlarged over 1 Volt to 2.5 Volts.

From *fig 3.3.2* it is apparent that with falling temperature, both the forward and reverse current decreases. This suggests that the decrease in temperature causes fewer carriers to contribute to the current.

When taking current-voltage measurements at very low temperatures, for example 107K and 117K, the output seen is very unstable due to system noise. There is a plateau region present on the forward characteristics, this is assumed to be due to oxidation of the aluminium contact. Aluminium oxidises rapidly in air and is thought to produce carrier traps at a fixed energy level. As can be seen on the forward characteristics, the current initially rises, but when the carriers reach the energy at which the traps are located, the traps are filled and these carriers can thus not contribute to the

current flow, this is when the plateau region is seen. Here, an increase in voltage does not produce an increase in current until all of the traps are filled, then all free carriers are able to contribute to the current flow and the output current again continues to rise. The figure also shows that with increased temperature, the measured current at the plateau region rises. This is probably due to a change of Fermi level in the neutral region and hence a change in the height of the barrier.

There is also lateral shift in the negative direction present in the characteristics. When zero voltage is applied to the diode, there should for a perfectly stable diode, be zero current. This is assumed to be due to the diode storing charge thus offsetting the output current by the amount of charge stored or due to displacement current adding to the measured current. Therefore, when zero voltage is applied, the diode actually has some extra charge present and this is seen on the output characteristics. The characteristics are shifted by 2.5 volts. This affects the results seen, for example, when 10 volts is applied, the stored charge also needs to be taken into consideration, therefore the actual applied voltage could be 10 volts plus or minus the offset voltage. This effect is not consistent with each diode fabricated and could be due to impurities present during the fabrication process.

According to the theory studied previously in section 3.2, the theoretical and experimental results are in agreement as with a change in temperature, a change in output current is seen.

3.3.3 Relationship between Current and Temperature

To determine the effect that temperature has on the operation of Schottky diodes it is necessary to understand the relationship between the measurement temperature and current obtained. *Fig 3.3.4* details the

measurement temperature against the measured current at a particular voltage applied, taken from the previous results in *fig 3.3.2*, on a linear-linear plot. The results were taken at 3.8 volts in the forward current direction. As can be observed, there appears to be an exponential relationship between the temperature of measurement and the output current obtained at a particular applied voltage. After 250 Kelvin there is a dramatic increase in the output current with temperature.

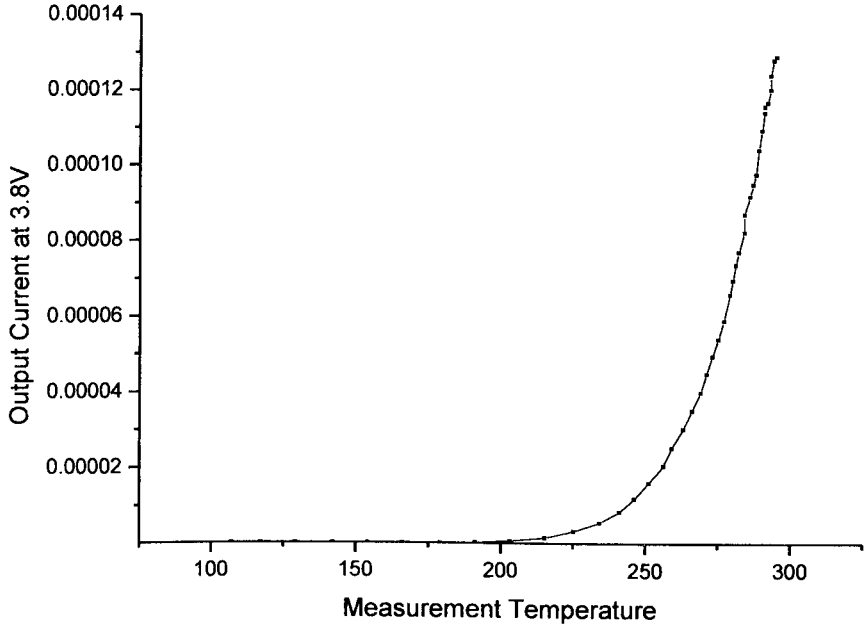

Fig 3.3.4. Measurement temperature plotted against current at 3.8 volts applied to the aluminium contact on a linear axis.

For a Schottky diode the current density is given by *eqn 2.2.29*. This states that the output current has an exponential relationship. As the measurements are taken at a constant voltage and only the temperature is varied, this shows that the current is related to the temperature. To investigate this, the current was plotted on a semi-logarithmic scale, this is shown in *fig 3.3.5*.

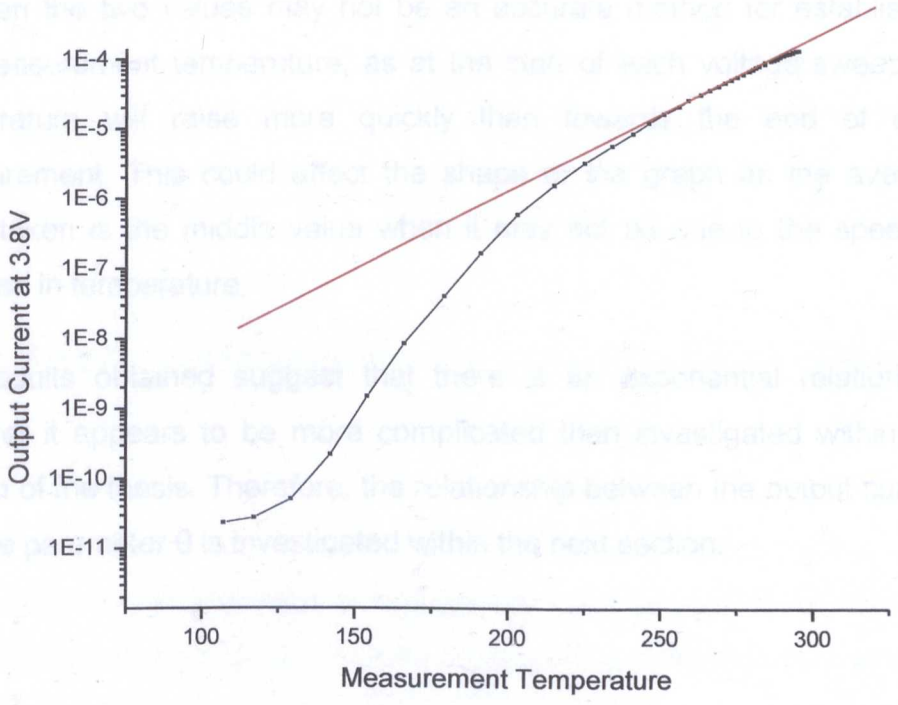

Fig 3.3.5. Measurement temperature plotted against output current at 3.8 volts applied to the aluminium contact on a semilogarithmic axis.

The figure shows that the points plotted at a higher temperature produce a linear graph when the axis is set to exponential. The measurement temperature plotted is the average temperature over the whole period of the measurement. Therefore, the temperature at the start and end of the measurement is noted and an average taken.

At lower temperatures, the difference between the initial and final measurements is greater than at higher temperatures. Therefore, the plotted points at lower temperatures are actually over a large range of temperature compared to those plotted at higher temperatures.

At lower temperatures there is a rapid increase in temperature over the time taken to complete the measurement. The rate of increase in temperature reduces as the temperature rises, therefore taking the average between the two values may not be an accurate method for establishing the measurement temperature, as at the start of each voltage sweep the temperature will raise more quickly than towards the end of each measurement. This could affect the shape of the graph as the average value taken is the middle value when it may not be due to the speed of increase in temperature.

The results obtained suggest that there is an exponential relationship however it appears to be more complicated than investigated within this section of the thesis. Therefore, the relationship between the output current and the parameter θ is investigated within the next section.

3.3.4 Relationship between Current and Theta

This section will investigate the dependence of temperature on the output current of the Schottky diodes to establish whether the derived relationship for theta has been obtained from the experimental results.

Shown in *fig 3.3.6* is the current at a particular voltage plotted against the value of theta.

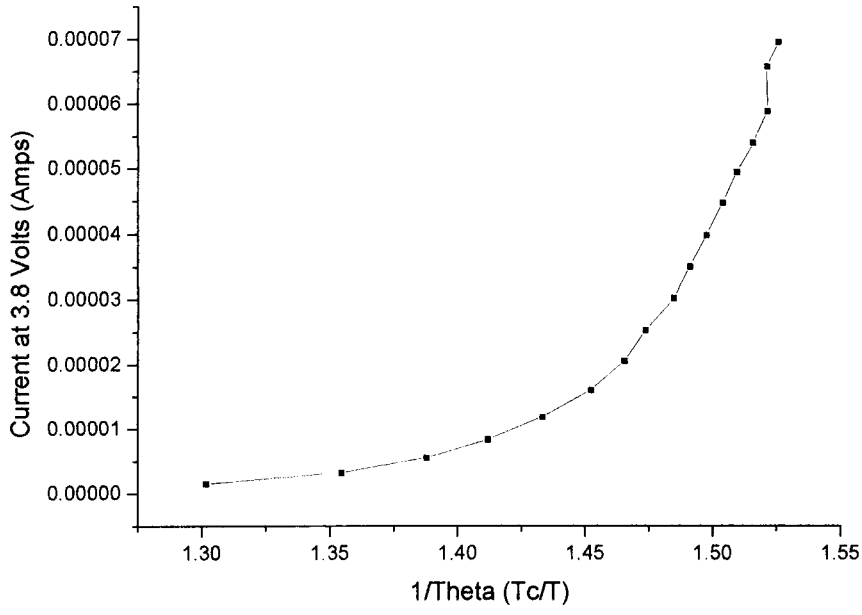

Fig 3.3.6 Details the output current at 3.8 Volts applied versus theta

As can be observed within the figure, the variation in output current again appears to have an exponential relationship to the value of theta. This can be further observed in *fig 3.3.7* when the current is plotted on a logarithmic scale.

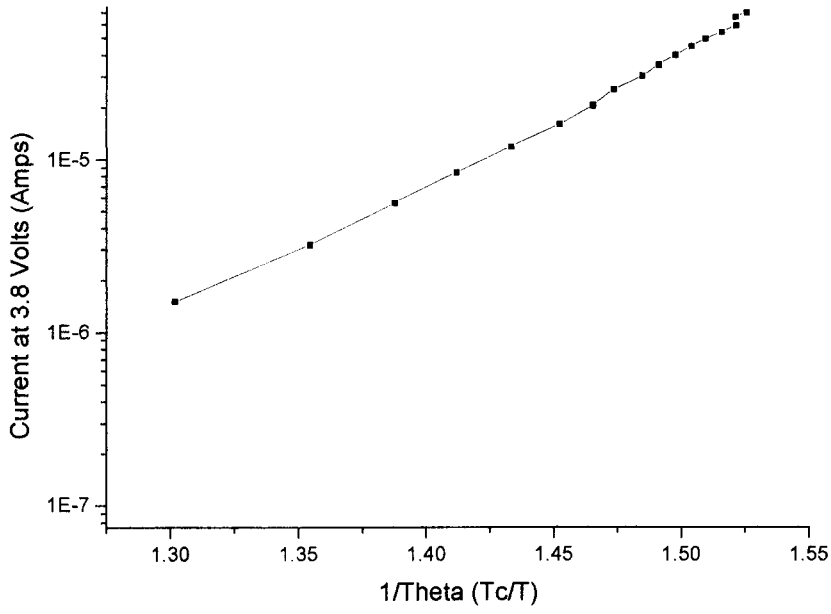

Fig 3.3.7 Details the output current at 3.8 Volts applied versus theta on a semi logarithmic scale

As can be observed within the graph, there is a definite exponential relationship between the output current and theta when plotted on a semi logarithmic scale. This is a much better relationship than obtained previously. The results indicate that the devices produce a relationship between the output current and theta as predicted for disordered material.

3.3.5 Effect of Temperatures on Parameters of the Diodes

The parameters of the diode were obtained for a range of temperatures to establish the effect of temperature on the results obtained. Firstly the mobile carrier density of the polymer was calculated, this was to establish the effect of temperature on the number of carriers able to contribute to the

current flow. Detailed below is a range of parameters calculated for various temperatures over the entire range of temperatures examined.

Temperature	Mobile carrier density m^{-3}	Carrier Mobility $m^2V^{-1}s^{-1}$	Ideality Factor
117 K	1.11×10^{21}	1.36×10^{-13}	-
142 K	1.305×10^{24}	6.625×10^{-16}	-
191 K	1.412×10^{23}	7.402×10^{-13}	5.856
234 K	1.41×10^{23}	5.53×10^{-10}	1.3967
273 K	3.63×10^{23}	1.18×10^{-9}	3.2882
287 K	4.75×10^{23}	1.22×10^{-9}	3.2997
295 K	8.13×10^{23}	1.17×10^{-9}	2.8837

As can be seen the doping density increases with increased temperature. This is the expected result and was discussed theoretically earlier. This is due to the increase in carriers available to contribute to the current at higher temperatures.

The next parameter to calculate is the carrier mobility. Shown in the above table are the calculated carrier mobilities for the same range of temperatures that the doping density was calculated for.

The results indicate that at low temperatures the carrier mobility is reduced and at higher temperatures the mobility is increased. There are orders of magnitude difference in the carrier mobility at low temperatures however at higher temperatures, almost room temperature, the carrier mobility appears to stabilise at around 10^{-9} $m^2V^{-1}s^{-1}$. It is expected that the mobility increases at higher temperatures, this can be explained with reference to the Fermi Dirac statistics as at higher temperatures, more carriers are in the higher

states which are more mobile that the lower states, thus the mobility is dependent on temperature. This confirms the theory discussed previously within section 3.2.1.

The final parameter is the doping density. This is again detailed within the above table. This shows that the ideality factor is smaller at the lowest temperature however remains fairly constant at the higher temperatures at around 3. It was not possible to obtain the characteristics over the same range as previously as the lower temperature measurements showed much instability and results could not be obtained from them. This suggests that the ideality factor is dependent on temperature, however closer to room temperature, the effect is not significant.

The effect of temperature on there parameters needs to be taken into consideration when using PTAA Schottky diodes for circuit design as it has been shown that the parameters alter with temperature. These could effect the operation of the device if it were used outside of its ideal temperature range and could affect the overall results seen from the device as the diode would not function correctly.

3.4 Summary

Theory was studied to understand the effect of temperature on the occupancy of energy levels within Schottky diodes together with the variation in position of the Fermi level with temperature. The ratio of free to total charge was also studied to establish its temperature dependence.

It has been established that the output characteristics of the Schottky diode alter under different temperature conditions. At lower temperatures both the forward and reverse currents decrease compared to applying the same potential at a higher temperature.

It has been shown that the output current is proportional to theta when plotted on a semi logarithmic scale. This was not the expected result for disordered material and it appears that the polymer behaves more like ordered material, as for ordered material it was predicted that there would be an exponential relationship between current and theta.

The parameters show that temperature affects the parameters obtained from the diodes. This is most noticeable in the results for the doping density and the carrier mobility.

It is possible that impurities introduced during the fabrication process contribute to some of the effects seen on the output characteristics. Also air exposure on the devices could have effects on the device, for example the effect seen with the plateau region of the graph. To resolve this would require a sterile environment for fabrication and a method of characterising the diodes without allowing them to come into contact with air and debris. This was not possible with the apparatus available, but if future work on this subject was carried out, eliminating these conditions would prove useful in further analysis of the diodes.

3.5 References

[1] S.M.Sze. Semiconductor Devices Physics and Technology. John Wiley & Sons, 1985, p 17.

[2] S.M.Sze. Semiconductor Devices Physics and Technology. John Wiley & Sons, 1985, p 26.

[3] S.M.Sze. Semiconductor Devices Physics and Technology. John Wiley & Sons, 1985, p 27.

[4] T. H. Nguyen, S. K. O'Leary. Journal of Applied Physics, Volume 88, Issue 6, 2000, p 3479.

[5] S. Nešpůrek, O. Zmeškal, J. Sworakowski. Thin Solid Films, Volume 516, Issue 24, 2008, p8949-8962.

[6] M, W. G. Ponjee, M. A. Reijme, A. W. Denier, Van Der Gon, H. H. Brongersma, B. M. W. Langeveld-Voss. Polymer, Volume 43, Issue 1, 2002, p 77-85.

Chapter 4

Capacitance of Schottky Diodes

Investigated is the effect of doping, frequency and voltage on the capacitance and depletion region width of polymer Schottky diodes. This was investigated by obtaining the capacitance of the diodes as a function of applied voltage and observing the effect of dopant and frequency.

4.1 Introduction

It is important to understand the variation of capacitance within Schottky diodes since it provides greater understanding of the devices. This is due to the capacitance of the diode being directly related to the width of the depletion region. The edges of the depletion region act like the plates of a capacitor. As the depletion region alters in width with applied voltage so does the width of the neutral region and its resistance. This chapter describes the theory of the capacitance of a Schottky diode together with experimental verification. It involves the variation of capacitance with frequency, applied voltage and doping density. This is important for theoretical and practical circuit design. The results obtained from experimental work are compared with theory.

4.2 Theoretical Schottky Diode Capacitance

A schematic representation of the cross-section of a Schottky diode is shown in *Fig 4.2.1.*

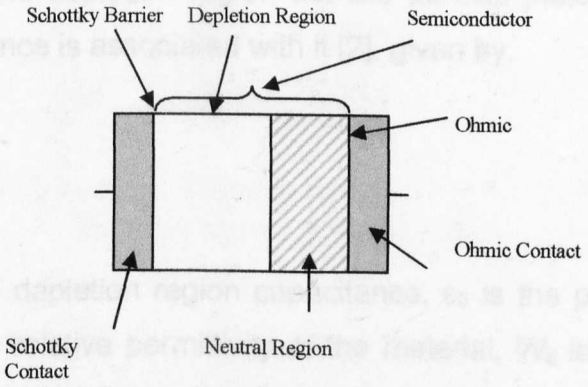

Fig 4.2.1. Schematic representation of a Schottky diode.

As can be seen from *Fig 4.2.1* there is a depletion region and a neutral region present which make up the entire width of the semiconductor region, between the two metal contacts. When a potential is applied to the device, the neutral region and depletion region alter in width. [1] There is a resistance R_n associated with the neutral region,

$$R_n = \frac{W_n}{\sigma A} \qquad 4.2.1$$

where W_n is the width of the neutral region, A is the cross-sectional area of the diode and σ is the electrical conductivity of the material. It is equal to the product of the carrier density, electronic charge and the carrier mobility. It is clear that the resistance of the neutral region is dependent on the voltage as this directly affects the width of the neutral region. This can then be substituted into *eqn 4.2.1* to give,

$$R_n = \frac{W_n}{nq\mu A} \qquad 4.2.2$$

This equation reproduces *Fig 4.2.1* in terms of more fundamental quantities.

The edges of the depletion region act like parallel plates of a capacitor, thus, a capacitance is associated with it [2], given by,

$$C_d = \frac{\varepsilon_0 \varepsilon_p}{W_d} A \qquad 4.2.3$$

where C_d is the depletion region capacitance, ε_0 is the permittivity of free space, ε_p is the relative permittivity of the material, W_d is the width of the depletion region and A is the diode area.

As the depletion region changes in width with the application of an applied voltage across the device, it is necessary to derive an expression for this

width to allow it to be eliminated from the expression given in *eqn 4.2.3* which will also allow the dependence of the capacitance on the applied voltage to be established.

To derive an expression for the width of the depletion region it is necessary to consider Gauss' Law [3]. It is also necessary to assume that the edge of the depletion region is abrupt.

$$\varepsilon_0 \varepsilon_p F_{\max} A = q N_D W_d A \qquad 4.2.4$$

where F_{max} is the maximum field strength within the Schottky diode.

$$\varepsilon_0 \varepsilon_p F_{\max} = q N_D W_d \qquad 4.2.5$$

It is then necessary to consider the variation of field with distance in a uniformly doped depletion region. This is shown in *fig 4.2.2*.

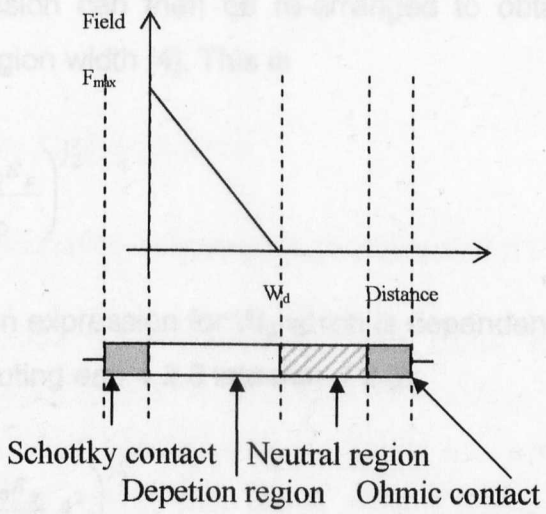

Fig 4.2.2 Variation of field with distance throughout a uniformly doped depletion region.

As can be seen from the figure, the relationship between field and distance is linear, with the maximum field at the Schottky barrier and reducing in size up to the edge of the neutral region. Thereafter the field is zero. The area beneath the triangle is equal to the potential drop across the depletion region, thus,

$$V_C = \frac{F_{max} W_d}{2} \qquad 4.2.6$$

where $V_C = \Phi_B + V_{app}$ and Φ_B is the difference in work functions between the metal and semiconductor, or the barrier height. It is then possible to combine *eqns 4.2.5* and *4.2.6* by eliminating F_{max} from the expressions. This is shown below,

$$\frac{qN_D W_d}{\varepsilon_0 \varepsilon_p} = \frac{2V_C}{W_d} \qquad 4.2.7$$

This expression can then be re-arranged to obtain an equation for the depletion region width [4]. This is

$$W_d = \left(\frac{2V_C \varepsilon_0 \varepsilon_p}{qN_D} \right)^{1/2} \qquad 4.2.8$$

This gives an expression for W_d which is dependent on the applied voltage. After substituting *eqn 4.2.8* into *eqn 4.2.3:*

$$C_d = \left(\frac{qN_D \varepsilon_0 \varepsilon_p}{2V_C} A^2 \right)^{1/2} \qquad 4.2.9$$

This equation details the variation of the capacitance within the depletion region of a Schottky diode and how the capacitance is affected by the applied voltage.

It is also now possible to substitute *eqn 4.2.8* in the *eqn 4.2.2*, to eliminate W_n as W_n is equal to $W_t - W_d$, thus,

$$R_n = \frac{W_t - \left(\frac{2V_C\varepsilon_0\varepsilon_p}{qN_D}\right)^{1/2}}{nq\mu A} \qquad 4.2.10$$

where W_t is the width of the polymer film. This then gives an expression for R_n which is dependent on the applied voltage.

A further expression can be considered which may be of use in describing the relationship between the capacitance of the diode and the frequency of measurement. This is the capacitive reactance [5] and is shown in *eqn 4.2.11*.

$$X_C = \frac{1}{2\pi fC} \qquad 4.2.11$$

4.3 Diode Capacitance

4.3.1 Relationship between Capacitance and Frequency

Schottky diodes were fabricated on a glass substrate with gold and aluminium contacts and PTAA doped with DDQ at percentage by weight. A DC voltage was then applied to the device and the capacitance was measured. The voltage was swept from -5 volts to 1 volt. The measured capacitance ranged from 0 to approximately 3200 Pico Farads.

Fig 4.3.1 shows a typical capacitance-voltage characteristic for a PTAA Schottky diode. This was obtained from a diode doped with 1% DDQ. This illustrates the effect of frequency on diode capacitance.

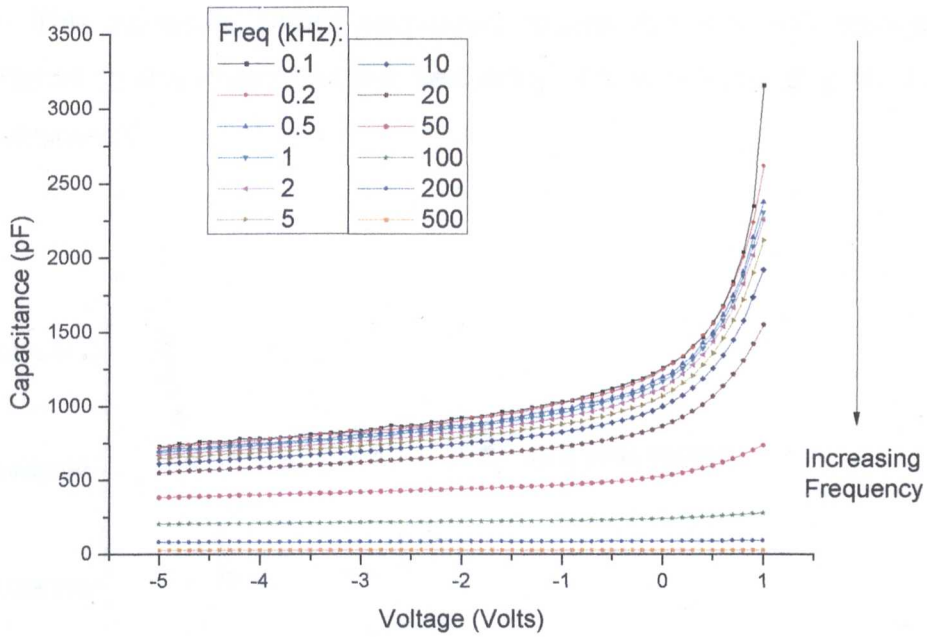

Fig 4.3.1 Capacitance-voltage characteristics for a gold-PTAA-aluminium Schottky diode, doped with DDQ at 1% by weight, taken at various frequencies.

The results from the Schottky diode were obtained at various frequencies from 0.1 kHz to 500 kHz.

As can be seen, the capacitance of the diode decreases with increasing frequency. The capacitance associated with the depletion region is defined in *eqn 4.2.3.* However, this assumes that the supply of carriers to and from the edge of the depletion region via the neutral region, on alternate half-cycles, is sufficient to provide the amount of charge demanded by this equation. The capacitance measurement senses the amount of charge that flows in one half of the cycle as C=Q/V. At higher frequencies insufficient charge is provided, some of the voltage falls across the neutral region and so less falls across the depletion region. Under these circumstances the capacitance is less than that predicted by *eqn 4.2.3.*

It is possible to now consider the capacitive reactance equation, *eqn 4.2.11.* This equation, when rearranged, states that the capacitance is proportional to the inverse of the frequency. To investigate this *fig 4.3.2* was considered.

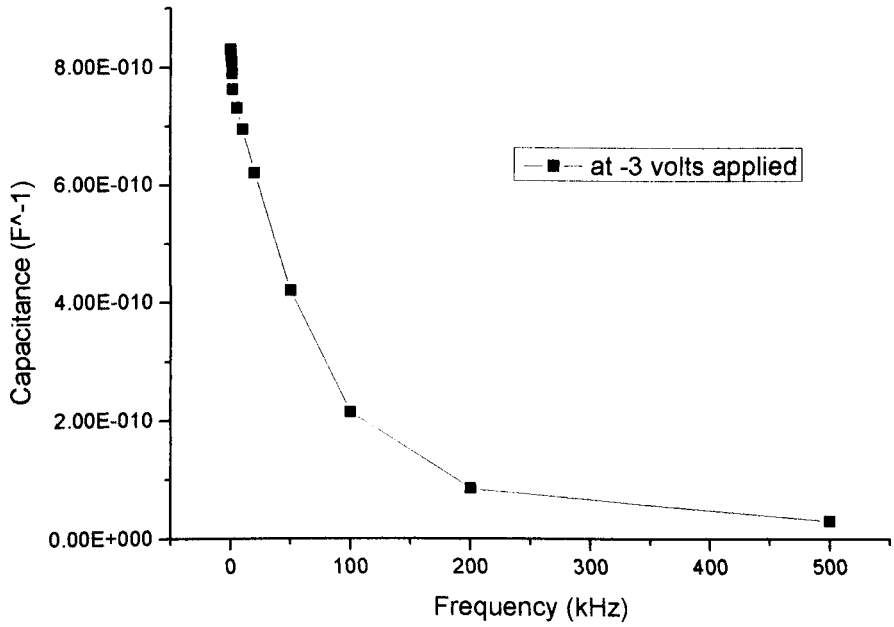

Fig 4.3.2 Details the frequency versus the capacitance at -3 volts

This figure shows a plot of the obtained capacitance at various frequencies when the applied voltage was equal to -3 Volts. This shows that there is an inverse relationship between the two parameters. To confirm this, the frequency was plotted against the inverse of the obtained capacitance and is shown in *fig 4.3.3.*

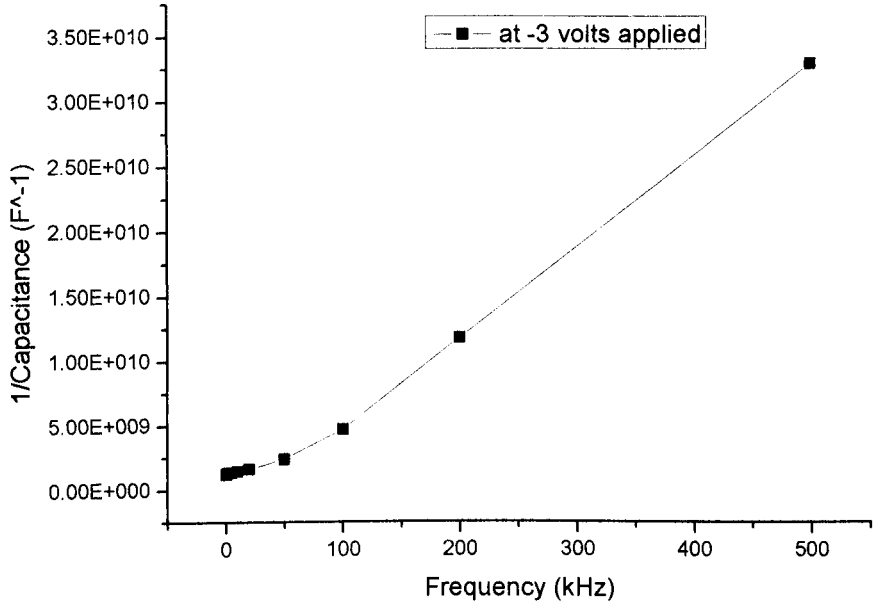

Fig 4.3.3 Details the frequency plotted against the inverse of the capacitance at -3 Volts applied.

However, observing the results in *fig 4.3.3* it is apparent that the frequency versus the inverse of the capacitance produces a fairly linear relationship. This behaviour is relatively simple to understand. If the frequency of measurement is doubled then the supply of carriers to the depletion region is halved. Thus the measured capacitance is halved. However, it is also possible that the distance the charge has to move also effects the results and this alters with the applied voltage.

There appears to be some deviation from a linear plot with the lower frequency readings. This could be due to the time for a half cycle being large enough so that there is time for the charge to reach its steady state value. In comparison, at higher frequencies the capacitor is not allowed to

charge for as long as it is at lower frequencies and may not fully charge. This could effect the results obtained and will require further investigation.

4.3.2 Relationship with Doping Density

This section investigates the effect of the doping density of the diodes on their capacitance. The diodes were fabricated on a glass substrate with gold and aluminium contacts and PTAA doped with DDQ at percentage by weight. The dopant was varied from 0.1% to 1% by weight. Voltage was then applied to the devices and the capacitance measured. The voltage was swept from -5 volts to 1 volt and the measured capacitance ranges from 0 to approximately 3200 Pico Farads.

Fig 4.3.4 shows the results obtained from various diodes with different doping levels.

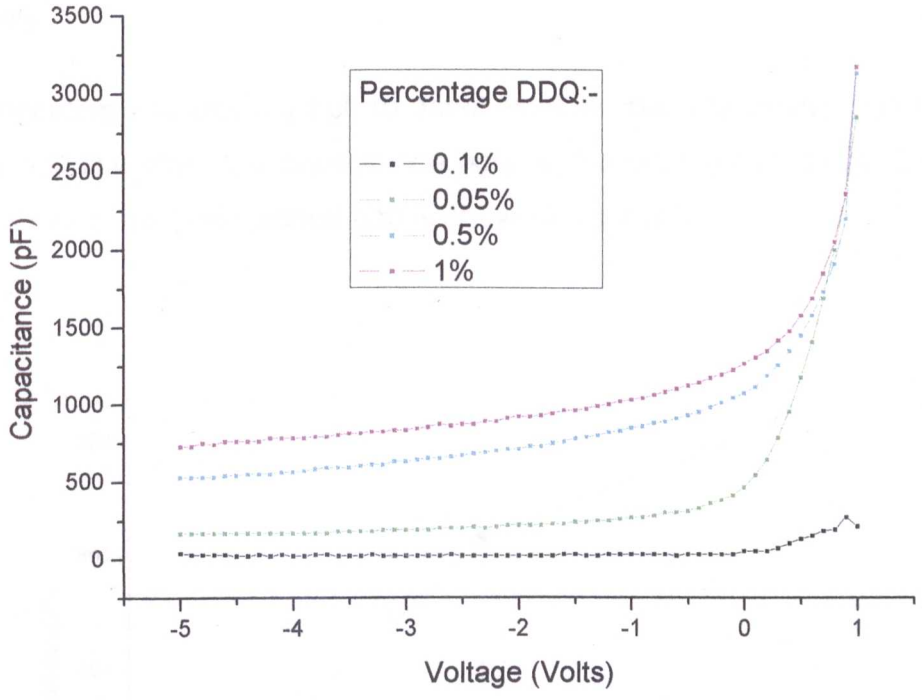

Fig 4.3.4 Capacitance-voltage characteristics for gold-PTAA-aluminium Schottky diodes, with various doping densities, taken at a frequency of 0.1 kHz.

The figure shows that with increased doping of the polymer, the measured capacitance increases. From *eqn 4.2.9* it is clear that the capacitance of the depletion region and the doping density of the material are related. Therefore, the expected relationship between capacitance and doping density is,

$$C_d \propto N_D^{1/2} \qquad 4.3.1$$

The resistivity of the neutral region falls and length of the neutral region is reduced as the depletion region widens under reverse bias. The supply of charge depends on the effective carrier mobility in the neutral region. The

carrier density increases with added dopant and so does its effective mobility.

It is necessary to plot a graph to detail whether this relationship has been obtained. Therefore the capacitance against the doping density at -3 volts and 0.1 kHz has been plotted and is shown in *fig 4.3.5*

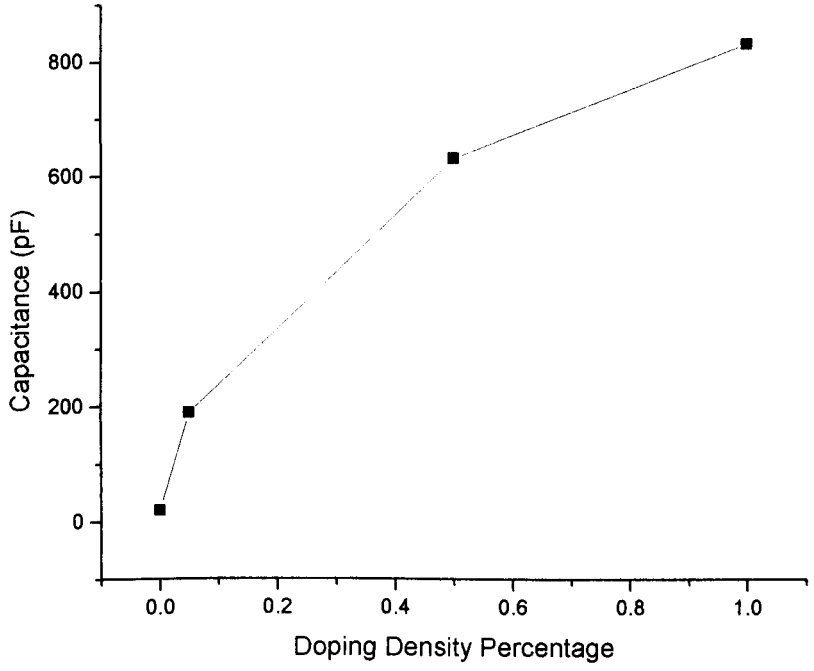

Fig 4.3.5 Details the capacitance versus the doping density percentage at -3 volts applied at a frequency of 0.1 kHz

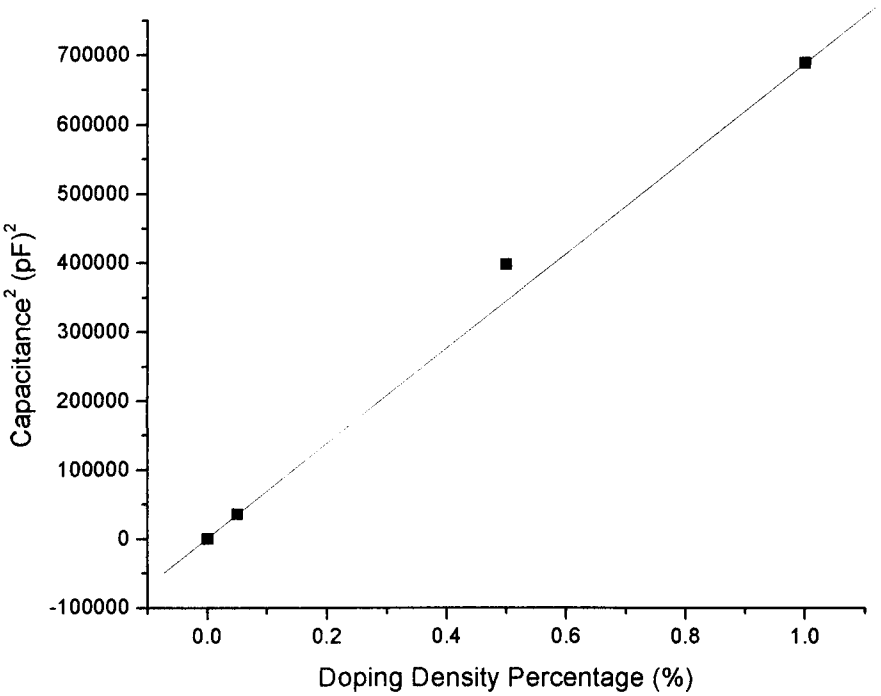

Fig 4.3.6 Capacitance squared of the Schottky diode against the doping density percentage

As can be seen in this graph, the results produce a linear relationship. The single point off the line could easily be accounted for in terms of experimental error particularly with regard to concentration of DDQ in the solution.

4.3.3 Relationship with Applied Voltage

Here the effect of voltage on the capacitance of Schottky diodes is investigated. To achieve this, the capacitance was measured at various

applied voltages and the results observed. This was carried out over a range of frequencies to establish the behaviour of the diodes. *Fig 4.3.7* shows the applied voltage versus the measured capacitance of the diodes.

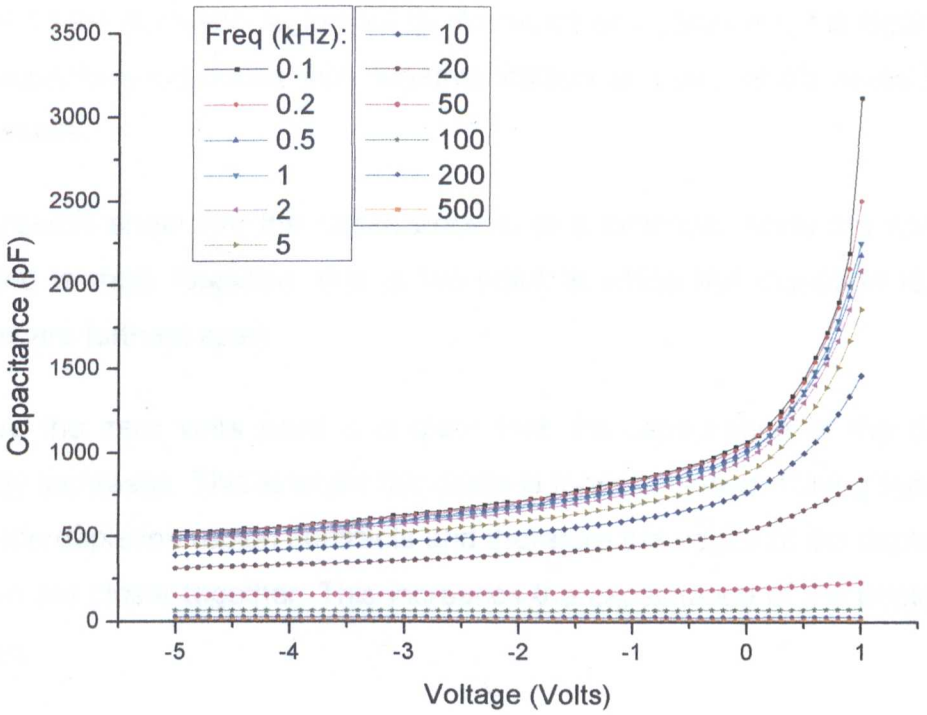

Fig 4.3.7 Capacitance-voltage characteristics for gold-PTAA-aluminium Schottky diodes, doped at 0.5% with DDQ by weight, taken at various frequencies.

As can be seen from the figure, the effect of voltage on the capacitance of the Schottky diodes is negligible at high frequencies. At lower frequencies however, the effect is very noticeable. With increasing voltage there is an increase in the capacitance of the diodes, however, this is more obvious at higher voltages, for example at voltages over 0 volts. As can be seen, there

is a dramatic increase in the measured capacitance at positive applied voltages.

The results obtained show the capacitance of the diode under reverse bias. During reverse bias the depletion region of the diode expands. As the edges of the depletion region act as the plates of a capacitor, it is clear that the capacitance reduces with negative voltage and can be observed from the results.

The results show that the capacitance is at a minimum when the voltage applied is most negative, this is the point at which the depletion region edges are furthest apart.

Above the zero volts point it is clear that the capacitance of the diode rapidly increases. This is when the diode is forward biased. During forward bias the depletion region contracts and therefore the edges of the depletion region are closer together. This increases the capacitance of the depletion region.

Shown in *fig 4.3.8* is a plot of the voltage versus the square of the inverse of the capacitance.

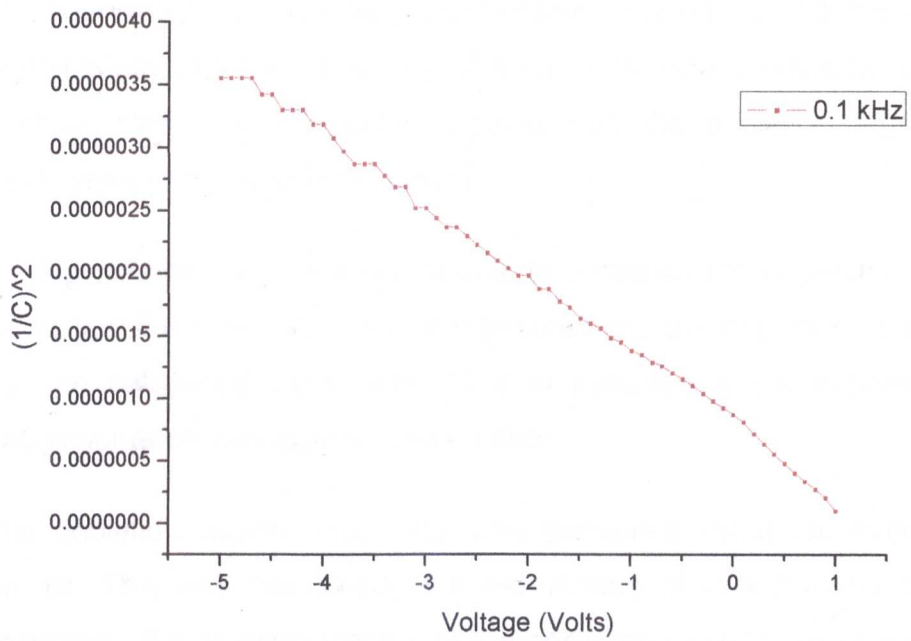

Fig 4.3.8 Details the Measurement voltage versus the square of the inverse of the capacitance taken at 0.05 kHz.

As can be seen in the figure there is a linear relationship between the voltage and the square of the inverse of the capacitance at this very low frequency. This confirms that the capacitance is inversely proportional to the root of the applied voltage as predicted in *eqn 4.2.9*.

4.4 Depletion Region Width

4.4.1 Relationship with Frequency of Measurement

Observing *eqn 4.2.3*, it is clear that an equation for the depletion region width can be obtained by simple re-arrangement. This equation shows that the depletion region width is inversely proportional to the capacitance, therefore as the capacitance increases, the depletion region width

decreases. It has also been established that the capacitance and frequency of measurement are inversely proportional. This means that the depletion region width and the frequency of measurement are proportional to one another. Hence, the equation predicts that the depletion region width increases with increased frequency.

Having obtained experimental results to establish the dependence of the capacitance on the frequency of measurement, the depletion region width can be calculated using *eqn 4.2.3* to establish if the theoretical and experimental results support one another.

The depletion region width, W_d, was calculated using the experimental results. This was calculated at a set voltage of -3 volts and a varying frequency. It was established that the depletion region is at its smallest at the lowest measurement frequency of 0.1 kHz and was found to be 2.5×10^{-8} m. It was found to be at its largest at the highest frequency of 500 kHz, the value of W_d was 6.8×10^{-7} m. The calculated results show that the as the frequency of measurement is increased, the depletion region width increases as predicted.

4.4.2 Relationship with Doping Density

The depletion region width is predicted to be proportional to the root of the inverse of the doping density according to *eqn 4.2.8*. To investigate this, the depletion region width must be obtained from the experimental results for various doping densities.

The depletion region width was calculated for various doping densities at a frequency of 0.1 kHz and an applied voltage of -3 volts. It was found that the width of the depletion region was largest with 0% dopant and smallest with 1% dopant. The range of depletion region width was from 2.513×10^{-8}

m to 1.043×10^{-6} m. From the obtained results it is clear that the depletion region width increases with a lower doping density and decreases with higher doping as predicted in *eqn 4.2.8.*

4.4.3 Relationship with Applied Voltage

It is predicted that the depletion region width is proportional to the root of the applied voltage. This is according to *eqn 4.2.8.* It is therefore necessary to calculate the value of W_d for various applied voltages to establish whether the experimental results obtained support the theoretical results studied.

The depletion region width was calculated and found to increase with greater applied negative voltage. The calculations were obtained at a frequency of 0.1 kHz as there was a greater variation in capacitance with applied voltage with the lower frequency plots, therefore it was easier to observe the effect on the depletion region width with these results. The largest value calculated was at an applied voltage of -5 volts and is equal to 3.986×10^{-8} m. The smallest value of 6.686×10^{-9} m was obtained for an applied voltage of 1 volt. This confirms that the depletion region expands with a negative applied voltage as the diode is in reverse bias and confirms that the depletion region width is dependent on the applied voltage.

4.5 Summary

Equations for the width of the depletion region of a Schottky diode and the capacitance associated with it have been derived. These equations prove useful as they can describe the behaviour of the diode. These equations

were confirmed by experimental results on the effect of signal frequency, doping density and applied voltage on the capacitance of the diodes.

Studying the variation of capacitance with frequency, it has been confirmed that the capacitance is inversely proportional to the frequency of measurement. This is caused by the high resistivity of the neutral region which is due to the low drift mobility in these materials even in the presence of dopant.

Observing the effect on the capacitance obtained with variation in the doping density of the material it has been shown that the low frequency capacitance is proportional to the square root of the doping density.

Experimental results were also studied to establish the relationship between the depletion region width and the frequency of measurement, doping density and applied voltage and confirmed the theoretical equations.

It is of interest to note that these results have been explained without referring to carrier trapping. However at much higher frequencies, which may be required for potential applications, this may turn out to be the case and would thus require further study.

4.6 References

[1] A. Takshi, A. Dimopoulos, J. D. Madden. Applied Physics Letters, Volume 91, Number 8, 2007, 083 513-3.

[2] S.M.Sze. Physics of Semiconductor Devices, John Wiley & Sons, 1969, p 91.

[3] C. R. Paul. Electromagnetics for Engineers with Applications, John Wiley and Sons, 2004, p 71.

[4] S.M.Sze. Physics of Semiconductor Devices, John Wiley & Sons, 1989, p 89.

[5] R. L. Meade, R. Diffenderfer. Foundations of Electronics, Circuits and Devices. Thomson Delmar Learning, Edition 4, 2003, p 586.

Chapter 5

Impulse Response of Schottky Diodes

Presented within this chapter of the thesis is an investigation into the impulse response of Schottky diodes. To achieve this, Schottky diodes were fabricated using gold and aluminium contacts and doped PTAA. Once fabricated, square waves of varying frequencies were applied to the diodes and the output observed. Discussed within this chapter is the effect of frequency on the impulse response of Schottky diodes. Also presented in this chapter is an investigation into the effect of temperature on the impulse response of Schottky diodes.

5.1 Introduction

The impulse response of Schottky diodes was studied to allow the operation of the diodes to be better understood, for example how the diode behaves under the application of a square wave input. This will allow the diodes to be modelled more accurately.

Detailed within this chapter is the theoretical analysis of the impulse response of Schottky diodes. This is described for both a simple case, where the resistance of the neutral region and the capacitance of the depletion region are independent of the applied voltage and also for a more complex case where the capacitance and resistance are dependent on the applied voltage.

The impulse response of Schottky diodes was then experimentally investigated for a variety of frequencies and the output observed. This was compared to theory.

This chapter also details the effect which temperature has on the impulse response of Schottky diodes. To investigate into this effect, the Schottky diodes were fabricated using gold and aluminium contacts and doped with PTAA. To obtain the impulse response, square waves were applied to the diodes and the output observed. To investigate the effect of temperature on the impulse response, the diodes were cooled using liquid nitrogen in a cryostat evacuated of air and allowed to slowly increase in temperature to room temperature. In comparison to the constant temperature measurements, a set frequency was used and only the temperature varied.

5.2 Theoretical Analysis of Schottky Diode Impulse Response

If a forward biased Schottky diode has a resistor in series, which is small in comparison to the internal resistance of the diode itself, a potential drop forms across the resistor as it is carrying the diode current. Also, according to Ohm's law, the potential drop across the resistor is proportional to the current flowing though the resistor. The depletion region of the Schottky diode acts like the plates of a capacitor and the distance between the plates changes due to the voltage applied to it. The circuit therefore acts as a simple RC circuit with variable R as the resistance of the neutral region and C as the capacitance of the depletion region.

If the supply voltage is removed, the capacitor will begin to discharge and the current reverses in direction, as it is initially driven by the full potential drop across the diode. The potential drop across the diode reduces approximately linearly as the diode discharges and the current reduces exponentially.

When considering disordered semiconductors, many carriers are in low energy (deep) traps. Thus they have to emit carriers into the higher energy levels which are more closely spaced to allow them to hop between the energy levels towards the contact. This behaviour predicts that the transient will have a long tail.

When the supply voltage is switched to forward bias the diode, all of the applied voltage initially falls across the neutral region and the current thus peaks and the voltage and current are proportional. The capacitor then begins to charge and thus takes up some of the applied voltage. The potential drop across the neutral region then falls and therefore so does the current through the resistor until the capacitor is charged, therefore the potential across the resistor is constant and a steady state current flows.

This describes the basic effects controlling the impulse response for a forward biased diode, however in reality there are more effects to be considered which can effect the output. For example, when the diode is forward biased the depletion region contracts, this means that the capacitance of the diode increases and the neutral region expands as does its resistance. This reduces the frequency response of the Schottky diode.

5.2.1 Derivation of Simple RC Equation

The simplest equivalent circuit of a Schottky diode for the impulse response consists of a capacitor and resistor both assumed to remain constant value, i.e. they are independent of the applied voltage, an example of which is detailed in *fig 5.2.1.*

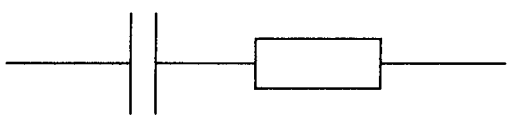

Fig 5.2.1 schematic representation of the equivalent circuit of a Schottky diode.

It is possible to develop an equation to describe the behaviour of the circuit. Firstly, since the charge is given by,

$$Q_d = C_d V_C \qquad 5.2.1$$

where Q_d is the charge in the depletion region, C_d is the capacitance of the depletion region and V_c is the voltage across the capacitor. Also, the current is defined as,

$$I = \frac{dQ_d}{dt} \qquad 5.2.2$$

where I is the current through the device, and dQ_d/dt is the variation in charge with time.

From *eqn 5.2.1* and *eqn 5.2.2*

$$I = \frac{C_d dV_C}{dt} \qquad 5.2.3$$

As the two components are in series, it is clear that the current is also given by,

$$I = \frac{V_R}{R} \qquad 5.2.4$$

where V_R is the voltage across the resistor and R is the resistance of the neutral region.

It is then possible to set *eqn 5.2.3* equal to *eqn 5.2.4* to eliminate I from the expression. The equation can then be rearranged to allow integration of both sides of the equation. This is given by,

$$\int \frac{1}{V_R} dV_C = \int \frac{1}{C_d R} dt \qquad 5.2.5$$

The expression can then be integrated by substitution with the limits of time between 0 and t and the limits of V_c between 0 and V_c, and also noting that the applied voltage, V_{app}, is initially equal to the voltage across the resistor, V_R and the voltage across the capacitor, V_C. Once integrated and rearranged, the following expression for V_c is obtained,

$$V_C = V_{app}\left[1 - \exp\left(\frac{-t}{C_d R}\right)\right] \qquad 5.2.6$$

This is the simplest equation which assumes that both the resistance of the neutral region and capacitance of the depletion region remain constant. If this were to be plotted this would show the charging of the depletion region of the Schottky diode. It is also of use to derive the expression for the discharging of the capacitor. This can be achieved in a similar manner to that above and is shown in *eqn 5.2.7*

$$V_C = V_{app}\left[\exp\left(\frac{-t}{C_d R}\right)\right] \qquad 5.2.7$$

5.2.2 Derivation of Complex RC Equation

The previously derived equation is not adequate to define the variation in V_c across a Schottky diode as the depletion region changes width with a variation in the applied voltage. This alteration in width in both the neutral and depletion region also means that the resistance of each is altered, thus both resistance and capacitance are dependent on the applied voltage. When a supply voltage is applied to the diode, the capacitor charges, however as this takes time, the voltage falls across the neutral region giving rise to a current which is equal to V_{app}/R, this is the charging current of the diode. As previously, *eqn 5.2.1* and *eqn 5.2.2* apply, and can be used to obtain an expression for the current, however, in this case, the capacitance is dependent on time, thus when combining the two equations the following is obtained

$$I = \frac{d(C_d V_c)}{dt} \qquad 5.2.8$$

Eqn 5.2.4 again applies and setting this equation equal to *eqn 5.2.8* results in

$$V_R = \frac{d(R_n C_d V_c)}{dt} \qquad 5.2.9$$

It is possible to obtain equations for R_n and C_d which can be substituted into *eqn 5.2.8* which are variable with the voltage applied to the device. These equations have been derived in Chapter 4. The resulting equation is,

$$R_n C_d = \frac{W_t - \left(\frac{2V_C \varepsilon_0 \varepsilon_p}{qN_D}\right)^{1/2}}{nq\mu A}\left(\frac{qN_D \varepsilon_0 \varepsilon_p}{2V_C} A^2\right)^{1/2} \qquad 5.2.10$$

Within this equation, the terms n and N_D are included separately, this is due to n being used for conduction processes and N_D being used for depletion regions. Although the two values are equal, they are included separately due to the complexity of the conduction process.

The mobility can be replaced with the universal mobility law [1], shown in *eqn 5.2.11*

$$\mu = Kn^m \qquad 5.2.11$$

Thus *eqn 5.2.10* becomes

$$R_n C_d = \frac{W_t - \left(\frac{2V_C \varepsilon_0 \varepsilon_p}{qN_D}\right)^{1/2}}{qKn^{m+1} A}\left(\frac{qN_D \varepsilon_0 \varepsilon_p}{2V_C} A^2\right)^{1/2} \qquad 5.2.12$$

To simplify,

$$R_n C_d = \frac{\left(\frac{qN_D \varepsilon_0 \varepsilon_p}{2V_C} A^2\right)^{1/2} W_t - \varepsilon_0 \varepsilon_p}{qKn^{m+1}} \qquad 5.2.13$$

A good approximation to this is given in *eqn 5.2.14*, this removes $\varepsilon_0\varepsilon_P$ from the expression as they have little impact on the results

$$R_n C_d = \frac{\left(\frac{q\varepsilon_0\varepsilon_p}{2V_C}A^2\right)^{1/2} W_t}{qKN_D{}^{m+1/2}} \qquad 5.2.14$$

Substituting this equation into *eqn 5.2.9* results in an equation for the voltage across the resistor where the resistance and capacitance are dependent on the applied voltage.

$$V_R = \frac{\left(\frac{\left(\frac{q\varepsilon_0\varepsilon_p}{2V_C}A^2\right)^{1/2} W_t}{qKN_D{}^{m+1/2}}\right) dV_C}{dt} \qquad 5.2.15$$

Again, V_R can be replaced by $V_{app} - V_C$ and is detailed below.

$$V_{app} - V_c = \frac{\left(\frac{\left(\frac{q\varepsilon_0\varepsilon_p}{2V_C}A^2\right)^{1/2} W_t}{qKN_D{}^{m+1/2}}\right) dV_C}{dt} \qquad 5.2.16$$

This can then be rearranged and the constants grouped to allow integration

$$\int dt = \int K^{1/2}\left(\frac{\left(\frac{1}{V_C}\right)^{1/2}}{(V_{app} - V_c)}\right) dV_C \qquad 5.2.17$$

This expression can then be integrated [2] with t between 0 and t and V_C between 0 and V_C to give

$$V_C = \left(V_{app}^{1/2} \tanh \frac{t V_{app}^{1/2}}{2k^{1/2}} \right)^2 \qquad 5.2.18$$

This is the complex equation for when the diode is charging, taking into account the variation in depletion region and neutral region widths. Again, it is possible to derive a similar equation for the discharging of the diode

$$V_C = \left(\left(2k^{1/2} \left(\frac{2k^{1/2}}{V_{app}^{1/2}} - t \right) \right)^{-1} \right)^2 \qquad 5.2.19$$

This then allows both the charging and discharging of the diodes to be modelled with these equations. These theoretical equations now need to be compared to experimental results.

5.3 Analysis of Schottky Diode Impulse Response

Having derived equations to represent the impulse response of Schottky diodes it is thus necessary to obtain experimental results. This was achieved by fabricating Schottky diodes using treated gold as the base contact, PTAA doped with DDQ and Aluminium as the top contact. Square waves were applied to the diode using a signal generator and the output observed across a series resistor. An example of the layout of the circuit is given in *fig 5.3.1.*

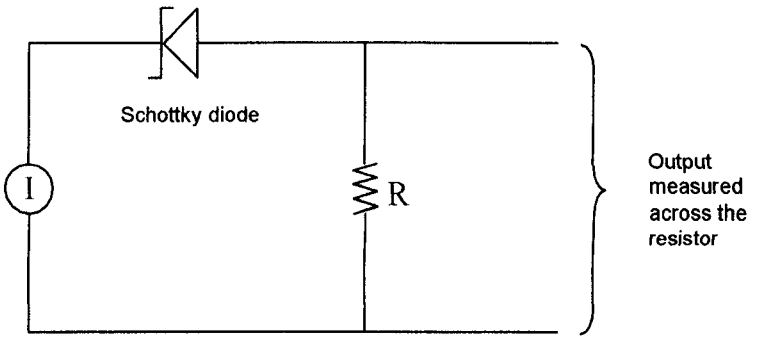

Fig 5.3.1 Layout of the circuit used to obtain the impulse response of the Schottky diodes.

The impulse response was taken at various frequencies to establish the effect of this on the output obtained.

Shown in *fig 5.3.2* is the output obtained when a -5V to +5V square wave of frequency 500 Hz was applied to the diode.

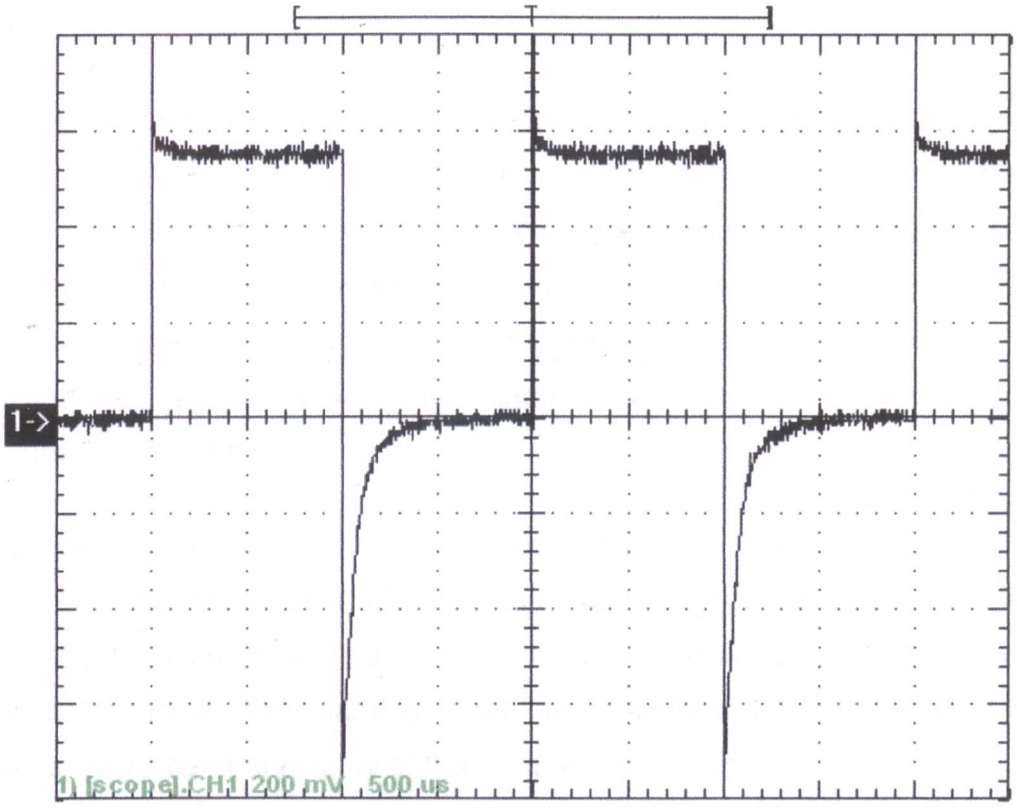

Fig 5.3.2. Impulse response of a Schottky diode when a -5V to +5V square wave of 500Hz was applied to the device.

When a square wave is applied to the Schottky diode, the diode switches between forward and reverse bias. When it initially switches to forward bias, all of the voltage initially falls across the neutral region of the diode and the voltage reaches a peak value as indicated by the spike on the characteristics. This causes the current to peak also as current and voltage are proportional.

The capacitor then charges and takes up some of the applied voltage, therefore not all of the voltage is now falling across the resistor. The voltage across the resistor falls until the capacitor is charged. This then results in a steady voltage drop across the resistor, therefore a steady current also

flows through the resistor, this is the diode current as the devices are in series.

When the polarity of the voltage is switched, the capacitor discharges and the current reverses as it is initially driven by the potential drop across the diode. The current and potential falls as the capacitor discharges. The current falls exponentially and has a fairly long tail, this is due to the polymer having carriers in deep traps, therefore the carriers have to be emitted into higher traps to allow them to be transported by hopping towards the contact.

It is possible to compare the experimental results to those obtained from the theoretical derivation of the impulse response. Shown in *fig 5.3.3* is the theoretical impulse response obtained from plotting *eqns 5.2.6* and *5.2.7*. *Eqn 5.2.6* models the charging of the capacitor and *eqn 5.2.7* models it discharging when the polarity of the voltage is switched.

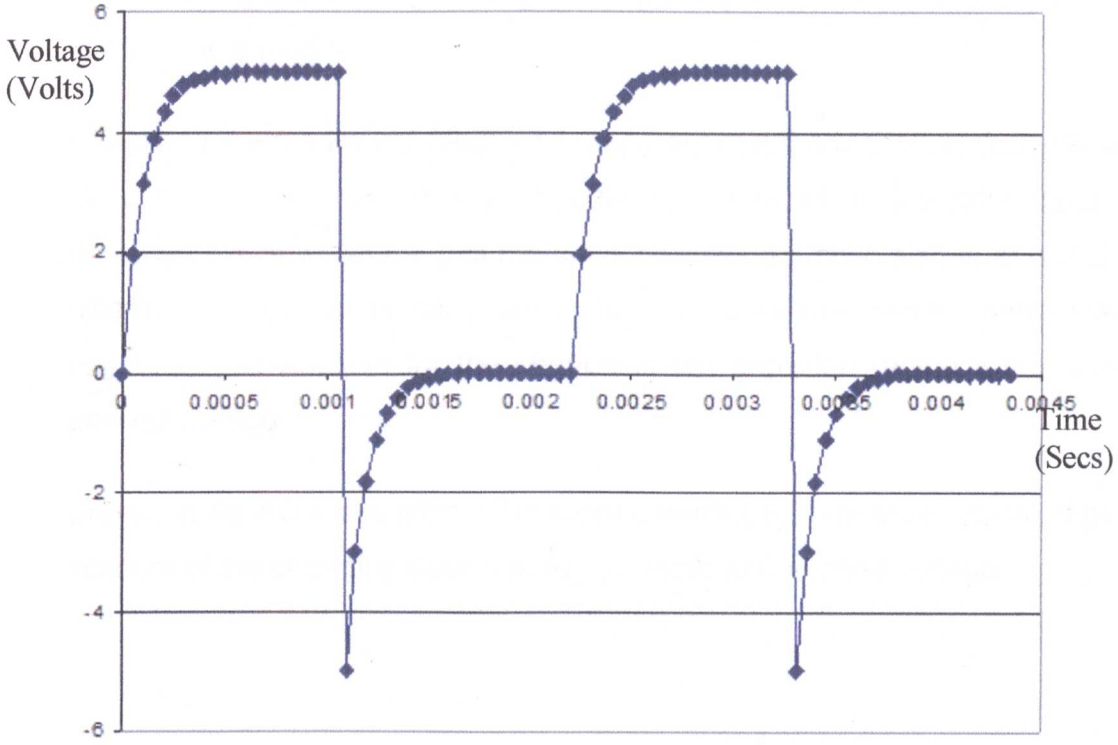

Fig 5.3.3 theoretical impulse response obtained from eqns 5.2.6 and 5.2.7.

As can be observed from *fig 5.3.3*, the theoretical results are quite similar to those obtained from the experimental results. Firstly, when observing the reverse characteristics of the impulse response, the theoretical results predict that the output voltage will immediately drop to a minimum and then rise exponentially until the voltage reaches zero volts. This effect is seen on the experimental results obtained and confirms that the reverse characteristics follow the simple RC equation.

When observing the forward characteristics, it is apparent that there are slight differences however the essential shape of the impulse response is the same. The theoretical results predict that the output will rise exponentially from zero volts to the applied voltage. The results obtained from the experiments show that the output voltage does settle at a maximum voltage, however instead of gradually rising, it initially peaks.

This is due to the initial switching of the polarity which is not accounted for in this simple model.

Observing the theoretical results it is apparent that the model produced is a fairly reasonable plot of the impulse response of a Schottky diode, however, it is important to plot the more complex equation also to establish whether this produces more accurate results as the simple theoretical results do not account for the change in the depletion region width with applied voltage.

Shown in *fig 5.3.4* is a plot of the more complex RC equation which takes account of the changing depletion region width with applied voltage.

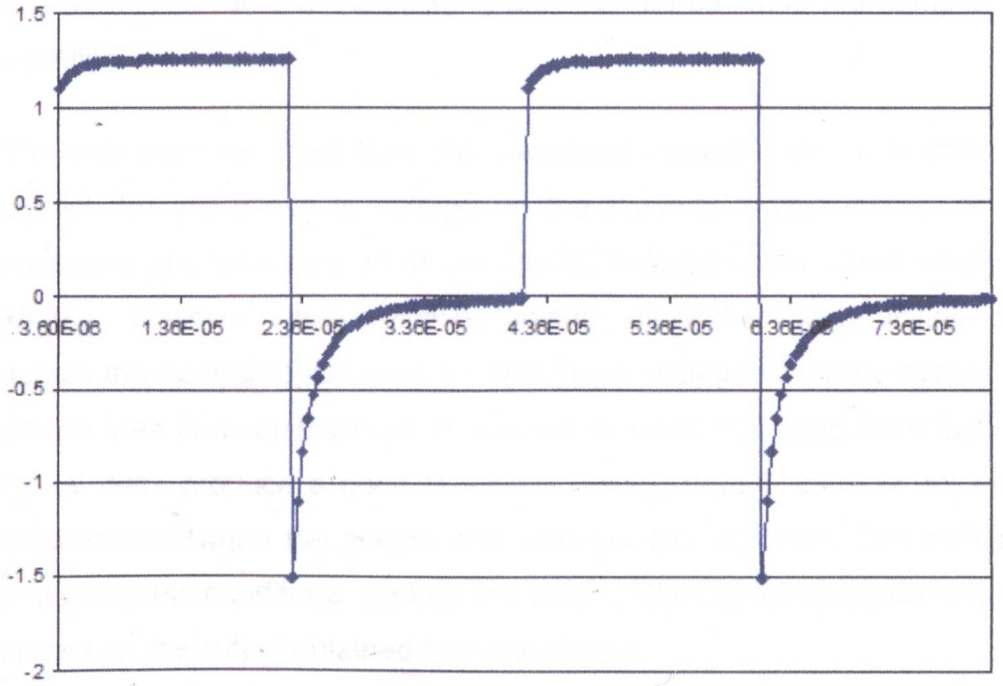

Fig 5.3.4. Theoretical impulse response obtained from eqn 5.2.18 and eqn 5.2.19.

Observing the theoretical results for the complex RC equation, which takes account of the variation in depletion region width with applied voltage, it is apparent that the reverse characteristics again show that the reverse voltage will immediately drop to its minimum and will rise exponentially. This is the same as obtained previously from the simple RC equation and matches the experimental results well. It appears that the variation in depletion region width does not affect the results obtained for the reverse current and both the simple and complex RC equations produce accurate results to model this.

Looking at the forward voltage results, it is apparent that the results obtained are again fairly similar, however with the complex RC equation, there is a sharper increase in the forward current compared to the simple RC equation. This therefore appears to more accurately model the characteristics of the Schottky diode compared with the simple RC equation.

The only error obtained from the theoretical results is that it is does not predict the sharp rise in voltage on the forward characteristics, as the equations just take account of the applied voltage which would simply be +/- V_{app}, however, when switching polarity, all of the voltage initially falls across the neutral region thus a much larger voltage would be across the device than is modelled here. It is however clear that apart from this, the model does produce a good fit for the results, though there is not much difference between the simple and complex RC equation. This indicates that under the conditions applied, the width of the depletion region has little impact on the output obtained from the device.

5.4 Analysis of the Effect of Temperature on Schottky Diode Impulse Response

This section investigates into the effect of temperature on the impulse response of Schottky diodes

Schottky diodes were fabricated on a flexible substrate with a treated gold base contact, PTAA doped with DDQ and aluminium top contact. Once fabricated the diodes were placed into a cryostat evacuated of air and the chamber then cooled with liquid nitrogen. The diodes were fabricated on a flexible substrate to allow the diodes to cool more quickly. Once the diodes reached a minimum temperature, the liquid nitrogen was removed and the diodes allowed to slowly return to room temperature. As the diodes were allowed to gain temperature, characteristics were obtained from them by applying -10 to +10 volts and recording the output current obtained. Shown in *fig 5.4.1* are the characteristics obtained from a single Schottky diode at a variety of temperatures. The temperatures of measurement are given below the figure.

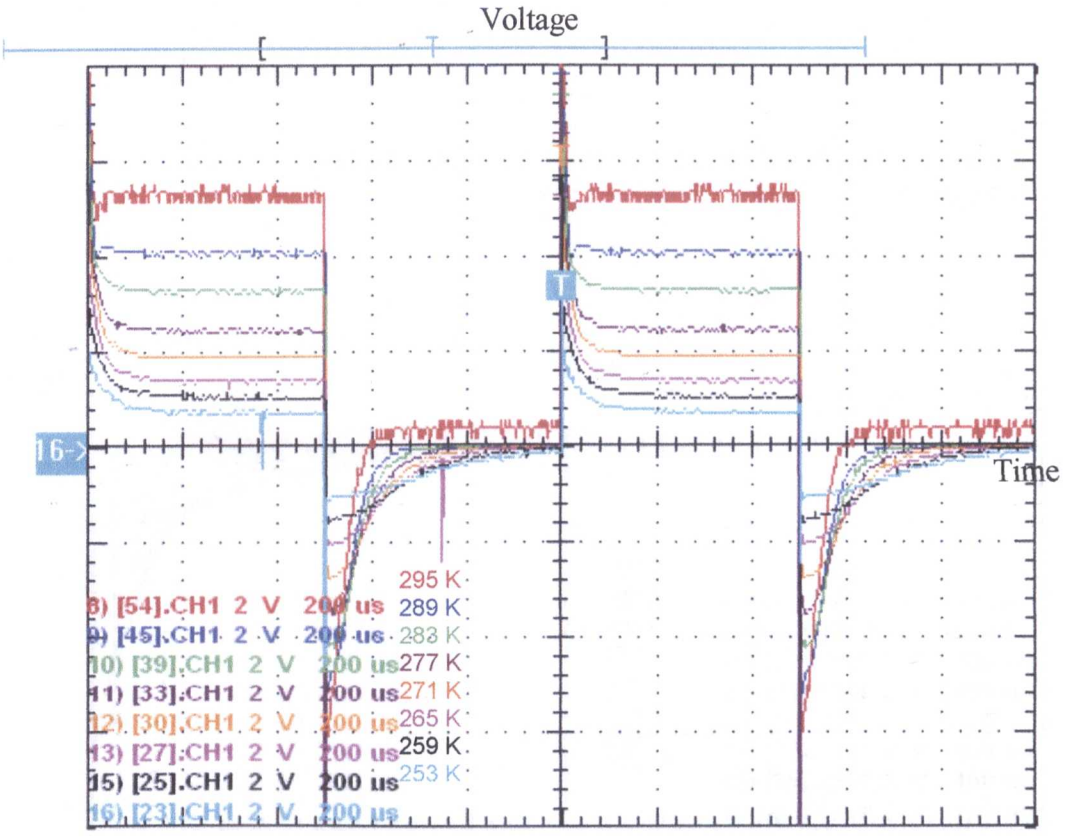

Fig 5.4.1 Impulse Response of a single Schottky diode at a variety of temperatures.

The measurement temperatures used were:

---- 295.15 K ---- 277.15 K ---- 259.15 K
---- 289.15 K ---- 271.15 K ---- 253.15 K
---- 283.15 K ---- 265.15 K

It is apparent that the characteristics alter with temperature, therefore, to more clearly observe the effect of temperature on the impulse response of the Schottky diodes, a single pulse is shown in *fig 5.4.2* together with arrows to indicate the movement of the characteristics with increased temperature.

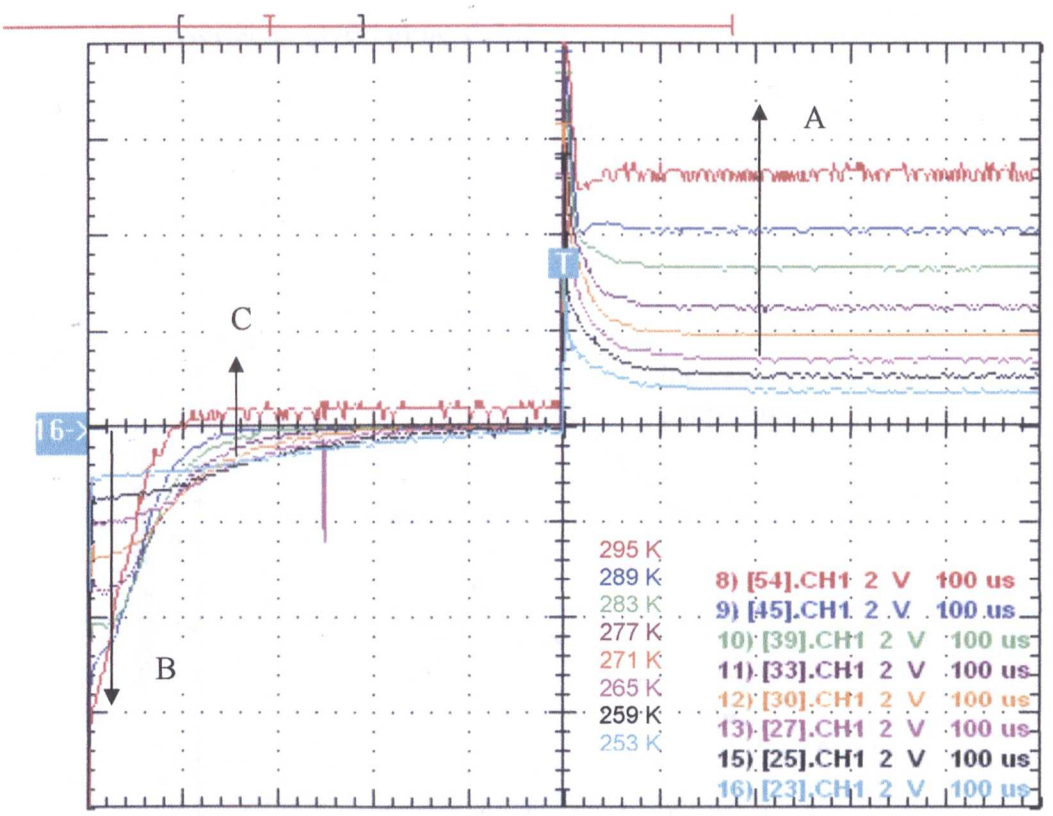

Fig 5.4.2 Impulse Response of a single Schottky diode at a variety of temperatures.

As can be seen from the figure, within the forward bias region of the impulse response, the voltage across the resistor increases with increased temperature. The carrier density and the effective mobility in the neutral region are temperature dependent and these cause a change in the resistance of the neutral region. Increasing temperature corresponds to a decreased resistance and a reduction in the time constant and can account for the difference in impulse response with temperature.

To confirm the relationship between current and temperature found in chapter 3 it is necessary to plot the variation in the output voltage against the parameter theta, which equals T/Tc. This is detailed in *fig 5.4.3*. The

output voltage observed was taken at 300μs during the forward bias region of the characteristics given in *fig 5.4.2.*

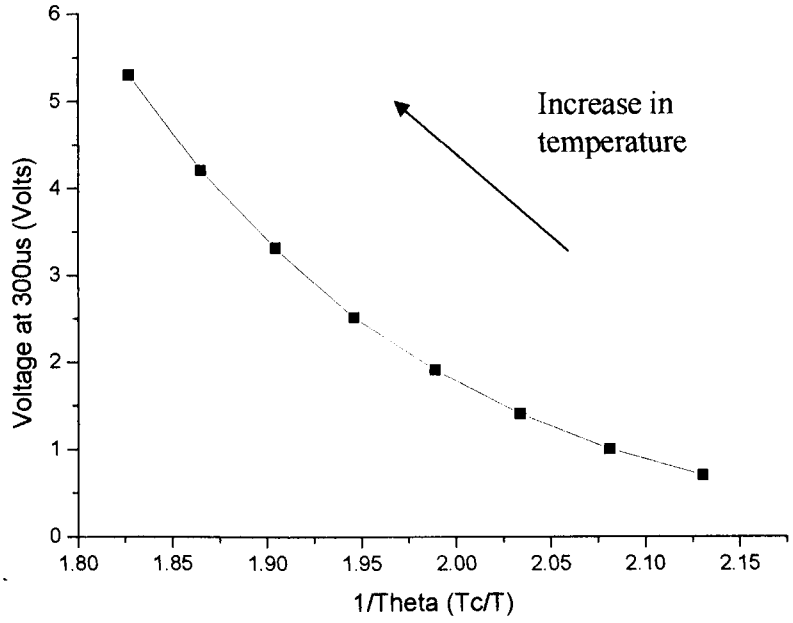

Fig 5.4.3 relationship between output voltage and theta plotted on a linear scale. Output voltage taken at 300μs during forward bias.

As can be observed in the figure, it is apparent that there is an exponential relationship between voltage and theta. In chapter 3 it was observed that there was an exponential relationship between theta and the current, thus it would be expected that an exponential relationship between voltage and theta was obtained as voltage and current are proportional to one another.

To confirm that the obtained relationship is exponential, the voltage was plotted on an exponential scale, this is shown in *fig 5.4.4.*

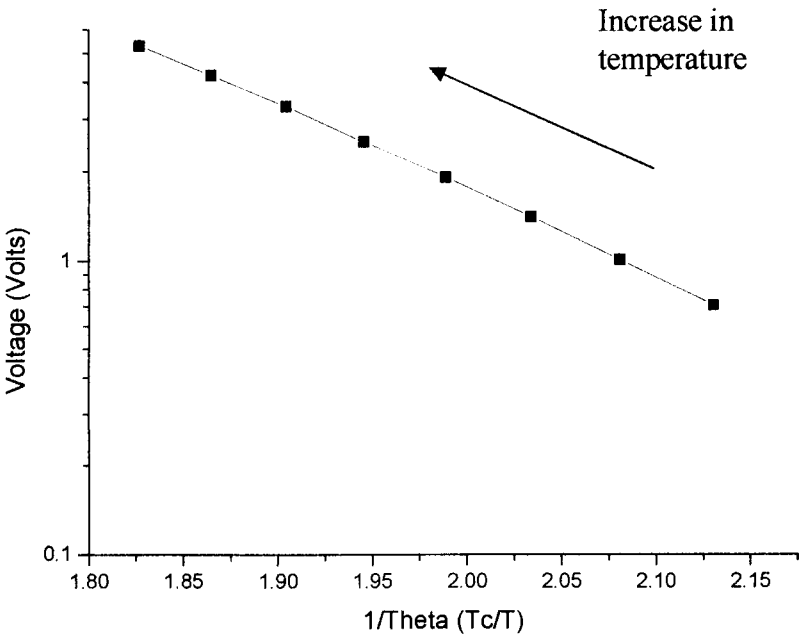

Fig 5.4.4 relationship between output voltage and theta plotted on a semi-logarithmic scale..

The figure shows that the plot does approximate to a straight line when plotted on a semi-logarithmic scale. This thus confirms the relationship between voltage and theta and also supports the work in chapter 3.

Referring back to *fig 5.4.2*, it is interesting to note that the red plot which is at the highest temperature of measurement is actually shifted upwards on the voltage axis. This could be a similar effect which has been seen in previous current voltage characteristics where the plot has shifted from the zero volts point. This could mean that the diode is storing some residual charge or perhaps this effect could be due to ion movement around the perimeter of the diode.

Another interesting point is the crossover of the curves in reverse bias. This could be explained if the carriers have more energy at higher temperatures, by picking up thermal energy, and are thus able to react quicker, therefore the capacitor would discharge quicker and produce this crossover.

It is important to determine whether the same effect is seen at different positions of the impulse response. The previous results were obtained from position A if fig 5.4.2, the results discussed below were obtained at position B on the same figure, these were obtained at 60us in reverse bias.

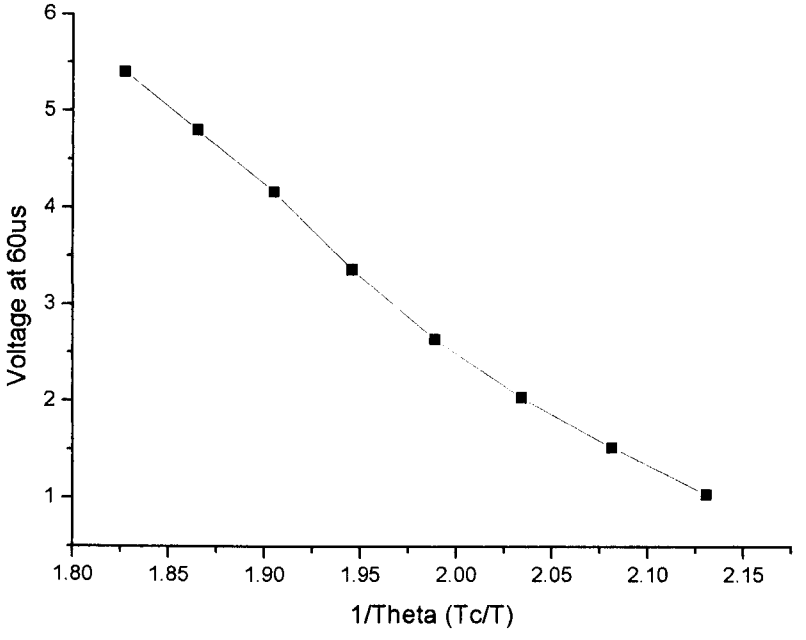

Fig 5.4.5 relationship between output voltage and theta plotted on a linear scale. Output voltage taken at 60μs during forward bias.

As can be seen from the figure, there again appears to be a linear relationship between the voltage and inverse of theta. This can be further confirmed with a semi logarithmic plot.

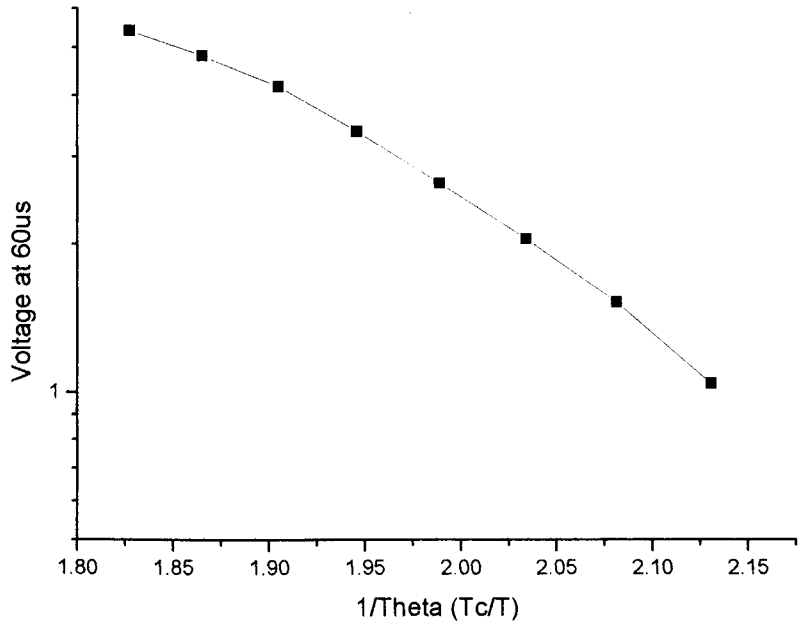

Fig 5.4.6 relationship between output voltage and theta plotted on a semi-logarithmic scale.

As observed in the above figure there appears to be more curvature to this graph than with the results obtained previously in the forward bias region. This could be due to the very small region over which it was possible to take results, or there may be a much more complex process happening. Either way, this would require further research.

5.5 Summary

This chapter has investigated the impulse response of Schottky diodes. Equations have been derived to model the behaviour of these devices. The first was a simple RC approximation which proved inaccurate in describing the behaviour. A second more complex equation was also derived which

takes into account the variation in the depletion and neutral region of the Schottky diode with applied voltage.

Experiments were performed to obtain the impulse response of the diodes to compare to the theoretical work. It is apparent that both the simple and complex RC equations are fairly similar and that both are a reasonable prediction of the impulse response of a Schottky diode. It appears that under the conditions used, the width of the depletion region has little impact on the results obtained.

The impulse response was also obtained under varying temperatures and has confirmed that the output voltage and therefore current does alter under different temperatures and supports the work carried out in chapter 3. It has been confirmed that the voltage and parameter theta have an exponential relationship as found previously.

5.6 References

[1] M. Fadallah, G. Billiot, W. Eccleston, D. Barclay. Solid-State Electronics, Volume 51, Issue 7, 2007, p1047-1051.

[2] Wolfram Research, Inc. Wolfram Mathematica Online Integrator. 1996. http://integrals.wolfram.com/index.jsp.

Chapter 6

Analytical Modelling of TFTs and Diodes on Small Molecule Organic Semiconductor Devices

Discussed within this chapter is the carrier transport through organic microcrystalline single crystal thin film transistors. This is modelled for both drift and diffusion in terms of grains and grain boundaries. Experimental results have been obtained to compare to the theoretical models.

6.1 Introduction

This chapter presents a study of Pentacene TFTs. The use of an exponential distribution of states to model devices actually pre-dates the use of organic materials and from the earliest days of thin film transistors it was found to represent a good approximation for modelling devices fabricated with polycrystalline materials. It therefore seems a natural extension of the work on diodes to extend it to polycrystalline TFTs. It is useful to have a TFT model that uses the same parameters as used for the diodes to allow direct comparisons between the two materials and there is some evidence that the TFT equations for disordered material, which are studied by other members of the Liverpool group, are very similar to those developed here for polycrystalline material. This makes the computer modelling of TFTs and diodes in disordered and polycrystalline material very similar, which was unexpected but convenient.

Pentacene devices have been modelled, using a new organic model, which takes account of the presence of grain boundaries consisting of highly disordered material and grains which consist of ordered material. The carrier traps within the grain boundaries are assumed to control the bending of the energy levels and the carriers in the grain are assumed to have a curvature that depends on the Debye length. There are two assumed modes of conduction, these are quasi-drift and quasi-diffusion and the models developed are based on these.

6.2 Pentacene

Pentacene is a polycyclic aromatic hydrocarbon (PAH) molecule. PAH's are molecules which consist of two or more aromatic rings [1] (a circular arrangement of atoms, which are alternately singly and doubly bonded to

one another, in which electrons are free to cycle around.) fused by sharing carbon atoms and do not contain heteroatoms (any atom which is not a carbon or a hydrogen atom) or carry substituents (atoms which are substituted in place of a hydrogen atom on the parent chain of a hydrocarbon). Pentacene is an organic semiconductor which is sensitive to both light and oxygen. Shown in *fig 6.2.1* is the structure of Pentacene [2], as can be seen it consists of five linearly fused benzene rings. It has the chemical formula $C_{22}H_{14}$.

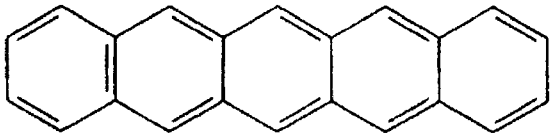

Fig 6.2.1. Schematic representation of Pentacene

Pentacene is the organic semiconductor used to fabricate the TFTs described within this chapter. It consists of regions of ordered and disordered material.

6.3 Organic Thin Film Transistor

Shown in *fig 6.3.1* is the structure of the top gate Thin Film Transistor.

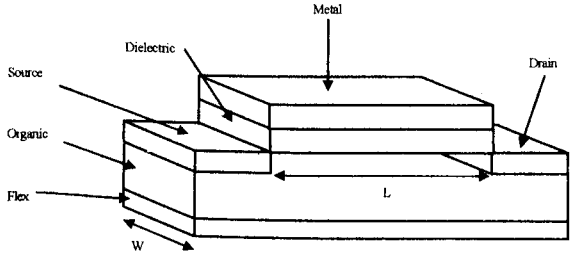

Fig 6.3.1. Thin Film Transistor structure.

As can be seen, the TFT is fabricated on a flexible substrate, on top of which is the organic layer, followed by the source and drain contacts, then the dielectric and the metal. The source and drain both make ohmic contact to the channel. This is the structure of the device used for the measurements described here.

Once results were obtained from the Pentacene TFTs, parameters were compared with those obtained from Schottky diodes. From the polymer Schottky diode characteristics, T_0, T_C and m were calculated. Firstly T_0 was calculated using the exponential region of the diode characteristics. Once T_0 was known, T_C was simply obtained from *eqn 2.3.6*.

The value of m is again calculated from the slope, G, of the exponential region of the diode characteristics. The values obtained are substituted into

$$\eta = \frac{q}{kTG} \qquad 6.3.1$$

to obtain a value for η. This can then be substituted into *eqn 6.3.3* to obtain the value for m.

$$m = \frac{1}{\eta - 1} \qquad 6.3.2$$

The obtained value for T_C can be compared with calculated values from polycrystalline TFTs. From these results, it is possible to determine whether the value for both disordered and polycrystalline material are similar: the diode is fabricated with disordered material. It will also indicate whether disordered and polycrystalline materials have a similar distribution of trap density with energy.

6.4 Carrier Transport in Pentacene TFTs

6.4.1 Single Grain Energy Level Diagram

Shown in *fig 6.4.1* is a simple model of small molecule organic material [3]. This shows how a single energy level varies with distance from the grain boundary for a semi-infinite grain size.

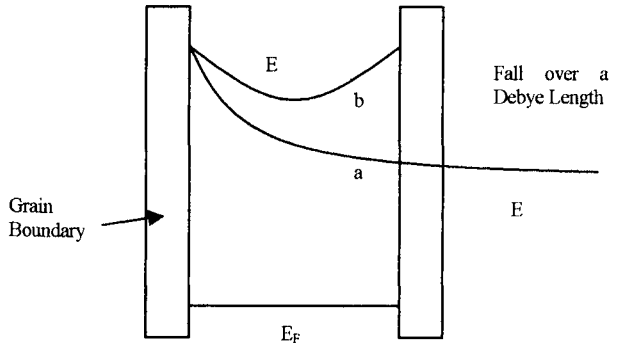

Fig 6.4.1. Simple structure of energy levels within a grain of a small molecule organic material.

The diagram illustrates the cases where one or two grain boundaries are present within a single grain. In the grain region there is a Fermi-level, E_F, and energy level, E, shown. As can be seen, the energy level extending to the right, labelled 'a', reaches the energy level expected for single crystal at infinity. This is due to the energy level being pinned at a point on the grain boundary and reducing in energy over a Debye length for undoped material.

When there are two grain boundaries present, there is a dip in the energy level mid way between them. This dip is associated with the combination of the Debye Lengths coming from the adjacent gains.

The Debye length, L_{De}, is

$$L_{De} = \left[\frac{k\,T\,\varepsilon_0\,\varepsilon_g}{2q^2\,n_g(y)} \right]^{1/2} \qquad 6.4.1$$

where k is Boltzmann's constant, T is the absolute temperature in Kelvin, ε_0 is the relative permittivity of free space, ε_g is the relative permittivity of the grain material, and $n_g(y)$ is the density of carriers at the centre of the grain.

If a greater number of carriers were induced within the grain, this would increase the carrier density at the midpoint of E, i.e. it would have a greater curvature. This is due to the mid point of the energy level being closer to the Fermi level, therefore increasing the density of carriers at that point.

The carrier flow between the grains is impeded by the potential barriers created by the dips in the energy levels.

Grains are regions of solid state matter which are assumed to have the structure of single crystal material. These regions can range in size from a few nanometres to several millimetres. Most material is polycrystalline, this means that is consists of regions of single crystals which are held together by areas of amorphous solid.

The grain boundaries are the regions where the crystalline material meets. Grain boundaries are assumed to consist of amorphous material and contain the atoms of the material which were unable to form into crystalline material, for example dislocations, impurities etc.

Grain boundaries are assumed to contain highly disordered discontinuities in the crystalline structure of materials, therefore, they will trap charge.

6.4.2 Quasi-Diffusion Model of Carrier Flow

When there are many grains and grain boundaries within the material, with no applied potential, *fig 6.4.2* applies [3].

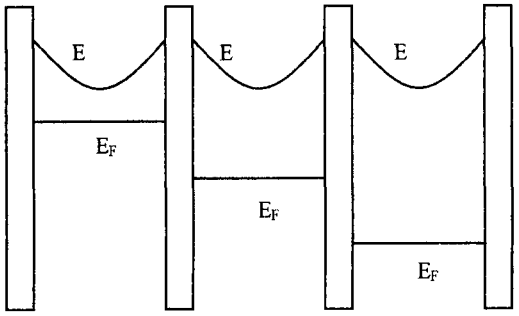

Fig 6.4.2. Quasi-diffusion model.

At low currents, there is no potential drop down the channel, except at the drain, which absorbs the voltage.

The flat Fermi-level in the grains falls in energy between the grains. The energy level, E, remains the same for each grain, however, the Fermi-level changes from grain to grain, therefore, so does the carrier concentration in each consecutive grain. This means that as the Fermi-level moves further away from the energy level there are fewer and fewer carriers in the lowest region of the energy level. The lowest region has the largest concentration of carriers.

This is comparable to diffusion in ordered semiconductors, therefore it is termed quasi-diffusion. This does not suggest that there is zero potential

difference between drain and source, instead it implies that there is insufficient field for the current to controlled by drift.

6.4.3 Quasi-Drift Model of Carrier Flow

If a larger potential is applied to the drain relative to the source, the energy level diagram will alter, this effect of an applied field on the heights of barriers for forward and reverse flow of carriers is shown in *fig 6.4.3* [3].

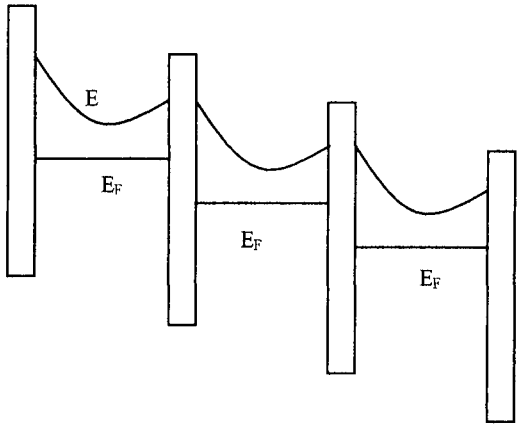

Fig 6.4.3: Quasi-drift model.

Again it is assumed that the Fermi level is flat across a grain, but changes energy across the grain boundary. The potential barriers are lowered however, by the application of drain voltage and carriers drift across them.

This means that the energy levels are progressively lower than the previous grain, however the difference between the energy level and E_F levels remain constant, therefore the number of carriers is constant. This applies at higher values of gate voltage and current and the process is known as quasi-drift.

6.4.4 Quasi-Diffusion and Quasi-Drift Model of Carrier Flow

If there is a combination of both quasi-drift and quasi-diffusion contributing to the current flow, then a combination of the effects are seen in the energy level diagram. This is shown in *fig 6.4.4* [3].

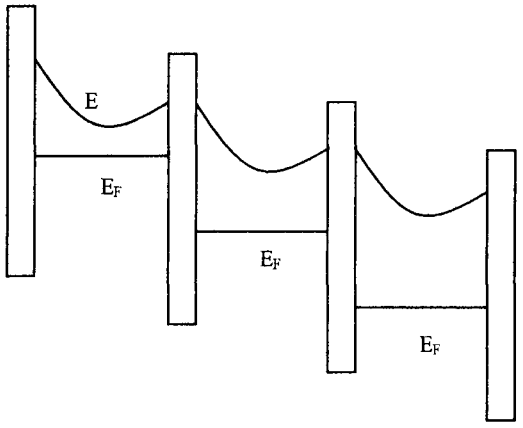

Fig 6.4.4. Energy level diagram for a combination of both quasi-diffusion and quasi-drift.

As can be seèn from *fig 6.4.4* above, both the Fermi-level and the energy level change energy between grains. The energy levels fall in energy between consecutive grains and the energy gap between the energy level and the Fermi-level becomes greater between consecutive grains.

This is the general case for current flow, which includes both quasi-drift and quasi-diffusion.

6.4.5 Flux of carriers

Flux is defined as number of carriers passing through unit area in unit time.

The grain boundaries illustrated above, form a series of potential hills which carriers need to overcome, these hills impede the motion of the carriers

through a material. *Fig 6.4.5* shows the case without an applied bias and *Fig 6.4.6* shows a simplified model to represent *fig 6.4.4*.

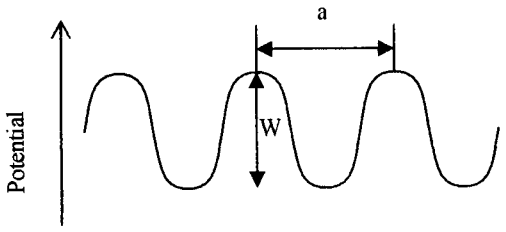

Fig 6.4.5. Simplification of the potential barriers caused by the grain boundaries. Here, W is the height of the potential barrier and a is the distance between successive peaks.

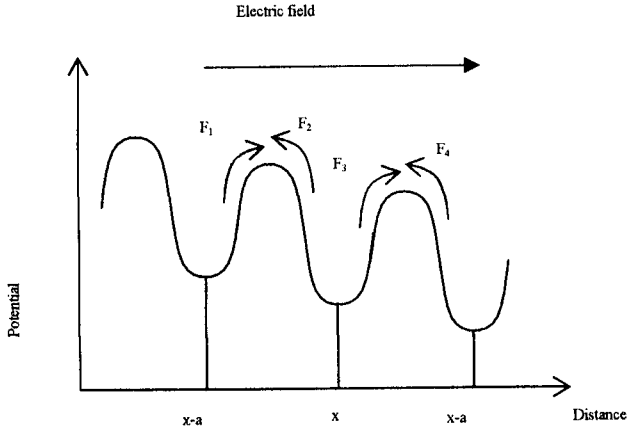

Fig 6.4.6. Details the potential barriers caused by the grain boundaries when a potential has been applied. Also detailed are the fluxes which are present at each peak.

As can be seen from *fig 6.4.6*, the potential distribution becomes 'tilted' with a constant electric field applied and it is easier for carriers to navigate to the right rather than to the left.

Combining *fig 6.4.4* and *6.4.6*, the fluxes present at each peak can be shown on the diagram for the grains. This is detailed within *fig 6.4.7.*

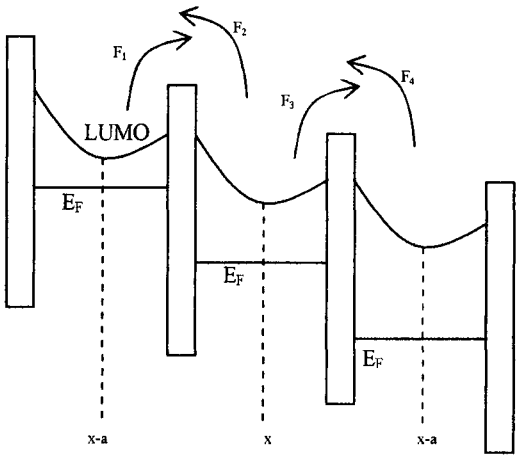

Fig 6.4.7: Details the potential barriers caused by the grain boundaries when a potential has been applied. Also detailed are the fluxes which are present at each peak.

6.5 Derivation of Current Equation

It is possible to derive an equation for the current down a thin film transistor channel. This is achieved by combining Poisson's equation, *eqn 6.5.1*, with the carrier concentration in the semiconductor, *eqn 6.5.2.*

$$\frac{d^2\phi}{dx^2} = -\frac{q\,n}{\varepsilon_0\,\varepsilon_P} \qquad 6.5.1$$

$$n_0 = n_i \exp\left(\frac{q\,\phi}{k\,T_C}\right) \qquad 6.5.2$$

where n_0 is the equilibrium carrier concentration at a reference level, q is the electronic charge, Φ is the potential, k is Boltzmann's constant, T is the temperature in Kelvin.

Eqn 6.5.3 shows the results after combining *eqn 6.5.1* and *6.5.2.*

$$F\frac{dF}{dx} = \frac{q}{\varepsilon_0\,\varepsilon_P}\,n_i \exp\left(\frac{q\,\phi}{k\,T_C}\right)\frac{d\phi}{dx} \qquad 6.5.3$$

where F is the field. *Eqn 6.5.3* can then be integrated to obtain an equation for the field, with F between 0 and F and Φ between 0 and Φ .This is detailed within *eqn 6.5.4.*

$$F \approx \left[\frac{2\,n_i\,k\,T_C}{\varepsilon_0\,\varepsilon_P}\,\exp\left(\frac{q\,\phi}{k\,T_C}\right)\right]^{1/2} \qquad 6.5.4$$

The application of Gauss' law to an infinitely thin cylinder, drawn normal to the interface is described in *eqn 6.5.5*

$$\varepsilon_D\,F_D = \varepsilon_S\,F_S \qquad 6.5.5$$

where F_D is the field strength on the dielectric side of the interface and F_S is the value on the semiconductor side, ε_D is the permittivity of the dielectric and ε_S is the permittivity of the semiconductor. The charge in such a cylinder must be zero. The field F_D is defined as

$$F_D = \frac{V_{G'} - V_x}{x_t} \qquad 6.5.6$$

where $V_{G'}$ is the gate voltage minus the threshold voltage, V_x is the voltage at the point x down the channel, x_t is the length of the channel. It is then possible to substitute the derived equation for the field, *eqn 6.5.4*, together with the expression for F_D *eqn 6.5.6*, into *eqn 6.5.5*

$$\varepsilon_D \frac{V_{G'} - V_x}{x_t} = \varepsilon_S \left[\frac{2\, n_i\, k\, T_C}{\varepsilon_0\, \varepsilon_P} \exp\left(\frac{q\, \phi}{k\, T_C} \right) \right]^{1/2} \qquad 6.5.7$$

Rearranging *eqn 6.5.7* and setting to the power (m+1/2) gives further use later in the derivation

$$\exp\left(\frac{q\, \phi}{k\, T_C} \right)^{m+1/2} = \left(\frac{\varepsilon_D}{x_t\, \varepsilon_S} \right)^{2m+1} \left(\frac{\varepsilon_0\, \varepsilon_P}{2\, n_i\, k\, T_C} \right)^{m+1/2} \left(V_{G'} - V_x \right)^{2m+1} \qquad 6.5.8$$

It is possible to define an equation for the current which can be obtained from J=nqμF, if the area is taken to be Wdz and replacing the mobility with the universal mobility law.

$$I = W q K F \int_0^{\varphi} \frac{n_i^{m+1}}{F_D}\, d\phi \qquad 6.5.9$$

After integrating *eqn 6.5.9* with the limits of Φ between 0 and Φ, and simplifying the result, *eqn 6.5.10* is obtained.

$$I = W q K F \left(\frac{\varepsilon_D}{x_t\, \varepsilon_S} \right)^{2m+1} \frac{1}{q\left(m+1/2\right)} \left(\frac{\varepsilon_0\, \varepsilon_P}{2} \right)^{m+1} \frac{1}{(k\, T)^m} \left(V_{G'} - V_x \right)^{2m+1} \qquad 6.5.10$$

F can then be replaced and after integrating x between 0 and L and V_X between 0 and V_D, *eqn 6.5.11* is obtained.

$$I = \frac{W}{L} K \left(\frac{\varepsilon_D}{x_t\, \varepsilon_S} \right)^{2m+1} \frac{1}{\left(m+1/2\right)} \left(\frac{\varepsilon_0\, \varepsilon_P}{2} \right)^{m+1} \frac{1}{(k\, T)^m} \frac{1}{2m+2} \left[-\left(V_{G'} - V_D \right)^{2m+2} + V_{G'}{}^{2m+2} \right] \qquad 6.5.11$$

This is the equation for the current within the accumulated channel of a polycrystalline TFT.

6.6 Electrical Characteristics

Transfer characteristics of a pentacene TFT, provided by Joanneum research, are shown in *fig 6.6.1*. The fitted data shows the agreement of the experimental data with the models.

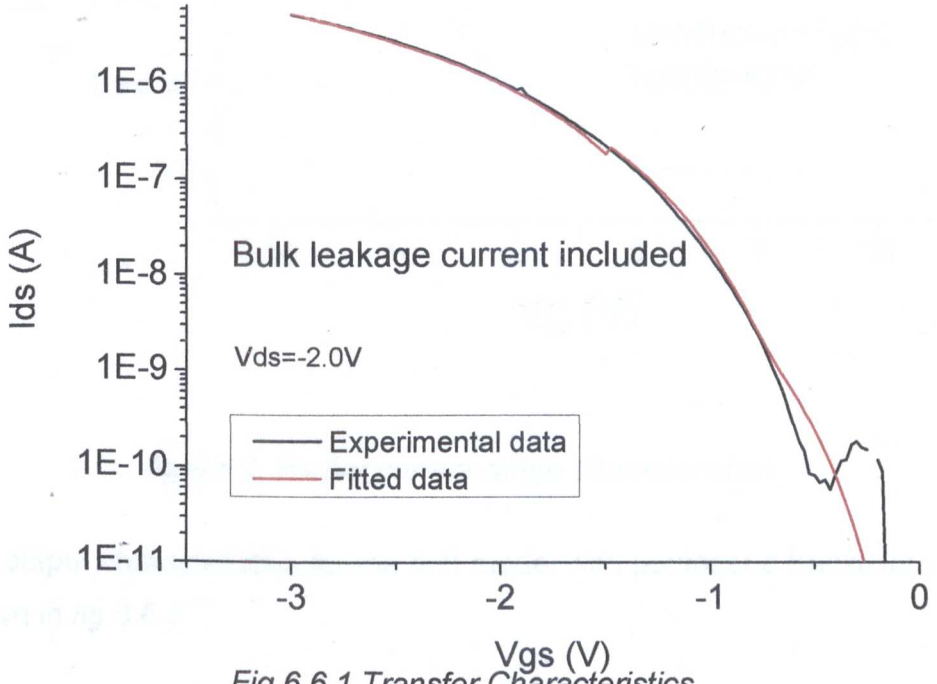

Fig 6.6.1 Transfer Characteristics

The results shown in *fig 6.6.2,* again supplied by Jonneaum, detail the higher current range. As can be seen, two values of T_C have been obtained.

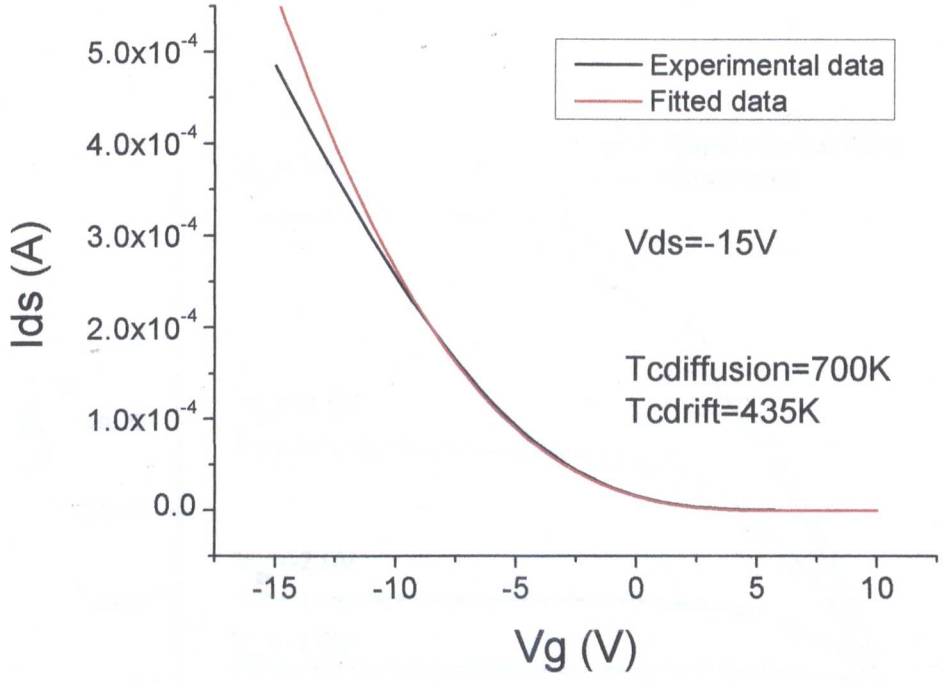

fig 6.6.2. Higher current range characteristics.

The output characteristics for the drift model with pentacene transistors are shown in *fig 6.6.3.*

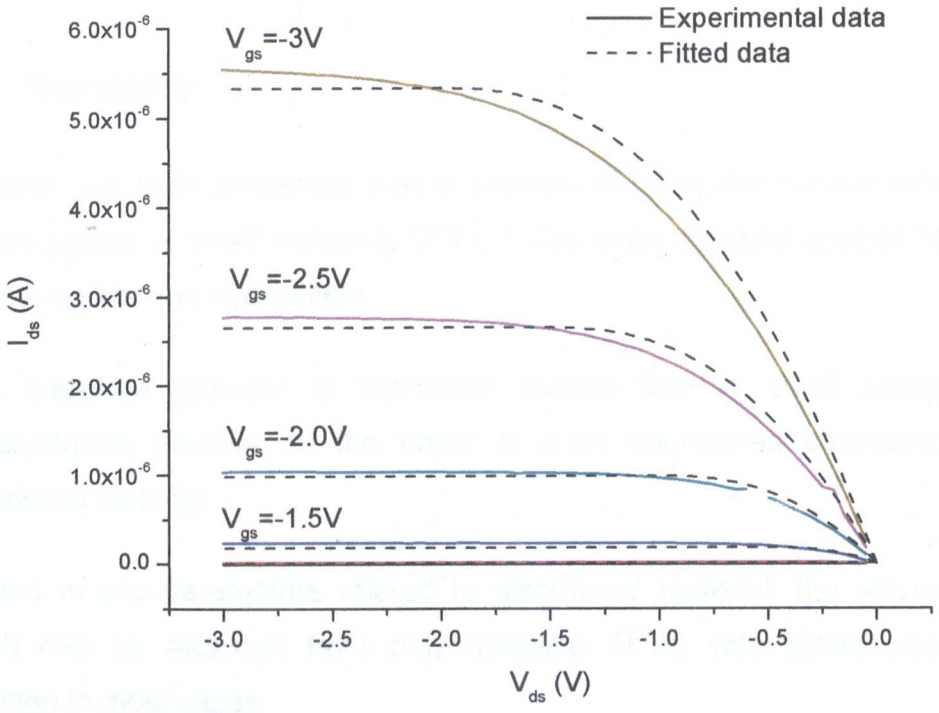

Fig 6.6.3 Output characteristics

The model has been fitted to the electrical characteristics of the pentacene devices. The results are shown in *fig 6.6.1, 6.6.2* and *6.6.3*. The agreement is excellent. The higher and lower current values of T_C are different. A similar effect has been seen in transistors on disordered material.

Also, comparing the T_C value calculated for the disordered diodes, it is clear that the value obtained (447K) is very similar to that obtained for T_{Cdrift} (435K) from the TFTs. This indicates that the two materials are behaving in a similar manner. The higher value obtained for $T_{Cdiffusion}$ (700K) could be

due to dopant present in the grain boundary or it could actually be a measure of T_0 not T_C, however this needs further investigation.

6.7 Summary

A model has been presented that is capable of fitting the current voltage characteristics of small molecule TFTs. It has been checked against TFTs and the agreement is excellent.

It is therefore possible to represent current flow in small molecule polycrystalline devices on the basis of grain boundaries consisting of disordered material.

T_C and m are parameters related to disordered material, the values of which can be deduced from polycrystalline TFTs, with similar results obtained in most cases.

Disordered metal semiconductor diodes give similar values of T_C and m but analysis of polycrystalline diodes has proved more problematical and is in need of analytical modelling of the behaviour at the top of the barrier.

Polycrystalline diodes are presently not reproducible, this could be due to the peak of the barrier either coinciding with a grain or a boundary which may affect the results obtained. It appears that the process is controlled by the grains not the boundaries, however, this requires further analysis.

6.8 References

[1] R. L. Crawford, D. L. Crawford. Bioremediation Principles and Applications, University of Cambridge Press, 1996, p125

[2] D. Gamota. Printed Organic and Molecular Electronics, Springer, 2004, p11

[3] W. Eccleston. Analysis of Current Flow in Polycrystalline TFTs, IEEE Transactions on Electron Devices, Volume 53, Number 3, 2006.

Chapter 7

Conclusions and Recommendations for Further Work

Presented in this chapter are the main conclusions drawn form the work discussed within the thesis. Also presented are recommendations for future work

7.1 Conclusions

7.1.1 Chapter 2

Expressions were derived for the carrier concentration within disordered semiconductors, current density within a Schottky diode, space charge limited current under various conditions and the universal mobility law.

A series of Schottky diodes were fabricated using gold, platinum/palladium and copper for the ohmic contact with PTAA doped with DDQ and aluminium as the Schottky contact. From these diodes it was found that the rectification ratio was approximately three orders of magnitude.

7.1.2 Chapter 3

The effect of temperature on the performance of Schottky diodes was investigated theoretically to determine how the occupancy of energy level and hence the output current would be affected under different temperatures of operation. Also studied was the position of the Fermi level with temperature and the temperature dependence of the parameter theta, the ratio of free to total charge. Each of these could contribute to the temperature dependence of Schottky diodes.

Schottky diodes were fabricated and characterised under various temperatures. Observing these results, it is apparent that there is a temperature dependence of the output current. At lower temperatures both the forward and reverse currents decrease compared to applying the same potential at a higher temperature.

By plotting theta against the output current at a particular voltage applied, it has been established that the output current has an exponential relationship to the theta.

Parameters were calculated from the characteristics and this shows that temperature effects the parameters obtained from the diodes. This is most noticeable in the results for the doping density and the carrier mobility.

There are a number of issues to consider with these diodes, for example, it is possible that impurities have been introduced during the fabrication process. This could alter the results seen from the diodes. Another problem is that the diodes have been exposed to air, this could alter the devices behaviour, as metals can become oxidised and the polymer can become more doped.

7.1.3 Chapter 4

Expressions were derived in relation to the capacitance within Schottky diodes, these were namely the width of the depletion region of a Schottky diode and the capacitance associated with the depletion region.

Schottky diodes were fabricated to experimentally investigate the capacitance within Schottky diodes and how it is affected by frequency, doping of the polymer and voltage applied to the device. Studying the experimental results, it has been established that they support the theoretical equations.

7.1.4 Chapter 5

The impulse response of Schottky diodes was modelled by deriving expressions for both a simple case, where the capacitance and resistance independent of the applied voltage and for a complex case where the resistance and capacitance vary with applied voltage.

Having studied the impulse response theoretically, experiments were performed to determine whether accurate models had been derived. Both the simple and complex models produced similar results and also predict the experimental results with reasonable accuracy. It also appears that the variation in depletion region width has little impact of the obtained results under the conditions studied.

The impulse response was also studied under varying temperatures. This has confirmed that the output voltage seen is dependent on the parameter theta, the ration of free to total charge. This supports the previous conclusions regarding temperature measurements on Schottky diodes within chapter 3.

7.1.5 Chapter 6

It has been established that it is possible to represent current flow in small molecule polycrystalline devices on the basis of grain boundaries consisting of disordered material. This model has proven accurate in fitting the current voltage characteristics of small molecule TFTs.

It has been established that the parameters T_C and m which are related to disordered material, can be deduced from polycrystalline TFTs, and produces very similar results.

The main problem with polycrystalline diodes is that they are presently not reproducible. This could be due to the peak of the barrier either coinciding with a grain or a boundary which may affect the results obtained.

7.2 Recommendations for Future Work

7.2.1 Chapter 2

There is a variety of further work which could be considered in relation to metal semiconductor junctions. Firstly, it is possible to further study the performance of the diodes when using alternative materials. This could include using a different polymer or different contact materials, for example varying either the ohmic or Schottky contact.

It would also be of use to investigate into the use of a Schottky contact other than aluminium which does not oxidise when exposed to air. This could eliminate problems within the Schottky diodes.

A further possibility is to conduct further research using copper as the ohmic contact to the polymer as this is the material which is planned to be used within RF tagging devices, thus research into this area would prove useful.

Finally, to eliminate the effect of air on both the contacts and polymer, the fabrication of the devices could be performed within an air free environment, because although the devices discussed here were fabricated within a clean room atmosphere, they were still allowed to come into contact with air which could affect the quality of the devices fabricated. This could also extend to the area within which the diodes are characterised to establish whether this would improve the quality of the characteristics obtained.

7.2.2 Chapter 3

The further work to be completed from the temperature measurement on Schottky diodes is similar to that discussed for chapter 2.

A further item which could be considered is to examine the effect of heating the diodes from room temperature to establish whether the theory studied is supported when the measurement temperature exceeds room temperature as well as if the temperature is lowered.

7.2.3 Chapter 4

Having studied the capacitance and depletion region width of Schottky diodes whilst varying the measurement frequency, applied voltage and doping density of the devices, it has become apparent that a variety of further work could be completed.

It may be of use to extend the voltage measurements to include more positive applied voltages to establish what happens to the depletion region width and capacitance during forward bias as the main region of experimental results were obtained for reverse bias.

Another possibility is to carry out the measurements over a wider range of doping as only a relatively small range was previously carried out.

It would also be of interest to extend the frequency range of measurement to establish the effect of capacitance at much higher measurement frequencies.

Finally, the capacitance measurements could be carried out under different temperatures to determine whether this would affect the depletion region width within the Schottky diodes.

7.2.4 Chapter 5

It has become apparent that although the models developed do predict the general shape of the impulse response, they do not accurately model the forward characteristics. This is due to the initial 'spike' in voltage not being modelled. The current models use the applied voltage to produce the output, however it can not take into account the switching of polarity. It would therefore be interesting to develop a third more accurate model which could take this into account.

7.2.5 Chapter 6

Having completed work regarding the modelling of TFTs fabricated using Pentacene, it would be of use to repeat the experimental work using both polymers and different polycrystalline materials to establish how different materials can affect the results obtained and also how this compares to using disordered materials as apposed to materials with areas of ordered and disordered material.